Post-transcriptional regulation of neural stem cell fate by non-canonical Drosha functions

Inauguraldissertation

zur

Erlangung der Würde eines Doktors der Philosophie

vorgelegt der

Philosophisch-Naturwissenschaftlichen Fakultät

der Universität Basel

von

Niklas-Frank Iffländer

Basel, 2020

Genehmigt von der Philosophisch-Naturwissenschaftlichen Fakultät auf Antrag von

Prof. Dr. Verdon Taylor

Prof. Dr. Mihaela Zavolan

Prof. Dr. Markus Stoffel

Basel, den 26. Mai 2020

Prof. Dr. Martin Spiess
Dekan der Philosophisch-Naturwissenschaftlichen Fakultät

Acknowledgements

I especially would like to thank **Prof. Dr. Verdon Taylor** for the great mentoring and support of my PhD studies and the opportunity to work in his lab.

Special thanks goes also to **Dr. Chiara Rolando**, who worked closely together with me on this project and always helped and supported me during her time in the Lab. Another thanks goes to **Dr. Andrea Erni** for her help and input during her time in the lab and for the effort she put in the ground work that preceded this study. I would like to thank **Dr. Elli-Anna Balta** and **Dr. Tanzila Mukhtar** for their help and contribution to the paper. Another thanks goes to **Dr. Thomas Bock** and the proteomics facility of the Biozentrum of the University of Basel for the fruitful collaboration.

I am also grateful to **Prof. Dr. Mihaela Zavolan** and **Prof. Dr. Markus Stoffel**, who have been on my thesis committee and followed the progress of this study. They always provided valuable comments and helpful advice and encouragement.

I also would like to thank all the past and present members of **the Taylor Lab** for helpful discussions and a nice working atmosphere. I would also like to thank **Mr. Frank Sager** and the **Animal facility** of the DBM for excellent technical support.

Ultimately, I wish to thank **everyone** who supported me in any way during this exciting period of my life!

Table of Content

Summary

The ability of stem cells to differentiate in to a variety of cell types is the fundamental basis for life in all organisms. But also later in life, the contribution and ability of stem cells to differentiate in tissue specific cells is crucial and needs to be preserved in adulthood. Yet, stem cells can only be found in a suitable environment called stem cell niches. The niche maintains the stem cell properties of the cells or provides factors required for their differentiation. In the adult brain, there are two distinct niches of adult neural stem cells (NSCs) that can be found in the subventricular zone (SVZ) on the outside walls of the lateral ventricle and the subgranular zone of the hippocampal dentate gyrus (DG). In the latter, NSCs differentiate into granular neurons and astrocytes that may contribute to learning and memory formation. This process is not only strictly regulated on a genetic level, but also post-transcriptional regulation of RNA transcripts strongly contributes to the extremely fine-tuned regulation of adult neurogenesis. A key factor in this process is the microprocessor, a complex best-known for its involvement in the microRNA (miRNA) pathway. The microprocessor consists of Drosha and DGCR8, and processes the pri-miRNA into pre-miRNA by targeting and cleaving distinct hairpin (HP) structures in these transcripts. The main effector of this process is the RNAse III Drosha. However, Drosha has been shown to participate in many additional processes that are not related to miRNA biogenesis and thus are referred to as non-canonical functions. Of special interest for this study is the finding that Drosha is able to target evolutionary conserved HPs that are located in the untranslated regions (UTRs) of mRNAs coding for transcription factors that drive NSCs into specific cell fates. In the adult hippocampal DG, Drosha targets and cleaves the 3’ UTR HP of the mRNA of NFIB, which leads to de destabilization and degradation of the whole mRNA transcript. Drosha thus prevents NFIB protein expression and hinders the cell to undergo oligodendrogenesis. This downregulation of NFIB is required to maintain the DG NSC pool and guarantee proper neuronal development and

differentiation. Interestingly, NFIB contains two RNA HPs, located in the 5' and 3' UTRs. Both HPs are targeted by Drosha but only the 3' UTR HP is cleaved. As Drosha is ubiquitously expressed in the entire brain, it remained to be shown how transcripts can escape Drosha cleavage and express NFIB in a cell-specific manner when needed, for example during oligodendrogenesis in other brain regions. In order to answer this question, we developed strategies to identify regulatory proteins that control Drosha-mediated NFIB cleavage in DG NSCs. By using protein immunoprecipitation (IP) followed by dual mass spectrometry (MS^2), we identified Drosha interacting proteins in DG NSCs. Moreover, we also determined NFIB HP interacting proteins by RNA pulldown assays and MS^2. This data did not only allow us to investigate closer some putative regulators of Drosha cleavage, but also allowed us to characterize the Drosha interactome in NSCs. Additionally, we analyzed the differences between NFIB 3' UTR and 5' UTR interaction partners and could show that especially the 5' UTR HPs interacts closely with ribosomal protein and thus seems to be deeper involved in translation than the 3' UTR HP. In order to investigate the functional relevance of the Drosha and NFIB mRNA bound proteins, we developed an *in vitro* GFP reporter assay in DG NSCs to directly monitor Drosha activity upon overexpression of putative cleavage regulating partners. We found that overexpression of certain candidate proteins modulates Drosha cleavage, especially gain-of-function of Scaffold Attachment Factor B1 (Safb1) significantly reduced the read-out GFP signal on mRNA as well as protein levels. This reduction was found to be Drosha-dependent as *Drosha* cKO in DG NSCs could rescue the reduced GFP levels caused by Safb1 overexpression. Moreover, Safb1 overexpression also reduced the mRNA level of endogenous NFIB. We could confirm direct binding of Safb1 to Drosha by protein IP and to NFIB by crosslinking and immunoprecipitation (CLIP) experiments. To investigate whether Safb1 gain-of-function and the consequent increase in Drosha cleavage has an influence of cell fate determination we overexpressed Safb1 in SVZ NSCs, an oligodendrogenic population, and

found reduced oligodendrogenesis in the transfected cells. Thus we identified Safb1 as a key regulator of Drosha-mediated cleavage of NFIB mRNAs, and could show that Safb1 levels influence NSC differentiation and oligodendrogenesis.

Introduction

Review title, authors & status

Mechanisms of post-transcriptional regulation and its effects in adult neurogenesis;
Niklas Iffländer, Verdon Taylor;
in preparation – planned submission in spring 2020

Contribution

I wrote the following review article and prepared all the included figures.

Manuscript

Mechanisms of post-transcriptional regulation and its effects in adult neurogenesis

Niklas Iffländer,[1] and Verdon Taylor[1,5,*]

[1]Department of Biomedicine, University of Basel, 4058 Basel, Switzerland

[5]Lead contact

*Correspondence to: verdon.taylor@unibas.ch

Abstract

Post-transcriptional regulation is a powerful mechanism for the cell to control its proteome independent of genetic regulation. It is known to affect all stages of cellular RNA production and to be sufficient to control expression of the target protein. During adult neurogenesis, the process in

which neural stem cells generate new neurons and glia cells in the adult brain, many mechanisms of post-transcriptional regulations have been identified. In this review, we discuss the impact of RNA binding proteins, miRNA and the microprocessor in a general perspective and shine special light to their functional implications for adult neurogenesis. Understanding the complex factors and fine interplay between effectors of post-transcriptional regulation and adult neurogenesis is a fundamental step in order to understand the process of neurogenesis as a whole.

Introduction

Adult neurogenesis

Adult neurogenesis is a steady-state process, in which the adult brain continues to generate neurons in two specific and well defined niches, the subventricular zone (SVZ) on the lateral walls of the lateral ventricle and the subgranular zone of the hippocampal dentate gyrus (DG) (Doetsch et al., 1999; Furutachi et al., 2015; Seri et al., 2004) (Figure 1). The microenvironment of these niches maintains stem cell properties and the neural stem cell (NSC) population, but also can direct differentiation (Alvarez-Buylla and Lim, 2004). NSCs located in the lateral wall of the SVZ are multipotent and have the capacity to generate neurons, astrocytes and oligodendrocytes, a process modulated by the niche (Ihrie and Alvarez-Buylla, 2011). Immature neuroblasts migrate via the rostral migratory stream to the olfactory bulb where they differentiate into interneurons that can integrate into local neuronal circuits (Doetsch et al., 1999). Also the hippocampal NSCs of the DG have been found to produce granular neurons and astrocytes, but are unable to form oligodendrocytes under physiological conditions (Bonaguidi et al., 2011; Pilz et al., 2018; Rolando et al., 2016).

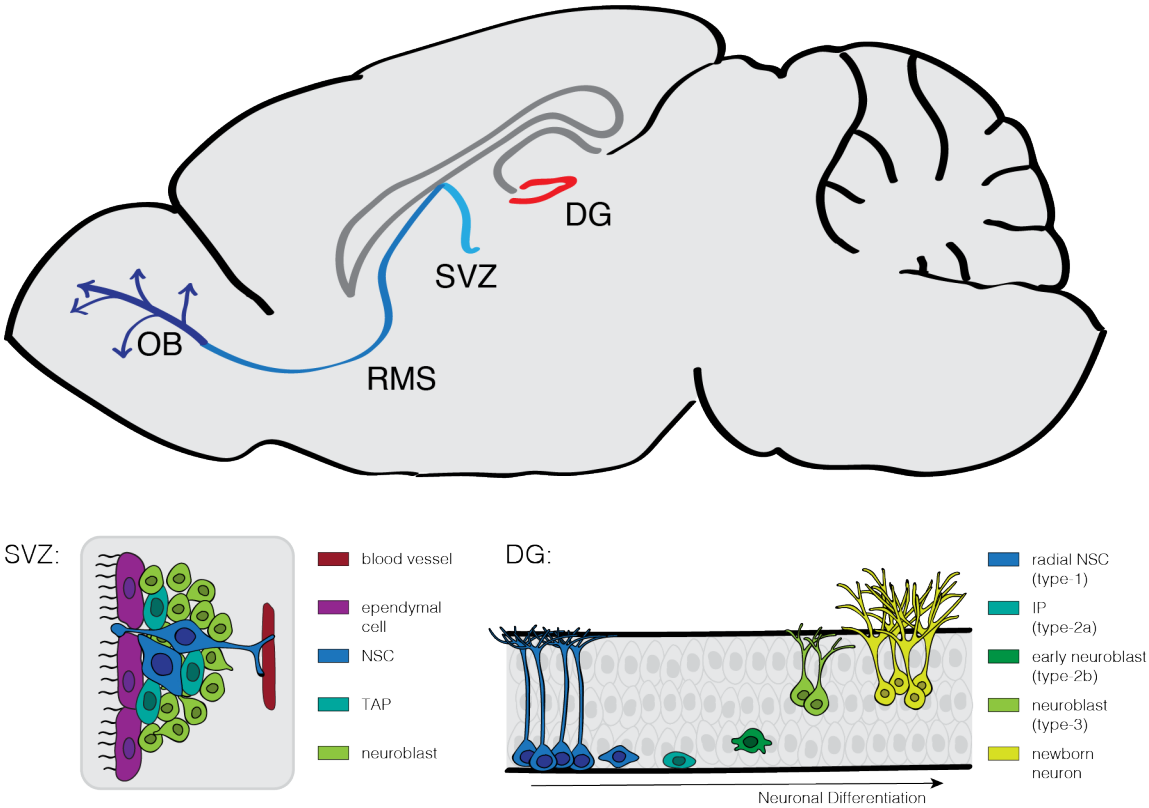

Figure 1: Neurogenic niches of the adult murine brain

The two niches of adult neurogenesis are the hippocampal dentate gyrus (DG) and the subventricular zone (SVZ), from where the cells migrate via the rostral migratory stream (RMS) to the olfactory bulb (OB). A detailed overview over the cell populations is displayed for the SVZ (bottom left) and for the DG (bottom right).

These DG NSC (type-1 cells) can be subdivided into two subpopulations with distinctly different morphologies: While radial type-1 cells characteristically divide very slowly and thus are defined as quiescent, the horizontal type-1 NSCs divide frequently and are considered active (Lugert et al., 2010; Lugert et al., 2012). During differentiation, the DG NSCs undergo several distinct stages: The initial type-2a intermediate progenitors (IP) are rapidly proliferating and progress towards a type-2b transitional stage before they eventually give rise to the migratory neuroblasts (type-3), exiting the cell cycle and ultimately committing to

granule neuron maturation (Gage, 2019; Goncalves et al., 2016; Lugert et al., 2012; Zhao et al., 2008) (Figure 1). These adult-born granule neurons integrate into functional circuits and adult neurogenesis contribute to learning and memory formation (Zhao et al., 2008) and general brain plasticity (Lledo et al., 2006). The capacity of the adult brain to generate newborn neurons has been observed in many mammals, including humans (Eriksson et al., 1998; Gage, 2019; Kempermann et al., 2018). Although still controversially discussed (Arellano et al., 2018; Sorrells et al., 2018), adult neurogenesis in humans could be linked to the process of memory formation, but also to neurodegenerative diseases (Boldrini et al., 2018; Kempermann et al., 2018; Tobin et al., 2019). Regulation of adult neurogenesis is a complex interplay between many factors including classic signaling molecules like BMPs and Notch (Basak et al., 2012; Mira et al., 2010; Zhang et al., 2019). However, also interplays between RNA, RNA binding proteins (RBPs) and other RNA regulators decisively shape the processes of adult neurogenesis in many aspects of post-transcriptional regulation.

Modes of post-transcriptional regulation

RNA Binding Proteins: critical regulators of RNA function

RNA binding proteins (RBPs) are involved in all stages of RNA translation and processing and are thus a fundamental pillar of cellular RNA regulation. Although RBPs are modular and hence able to fulfill a variety of functions in a cell, one limiting factor is the available pool of RNA binding domains (RBDs) (Lunde et al., 2007). Despite some diversity within the RBDs, some RBDs are found more commonly than others, including the RNA recognition motifs (RRMs), the DEAD box helicase, the hnRNP K homology (KH) domains, the zinc finger motif and the Pumilio-family (PUF) RNA binding repeats (Kilchert et al., 2019). Of these RBDs, the RRM is observed most frequently and has been identified in many species from bacteria up to humans. In humans, around 450 proteins have been

described which carry at least one RRM domain (Letunic and Bork, 2018). Yet, the number of RBDs and RBPs is steadily increasing, since increased experimental sensitivity and technologies like nucleotide-crosslinking allow the identification and location of novel protein-RNA interfaces, as shown for the previously unknown DUF2373 domain of the C7orf50 protein (Trendel et al., 2019). The identification of new RBPs is progressing faster than ever. Beginning with the development of the by now well established UV crosslinking and immunoprecipitation (CLIP) technique in 2003 (Ule et al., 2003), rapid advances in RNA mapping technologies (Lee and Ule, 2018) can be seen in the many methodological publications that have been published in the years that followed (Table 1).

METHOD	*NAME*	*USED IN*
CLIP	UV crosslinking and immunoprecipitation	(Ule et al., 2003)
HITS-CLIP	High-throughput sequencing CLIP	(Licatalosi et al., 2008)
PAR-CLIP	Photoactivatable-Ribonucleoside-Enhanced C.	(Hafner et al., 2010)
iCLIP	Individual-nucleotide resolution CLIP	(König et al., 2010)
miR-CLIP	MicroRNA CLIP	(Imig et al., 2015)
eCLIP	Enhanced CLIP	(Van Nostrand et al., 2016)
irCLIP	Infrared-CLIP	(Zarnegar et al., 2016)
fCLIP	Formaldehyde CLIP	(Kim et al., 2017)
s-CLIP	Simplified CLIP	(Kargapolova et al., 2017)
d-CLIP	Denaturing CLIP	(Rosenberg et al., 2017)
meCLIP	Monitored enhanced CLIP	(Hocq et al., 2018)
Proximity-CLIP	Proximity CLIP	(Benhalevy et al., 2018)
cTAG-CLIP	Conditionally tagged CLIP	(Ule et al., 2018)
spyCLIP	SpyTag based CLIP	(Zhao et al., 2019)
Quick-irCLIP	Quick-irCLIP	(Kaczynski et al., 2019)

Table 1: Evolution of CLIP based technologies

List of selected methods using UV crosslinking and immunoprecipitation (CLIP). After the development of the original CLIP protocol, a dramatic variation and specification in the methodological approaches has been seen.

A good example of methodical fine-tuning is the development of an enhanced CLIP (eCLIP) protocol in order to generate transcriptome wide RBP binding-maps at large-scale (Van Nostrand et al., 2016). This

enhancement greatly improves library generation efficiency and reproducibility, maintains single-nucleotide binding resolution and drastically decreases requirements for amplification reducing PCR generated duplicate reads. Moreover, technical optimization improves the eCLIP specificity for the exploration of novel RNA binding sites (Van Nostrand et al., 2016). In order to reduce the false binding site assignments that can be created by reading through cross-linked samples, two years later eCLIP was further evolved to monitored enhanced CLIP (meCLIP), allowing RNA purification prior to the reverse transcription (Hocq et al., 2018). These results funnel into brand new databases including the EuRBPDB for eukaryotic RBPs (Liao et al., 2020) and the oRNAment database for putative RBP target sites (Benoit Bouvrette et al., 2020). Anticipating these trends in analytical development and database initiations, we can expect even more sophisticated procedures and resources in the upcoming years.

Many RBPs have been found to cause disease in humans particularly in the nervous system, as examples, SMN1 and SMN2 in spinal muscular atrophy (SMA), FUS and TDP-43 in amyolateral sclerosis (ALS) and frontal temporal lobular degeneration (FTLD) and Qki in schizophrenia (Lukong et al., 2008; Mackenzie et al., 2010). Thus, better understanding of RBP mechanisms of gene regulation and control of the proteome will increase our ability to counteract certain dysregulated processes and to design new treatments for RBP caused diseases, and especially neurological disorders.

RBPs modulate different stages of neurogenesis

RBP regulation directly affects adult neurogenesis and impairs RNA metabolism which has an immediate impact on the maintenance of the NSC pool as well as in disease. A well-studied example is the fragile X mental retardation protein (FMRP), an RBP that has not only important roles in neural development but its loss also causes the fragile X syndrome. Moreover, FMRP is known to be a major contributor of autism and intellectual disability (Hagerman and Hagerman, 2015). In the brain of

adult mice, FMRP inhibits NSC proliferation, which decreases the amount of RGLs and IPCs and induces the generation of glia cells (Lazarov et al., 2012). Functional analysis of the RBP FMRP revealed that in addition to its regulation of the p53 pathway, FMRP binds the mRNA of GSK3β, inhibiting its translation. Dysregulation of GSK3β leads to reduced Wnt signaling pathway activity, altered Neurogenin1 expression and ultimately to fate changes in adult NSCs (Luo et al., 2010; Patzlaff et al., 2018). This also highlights the potential of RBPs to influence far downstream processes and provides an explanation of why some RBP effects on neurogenesis still remain elusive today. RBPs often act in higher hierarchical groups, usually as the same RBP families. This remains the case for the FRXs family, where besides FMRP also FXR1P and FXR2P have been shown to affect adult neurogenesis (Patzlaff et al., 2018).

The growing attention to study RBPs in adult neurogenesis and consequent scrutiny of new, but also already known RBP mechanisms in the last couple of years revealed some novel and additional RBP regulatory structures outside the main pathways. This is reflected in the analysis of Lin28, a RBP predominantly known for its close relation to Let-7 miRNA production, where Lin28 binds the pri-miRNA of Let-7 and thus blocks generation of mature Let-7 miRNAs (Viswanathan et al., 2008). However, subsequent investigations revealed that Lin28 directly influences postnatal neurogenesis independent of its inhibition of Let-7 production. Particularly, it was shown that constitutive Lin28 inhibited gliogenesis of murine postnatal cells, whilst in control cells inhibited for Let-7 by circRNA sponges, gliogenesis still occurs (Romer-Seibert et al., 2019).

Adult neurogenesis recapitulates embryonic processes that occurred during neurogenesis and thus resembles certain aspects of development. However, adult neurogenesis also has some unique, intrinsic mechanisms that cannot be extrapolated from earlier stages of development and these mechanisms considerably involved RBP-mediated processing. A recent study of the RBP HuR, which stabilizes or modulates the translation of numerous target proteins, reported that HuR specifically impairs adult

neurogenesis, whereas ablation in embryonic NSCs did not affect neurogenesis during development (Wang et al., 2019). Remarkably, the underlying cause was found to be the cellular translocation of HuR from the cytoplasm in the embryonic neural progenitors to the nucleus in adult NSCs, indicating that not only RBP expression, but already subcellular localization is sufficient to trigger RBP derived effects on neurogenesis (Wang et al., 2019).

miRNAs and neurogenesis

miRNAs are small non-coding RNA molecules that post-transcriptionally regulate gene expression via destabilization, inhibition of translation, deadenylation, and subcellular transport of target mRNAs (Eulalio et al., 2008). Like proteins, miRNA can be categorized into families based on sequence conservation of their HPs (Griffiths-Jones, 2006; Kaczkowski et al., 2008).They are mainly transcribed by the RNA pol II, which gives them also the pol II characteristic cap structures and poly(A) tails (Lee et al., 2004). After initial processing by the microprocessor and subsequent maturation by Dicer complexes in the cytoplasm, the mature miRNA is bound by the RNA-induced silencing complex (RISC) which processes the miRNA target mRNA, thus silencing the transcription product (Gregory et al., 2005) (Figure 2).

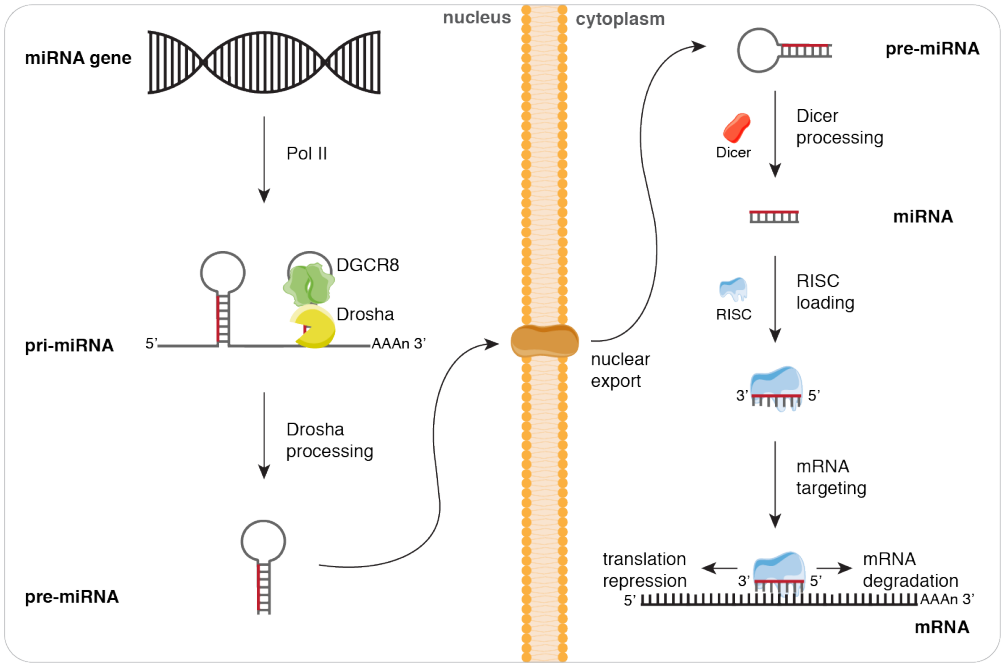

Figure 2: miRNA biogenesis pathway

Nucleus: pri-miRNA is transcribed by the RNA polymerase II (Pol II) and the hairpin loop structure gets targeted and cleaved by Drosha as part of the microprocessor. The pre-miRNA then is exported. Cytoplasm: After Dicer cleaves the loop structure, the miRNA negative strand is loaded on the RNA-induced silencing complex (RISC) and induces target mRNA degradation or translational repression.

Attempts to better understand the miRNA targeting efficacy lead to the development of a biochemical model of miRNA-mediated repression. This model is applicable to all miRNA sequence thanks to an *in silico* convolutional neural network, which substantially improved predictions of cellular repression (McGeary et al., 2019). Such computer-assisted tools will help us in the future to understand the regulatory roles of miRNA better. Of particular interest regarding the regulation of neurogenesis is the role of miRNAs in NSCs, especially in their maintenance and regulation of proliferation. Pioneering work in the *Drosophila* germline demonstrated for the first time that miRNAs actively regulate the division of stem cells (Hatfield et al., 2005). It is now accepted that stem cells of the *Drosophila* germline and their niche are not only rigorously controlled by miRNA in

order to regulate stem cell behavior upon stress, but also coordinate stem cell proliferation and differentiation (Shcherbata, 2019). Strict restrictions on proliferation are crucial, especially in complex organs including the vertebrate brain where uncontrolled stem cell division can lead to cancers. Downregulation of miRNA networks in mouse were shown to induce glioblastoma, the most aggressive forms of brain tumors, via downstream regulation of Oct4 and Sox2 (Lopez-Bertoni et al., 2015). The repression of miR-148a and miR-296-5p in particular was found to be required for the glioblastoma induction through this mechanism, the phenotype however could be rescued by miRNA overexpression. Based on the discovery of these cancer stem cell inhibiting miRNAs and thanks to state-of-the-art intracellular delivery techniques in nanomedicine, a miRNA based treatment design, so-called nano-miRs, were found to successfully treat gliomas in mice (Lopez-Bertoni et al., 2018). As we understand the implications of miRNA in disease better, miRNA-based treatments might reform modern medical approaches and offer an alternative to the classical drug based system.

The influence of miRNA on both embryonic and adult neurogenesis is undisputed, ranging from NSC self-renewal and proliferation, neural differentiation, migration, maturation and integration into neuronal circuits (Esteves et al., 2020). How the transition of NSCs between quiescent and active states is still not completely understood. It has become evident that Notch signaling is a key factor to maintain NSC quiescence in the SVZ as well as in the hippocampal DG (Ehm et al., 2010; Engler et al., 2018; Giachino and Taylor, 2014; Lugert et al., 2010; Zhang et al., 2019). Moreover, the miRNA miR-9 has been demonstrated to balance quiescent and proliferative NSC states through permitting efficient Notch signaling (Katz et al., 2016). This adds miR-9 to a larger group of several miRNAs that are essential to regulate NSC quiescence and activity. The miR-9 forms a complex with the Argonaute proteins, which is localized to the nucleus of NSCs mediated by TNRC6 proteins. Once in the nucleus, it is

promoting quiescence via Notch signaling activation, thus maintaining adult germinal pools (Katz et al., 2016). Similar behaviors have been seen for other genes including Hmga2, targeted by miRNA let-7 (Nishino et al., 2008) and Foxo3, targeted by the miRNA cluster miR-106b~25 (Brett et al., 2011). These are further examples of effectors, whose mRNA is targeted and controlled by miRNA which underlines the major contribution of miRNA towards NSC self-renewal and quiescence control. miRNAs also affect the neuronal progeny of the adult NSC and have been reported to assist migration of newborn neurons to their final homing site as well as modulating neuronal morpho- and synaptogenesis (Stappert et al., 2018). The miRNA miR-19 is highly expressed by adult neural progenitors and governs the migration of the newborn neurons while its expression steadily decreased during neural development in the adult hippocampus (Han et al., 2016). Gain- and loss-of-function experiments revealed that miR-19 directly targets Rapgef2 mRNA and moreover, in patient-derived iPSCs generated neurons that showed aberrant neuronal migration phenotypes, miR-19 is abnormally expressed hinting at potential links between miR-19 and neurodegenerative defects and schizophrenia (Han et al., 2016). In addition, the long-term impacts of miRNA impairment on cognitive function, particular the miRNA miR-17-92 cluster, resulted in defects in learning and memory (Pan et al., 2019). Strikingly, the miR-17-92 cluster knockout mouse performed significantly worse in a Morris water-maze assay compared to control mice and performed badly in other tests for novel odor and object recognition. One phenotype that was observed was a drastic reduction in the number of proliferating NSCs, neuroblast and neural differentiation in the DG compared to wild-type animals (Pan et al., 2019). These results indicate that miRNAs influence neuronal differentiation and even have long-term effects in cognitive, social and behavioral functions in mice.

Microprocessor and its diverse functions

During miRNA biogenesis, the conversion of pri-miRNA to pre-miRNA transcripts requires the precise cleavage and processing by the microprocessor, a trimeric complex that consist of Drosha and two DGCR8 proteins (Han et al., 2004; Nguyen et al., 2015). During pri-miRNA to pre-miR processing, the RNAse III Drosha cleaves the hairpin loop structure of the pri-miRNA at distinct locations in the hairpin stem, and serves as a molecular ruler to measure precisely 11 bp from the basal junction (Kim et al., 2017; Nguyen et al., 2015) (Figure 2). Deep-sequencing-based complementation and structural modeling revealed that Drosha with its double-stranded RNA-binding domain (dsRBD), recognizes an evolutionary conserved mGHG motif to place its catalytic center in the correct position for appropriate cleavage (Kwon et al., 2019). However, it is known that Drosha can also alternatively process some miRNAs and the resulting multiple miRNA variants are still recognized and processed by Dicer (Wu et al., 2009). The number of identified miRNA variants, called isomiRs, has drastically increased over the last couple of years as the results of improved RNA-seq based methods that allow for larger and more specific assays (Kim et al., 2019). This underlines the importance to understand all aspects of Drosha-mediated RNA processing in order to increase the efficiency of shRNA approaches in biological experiments and medical applications.

Although properly folded Drosha can act by itself as a functional core of the microprocessor albeit with low efficiency, only the combination with a DGCR8 dimer enables the exceptional fidelity of miRNA processing by the additional interaction of DGCR8 with the apical elements of the cleaved miRNA hairpin (Nguyen et al., 2015). DGCR8 recognizes an apical UGU motif and DGCR8 dimerization suppresses unproductive miRNA processing (Nguyen et al., 2015). The close interdependence between Drosha and DGCR8 is also reflected in their cross regulatory behavior. Both proteins regulate each other post-transcriptionally allowing them to

directly influence the expression of their corresponding microprocessor counterpart (Han et al., 2009).

The impact of the microprocessor itself on adult neurogenesis is more through Drosha and DGCR8 non-canonical functions. That makes the performance of the microprocessor towards neurogenic regulation, although indispensable, rather indirect, occurring via cleavage of miRNA or non-canonical RNA functions that then affect neurogenesis. It is not surprising, that a knockout of the ubiquitously expressed Drosha and the consequent impairment of the microprocessor causes obstruction of many cellular pathways, disturbing several molecular mechanisms including neurogenesis and leads to lethality by embryonic day 7.5 (E7.5) (Chong et al., 2010). It remains to be shown whether Drosha or DGCR8 proteins are able to directly bind adult neurogenesis regulating proteins as Drosha has been found to perform functions that are entirely independent of RNA (Gromak et al., 2013) and the large Drosha complex contains dozens of cell type-specific proteins with different cellular functions (Macias et al., 2015; Rouillard et al., 2016).

Non-canonical microprocessor functions as a miRNA-independent fate regulator

There are now several reports of Drosha and DGCR8 activity outside their classical mode of action in processing miRNAs (Burger and Gullerova, 2015; Johanson et al., 2013; Lee and Shin, 2017). The first solid evidence for a direct mRNA target of the microprocessor was the regulation of the mRNA of DGCR8 itself (Han et al., 2009; Kadener et al., 2009; Triboulet et al., 2009). Excess Drosha inhibits DGCR8 primary transcripts which causes a reduction in DGCR8 mRNA levels and thus protein synthesis, suggesting a negative feedback loop as auto-regulatory mechanism to control microprocessor expression levels (Han et al., 2009; Kadener et al., 2009). Drosha targets and processes the evolutionary conserved hairpins

in the 5' UTR of the DGCR8 transcripts resulting in mRNA destabilization and block of protein expression (Han et al., 2009; Triboulet et al., 2009). A more recent study revealed that Drosha not only controls DGCR8 expression but targets its own mRNA in order to modulate alternative splicing (Lee et al., 2017). A mechanistic analysis demonstrated that Drosha recognizes a hairpin that is conserved among species and spans a specific exon-intron junction. Strikingly, Drosha promotes constitutive or alternative intron splicing independent of its cleavage function, however, this behavior was only observed in human but not in mouse cells (Lee et al., 2017). The idea that Drosha competes with the spliceosome over exon-intron junctions was already proposed previously (Melamed et al., 2013). Gain and loss of function experiments of Drosha demonstrated that the miR-412, which is located at an exon-intron junction in the *Mirg* cluster, was spliced alternatively in high versus low expression levels of Drosha. The lower Drosha was expressed, the more spliceosome binding and exon inclusion was observed (Melamed et al., 2013). Thanks to modern approaches including genome wide mapping of Drosha cleavage sites, there is now a much better understanding of the Drosha targets and multiple new non-miRNA substrates have been identified (Kim et al., 2017). Applying a formaldehyde crosslinking, immunoprecipitation and sequencing (fCLIP-seq) approach allowed a precise nucleotide mapping of the target sites, which not only led to the discovery of more alternatively processed pri-miRNAs but also to the identification of new Drosha substrates. These substrates were not affected by Dicer knockout and three of these hairpins were validated to be indeed processed by Drosha (Kim et al., 2017). Drosha non-canonical activity has been found in many cell types (Burger and Gullerova, 2015; Lee and Shin, 2017; Rolando and Taylor, 2017). A particular example is Drosha's critical role in dendritic cells. Drosha deficiency completely interrupts dendritic cell development and manipulated myelopoiesis (Johanson et al., 2015). Drosha represses the expression of two mRNAs that encode inhibitors of myelopoiesis by directly cleaving hairpin structures within these mRNAs. The destabilized

mRNA is subject to degradation, and this process is needed for myelopoiesis (Johanson et al., 2015). Altogether, these examples demonstrate the various aspects of Drosha outside of its well-known function in miRNA processing. But not only Drosha, also its microprocessor partner DGCR8 is known to perform additional non-canonical tasks. For example, DGCR8 was found to form an alternative complex with the exosome, where it acts as an adaptor to target structured RNAs (Macias et al., 2015). DGCR8 binds the endosomal hRRP6 and that DGCRR8-exosome complex then controls the stability of the telomerase RNA component (hTR/TERC) in humans. Moreover, DGCR8 was proven to be essential for the recruitment of the exosome to snoRNAs and to human telomerase RNA (Macias et al., 2015). More recently, DGCR8 was reported to maintain the organization of heterochromatin and to attenuate aging in an non-canonical process (Deng et al., 2019). Accelerated senescence in human mesenchymal stem cells was observed to be increased by the expression of an N-terminal truncated DGCR8 variant, which was linked to heterochromatin maintenance by DGCR8. Moreover, also in both naturally and pathologically aged cells, DGCR8 was found to be expressed at low levels (Deng et al., 2019). A more specific role for DGCR8 in neurogenesis was found as non-canonical DGCR8 functions were essential for maintenance of neural progenitors during embryonic neurogenesis and carcinogenesis (Marinaro et al., 2017). Conditional deletion of DGCR8, but not Dicer, leads to premature differentiation of neural progenitor cells accompanied with $TBR1^{+}$ neuron overproduction. Interestingly, it was also found that the whole microprocessor, including Drosha, directly regulates the Tbr1 transcript by targeting evolutionary conserved hairpins in a miRNA-independent manner (Marinaro et al., 2017).

The role of Drosha in neurogenesis was the first *in vivo* evidence for non-canonical functions of components of the microprocessor (Knuckles et al., 2012) . Our lab has shown that Drosha regulates NSC maintenance and

differentiation of NSCs in the developing and adult brain (Knuckles et al., 2012) and in the hippocampal DG of the adult mouse (Rolando et al., 2016). However, as Dicer depletion could not reproduce these phenotypes it became evident that Drosha acts in miRNA-independent pathways in the central nervous system. In both the embryonic and the adult case, Drosha binds and cleaves evolutionary conserved hairpins in the mRNA of transcription factors driving NSC differentiation. Conditional genetics demonstrated that Drosha and DGCR8 have important functions in embryonic neurogenesis and lead to a loss in stem cell-ness and precocious differentiation (Knuckles et al., 2012). In the embryonic system, Drosha negatively regulates the expression of Neurogenin2 and NeuroD1 mRNAs (Knuckles et al., 2012) whereas in the adult hippocampal DG NSCs, Drosha targets and cleaves the hairpins of the mRNA of Nuclear Factor I/B (NFIB) (Rolando et al., 2016) (Figure 3).

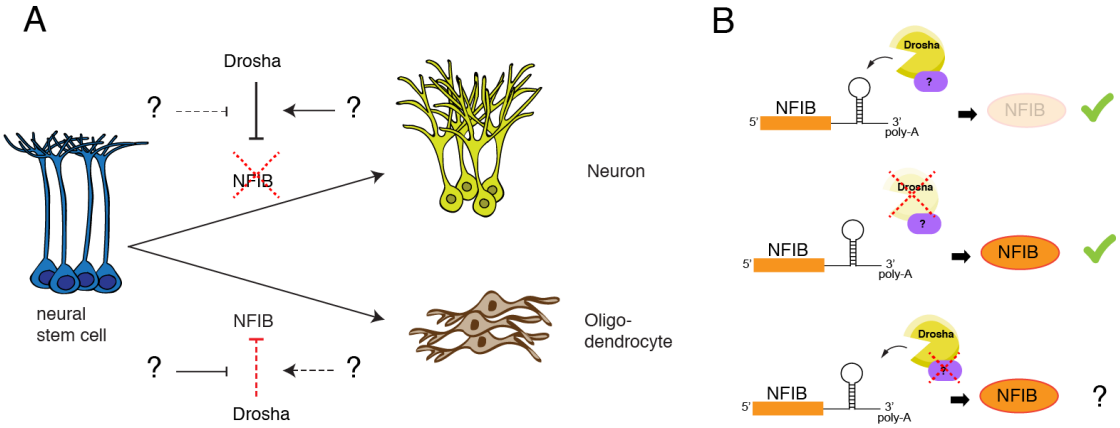

Figure 3: Drosha-mediated cleavage of the mRNA of NFIB regulates NSC fate

A) NSCs can adapt neuronal and oligodendrocytic fate. Drosha post-transcriptionally downregulates NFIB, which in turn drives oligodendrogenesis. Cellular expression of activating or inhibitory factors of Drosha might allow cell fate specific expression of NFIB. B) Detailed view of Drosha/NFIB interaction. Drosha recognizes and cleaves the 3' UTR hairpin of NFIB mRNA and thus prevents protein expression. Drosha cKO allows NFIB expression, however the absence of a regulating RBP might have the same effect.

NFIB drives NSCs into an oligodendrocytic cell fate and is required and sufficient for oligodendrogenesis by activating a differentiation program that includes Sox10 and NG2 (Deneen et al., 2006; Rolando et al., 2016). Inactivation of Drosha in DG NSCs leads to stabilization of NFIB mRNA transcripts and disinhibition of NFIB expression leading to exhaustion of the NSC pool, oligodendrocyte fate commitment, and premature arrest of neurogenesis (Figure 3B) . Knockdown of NFIB in Drosha-deficient DG NSCs rescues these defects indicating that the non-canonical role of Drosha on NFIB expression is a primary fate regulation in the adult hippocampus (Rolando et al., 2016). These findings demonstrate the involvement of Drosha in adult neurogenesis in an miRNA-independent fashion. However, as Drosha is ubiquitously expressed in the brain, the question arises how mRNAs in NSCs can escape Drosha cleavage to be expressed when needed by the cell.

Moreover, the regulatory mechanisms must ensure hairpin target specificity to avoid off-target cleavage of the several known Drosha mRNA targets. The most plausible explanation is that additional, modulatory proteins, either activate or inhibit Drosha activity on particular target transcripts. Different expression levels of a regulator would allow cell lineage and type-specific control of Drosha non-canonical activity, while canonical functions in miRNA biogenesis would still be maintained in these cells. These Drosha regulators are likely to be RBPs and able to bind the RNA themselves in a sequence-specific manner to provide the necessary target specificity. Unfortunately, none of these Drosha regulators have yet been identified, although their existence seems inevitable. Further, the role and requirement of DGCR8 during non-canonical Drosha cleavage remains debated and may differ from one mRNA target to the next. As Drosha is suspected to have more non-canonical mRNA targets and is likely to bind proteins that assist cleavage of potential targets, it is likely that there are more, currently unknown mechanisms of how Drosha might regulate embryonic as well as adult neurogenesis by targeting hairpins in crucial mRNA transcription factors.

Conclusion and future perspective

We have discussed how post-transcriptional regulation contributes to neurogenesis. The given mechanisms serve as examples to underline the close connectivity and interplay between different modes of post-transcriptional regulation, for example the microprocessor that influences adult neurogenesis via miRNA but also direct regulation of mRNA stability. There are many excellent up-to-date reviews about general mechanisms of post-transcriptional regulation and non-canonical functions of the microprocessor (Gebert and MacRae, 2018; Kilchert et al., 2019; Lee and Shin, 2017), however only few focus on adult neurogenesis (Esteves et al., 2020; Rolando and Taylor, 2017). In this review, we have discussed the rapidly growing technological discoveries in RNA binding motif recognition and RNA binding domains. This might be the driving factor for future RBP research, as the discovery of new RBPs will raise follow up questions about their functionality and relevance. Also the multiple roles of proteins and miRNA for different targets will need to be further addressed in order to unravel the full, non-canonical potential of the post-transcriptional machinery. This knowledge needs to be connected with the new findings in adult neurogenesis and only a combination of the two fields will lead to the full understanding of the whole picture.

References

Alvarez-Buylla, A., and Lim, D.A. (2004). For the long run: maintaining germinal niches in the adult brain. Neuron *41*, 683-686.
Arellano, J.I., Harding, B., and Thomas, J.L. (2018). Adult Human Hippocampus: No New Neurons in Sight. Cereb Cortex *28*, 2479-2481.
Basak, O., Giachino, C., Fiorini, E., Macdonald, H.R., and Taylor, V. (2012). Neurogenic subventricular zone stem/progenitor cells are Notch1-dependent in their active but not quiescent state. J Neurosci *32*, 5654-5666.
Benhalevy, D., Anastasakis, D.G., and Hafner, M. (2018). Proximity-CLIP provides a snapshot of protein-occupied RNA elements in subcellular compartments. Nat Methods *15*, 1074-1082.

Benoit Bouvrette, L.P., Bovaird, S., Blanchette, M., and Lecuyer, E. (2020). oRNAment: a database of putative RNA binding protein target sites in the transcriptomes of model species. Nucleic Acids Res *48*, D166-D173.
Boldrini, M., Fulmore, C.A., Tartt, A.N., Simeon, L.R., Pavlova, I., Poposka, V., Rosoklija, G.B., Stankov, A., Arango, V., Dwork, A.J.*, et al.* (2018). Human Hippocampal Neurogenesis Persists throughout Aging. Cell Stem Cell *22*, 589-599 e585.
Bonaguidi, M.A., Wheeler, M.A., Shapiro, J.S., Stadel, R.P., Sun, G.J., Ming, G.L., and Song, H. (2011). In vivo clonal analysis reveals self-renewing and multipotent adult neural stem cell characteristics. Cell *145*, 1142-1155.
Brett, J.O., Renault, V.M., Rafalski, V.A., Webb, A.E., and Brunet, A. (2011). The microRNA cluster miR-106b~25 regulates adult neural stem/progenitor cell proliferation and neuronal differentiation. Aging (Albany NY) *3*, 108-124.
Burger, K., and Gullerova, M. (2015). Swiss army knives: non-canonical functions of nuclear Drosha and Dicer. Nature reviews. Molecular cell biology *16*, 417-430.
Chong, M.M., Zhang, G., Cheloufi, S., Neubert, T.A., Hannon, G.J., and Littman, D.R. (2010). Canonical and alternate functions of the microRNA biogenesis machinery. Genes Dev *24*, 1951-1960.
Deneen, B., Ho, R., Lukaszewicz, A., Hochstim, C.J., Gronostajski, R.M., and Anderson, D.J. (2006). The transcription factor NFIA controls the onset of gliogenesis in the developing spinal cord. Neuron *52*, 953-968.
Deng, L., Ren, R., Liu, Z., Song, M., Li, J., Wu, Z., Ren, X., Fu, L., Li, W., Zhang, W.*, et al.* (2019). Stabilizing heterochromatin by DGCR8 alleviates senescence and osteoarthritis. Nat Commun *10*, 3329.
Doetsch, F., Caillé, I., Lim, D.A., García-Verdugo, J.M., and Alvarez-Buylla, A. (1999). Subventricular Zone Astrocytes Are Neural Stem Cells in the Adult Mammalian Brain. Cell *97*, 703-716.
Ehm, O., Goritz, C., Covic, M., Schaffner, I., Schwarz, T.J., Karaca, E., Kempkes, B., Kremmer, E., Pfrieger, F.W., Espinosa, L.*, et al.* (2010). RBPJkappa-dependent signaling is essential for long-term maintenance of neural stem cells in the adult hippocampus. J Neurosci *30*, 13794-13807.
Engler, A., Rolando, C., Giachino, C., Saotome, I., Erni, A., Brien, C., Zhang, R., Zimber-Strobl, U., Radtke, F., Artavanis-Tsakonas, S.*, et al.* (2018). Notch2 Signaling Maintains NSC Quiescence in the Murine Ventricular-Subventricular Zone. Cell Rep *22*, 992-1002.
Eriksson, P.S., Perfilieva, E., Bjork-Eriksson, T., Alborn, A.M., Nordborg, C., Peterson, D.A., and Gage, F.H. (1998). Neurogenesis in the adult human hippocampus. Nat Med *4*, 1313-1317.
Esteves, M., Serra-Almeida, C., Saraiva, C., and Bernardino, L. (2020). New insights into the regulatory roles of microRNAs in adult neurogenesis. Current Opinion in Pharmacology *50*, 38-45.
Eulalio, A., Huntzinger, E., and Izaurralde, E. (2008). Getting to the Root of miRNA-Mediated Gene Silencing. Cell *132*, 9-14.

Furutachi, S., Miya, H., Watanabe, T., Kawai, H., Yamasaki, N., Harada, Y., Imayoshi, I., Nelson, M., Nakayama, K.I., Hirabayashi, Y.*, et al.* (2015). Slowly dividing neural progenitors are an embryonic origin of adult neural stem cells. Nature Neuroscience *18*, 657-665.
Gage, F.H. (2019). Adult neurogenesis in mammals. Science *364*, 827-828.
Gebert, L.F.R., and MacRae, I.J. (2018). Regulation of microRNA function in animals. Nature Reviews Molecular Cell Biology *20*, 21-37.
Giachino, C., and Taylor, V. (2014). Notching up neural stem cell homogeneity in homeostasis and disease. Front Neurosci *8*, 32.
Goncalves, J.T., Schafer, S.T., and Gage, F.H. (2016). Adult Neurogenesis in the Hippocampus: From Stem Cells to Behavior. Cell *167*, 897-914.
Gregory, R.I., Chendrimada, T.P., Cooch, N., and Shiekhattar, R. (2005). Human RISC couples microRNA biogenesis and posttranscriptional gene silencing. Cell *123*, 631-640.
Griffiths-Jones, S. (2006). miRBase: microRNA sequences, targets and gene nomenclature. Nucleic Acids Research *34*, D140-D144.
Gromak, N., Dienstbier, M., Macias, S., Plass, M., Eyras, E., Caceres, J.F., and Proudfoot, N.J. (2013). Drosha regulates gene expression independently of RNA cleavage function. Cell Reports *5*, 1499-1510.
Hafner, M., Landthaler, M., Burger, L., Khorshid, M., Hausser, J., Berninger, P., Rothballer, A., Ascano, M., Jr., Jungkamp, A.C., Munschauer, M.*, et al.* (2010). Transcriptome-wide identification of RNA-binding protein and microRNA target sites by PAR-CLIP. Cell *141*, 129-141.
Hagerman, P.J., and Hagerman, R.J. (2015). Fragile X-associated tremor/ataxia syndrome. Annals of the New York Academy of Sciences *1338*, 58-70.
Han, J., Kim, H.J., Schafer, S.T., Paquola, A., Clemenson, G.D., Toda, T., Oh, J., Pankonin, A.R., Lee, B.S., Johnston, S.T.*, et al.* (2016). Functional Implications of miR-19 in the Migration of Newborn Neurons in the Adult Brain. Neuron *91*, 79-89.
Han, J., Lee, Y., Yeom, K.H., Kim, Y.K., Jin, H., and Kim, V.N. (2004). The Drosha-DGCR8 complex in primary microRNA processing. Genes Dev *18*, 3016-3027.
Han, J., Pedersen, J.S., Kwon, S.C., Belair, C.D., Kim, Y.K., Yeom, K.H., Yang, W.Y., Haussler, D., Blelloch, R., and Kim, V.N. (2009). Posttranscriptional crossregulation between Drosha and DGCR8. Cell *136*, 75-84.
Hatfield, S.D., Shcherbata, H.R., Fischer, K.A., Nakahara, K., Carthew, R.W., and Ruohola-Baker, H. (2005). Stem cell division is regulated by the microRNA pathway. Nature *435*, 974-978.
Hocq, R., Paternina, J., Alasseur, Q., Genovesio, A., and Le Hir, H. (2018). Monitored eCLIP: high accuracy mapping of RNA-protein interactions. Nucleic Acids Res *46*, 11553-11565.

Ihrie, R.A., and Alvarez-Buylla, A. (2011). Lake-front property: a unique germinal niche by the lateral ventricles of the adult brain. Neuron *70*, 674-686.
Imig, J., Brunschweiger, A., Brummer, A., Guennewig, B., Mittal, N., Kishore, S., Tsikrika, P., Gerber, A.P., Zavolan, M., and Hall, J. (2015). miR-CLIP capture of a miRNA targetome uncovers a lincRNA H19-miR-106a interaction. Nat Chem Biol *11*, 107-114.
Johanson, T.M., Keown, A.A., Cmero, M., Yeo, J.H.C., Kumar, A., Lew, A.M., Zhan, Y., and Chong, M.M.W. (2015). Drosha controls dendritic cell development by cleaving messenger RNAs encoding inhibitors of myelopoiesis. Nature immunology *16*, 1134-1141.
Johanson, T.M., Lew, A.M., and Chong, M.M.W. (2013). MicroRNA-independent roles of the RNase III enzymes Drosha and Dicer. Open Biology *3*, 130144-130144.
Kaczkowski, B., Torarinsson, E., Reiche, K., Havgaard, J.H., Stadler, P.F., and Gorodkin, J. (2008). Structural profiles of human miRNA families from pairwise clustering. Bioinformatics *25*, 291-294.
Kaczynski, T., Hussain, A., and Farkas, M. (2019). Quick-irCLIP: Interrogating protein-RNA interactions using a rapid and simple cross-linking and immunoprecipitation technique. MethodsX *6*, 1292-1304.
Kadener, S., Rodriguez, J., Abruzzi, K.C., Khodor, Y.L., Sugino, K., Marr, M.T., 2nd, Nelson, S., and Rosbash, M. (2009). Genome-wide identification of targets of the drosha-pasha/DGCR8 complex. RNA *15*, 537-545.
Kargapolova, Y., Levin, M., Lackner, K., and Danckwardt, S. (2017). sCLIP-an integrated platform to study RNA-protein interactomes in biomedical research: identification of CSTF2tau in alternative processing of small nuclear RNAs. Nucleic Acids Res *45*, 6074-6086.
Katz, S., Cussigh, D., Urbán, N., Blomfield, I., Guillemot, F., Bally-Cuif, L., and Coolen, M. (2016). A Nuclear Role for miR-9 and Argonaute Proteins in Balancing Quiescent and Activated Neural Stem Cell States. Cell Reports *17*, 1383-1398.
Kempermann, G., Gage, F.H., Aigner, L., Song, H., Curtis, M.A., Thuret, S., Kuhn, H.G., Jessberger, S., Frankland, P.W., Cameron, H.A.*, et al.* (2018). Human Adult Neurogenesis: Evidence and Remaining Questions. Cell Stem Cell *23*, 25-30.
Kilchert, C., Strasser, K., Kunetsky, V., and Anko, M.L. (2019). From parts lists to functional significance-RNA-protein interactions in gene regulation. Wiley Interdiscip Rev RNA, e1582.
Kim, B., Jeong, K., and Kim, V.N. (2017). Genome-wide Mapping of DROSHA Cleavage Sites on Primary MicroRNAs and Noncanonical Substrates. Mol Cell *66*, 258-269 e255.
Kim, H., Kim, J., Kim, K., Chang, H., You, K., and Kim, V.N. (2019). Bias-minimized quantification of microRNA reveals widespread alternative processing and 3' end modification. Nucleic Acids Res *47*, 2630-2640.
Knuckles, P., Vogt, M.A., Lugert, S., Milo, M., Chong, M.M., Hautbergue, G.M., Wilson, S.A., Littman, D.R., and Taylor, V. (2012). Drosha regulates

neurogenesis by controlling neurogenin 2 expression independent of microRNAs. Nat Neurosci *15*, 962-969.
König, J., Zarnack, K., Rot, G., Curk, T., Kayikci, M., Zupan, B., Turner, D.J., Luscombe, N.M., and Ule, J. (2010). iCLIP reveals the function of hnRNP particles in splicing at individual nucleotide resolution. Nat Struct Mol Biol *17*, 909-915.
Kwon, S.C., Baek, S.C., Choi, Y.G., Yang, J., Lee, Y.S., Woo, J.S., and Kim, V.N. (2019). Molecular Basis for the Single-Nucleotide Precision of Primary microRNA Processing. Mol Cell *73*, 505-518 e505.
Lazarov, O., Demars, M.P., Da Tommy Zhao, K., Ali, H.M., Grauzas, V., Kney, A., and Larson, J. (2012). Impaired survival of neural progenitor cells in dentate gyrus of adult mice lacking FMRP. Hippocampus *22*, 1220-1224.
Lee, D., Nam, J.W., and Shin, C. (2017). DROSHA targets its own transcript to modulate alternative splicing. RNA *23*, 1035-1047.
Lee, D., and Shin, C. (2017). Emerging roles of DROSHA beyond primary microRNA processing. RNA Biol, 1-8.
Lee, F.C.Y., and Ule, J. (2018). Advances in CLIP Technologies for Studies of Protein-RNA Interactions. Mol Cell *69*, 354-369.
Lee, Y., Kim, M., Han, J., Yeom, K.H., Lee, S., Baek, S.H., and Kim, V.N. (2004). MicroRNA genes are transcribed by RNA polymerase II. EMBO J *23*, 4051-4060.
Letunic, I., and Bork, P. (2018). 20 years of the SMART protein domain annotation resource. Nucleic Acids Res *46*, D493-D496.
Liao, J.Y., Yang, B., Zhang, Y.C., Wang, X.J., Ye, Y., Peng, J.W., Yang, Z.Z., He, J.H., Zhang, Y., Hu, K.*, et al.* (2020). EuRBPDB: a comprehensive resource for annotation, functional and oncological investigation of eukaryotic RNA binding proteins (RBPs). Nucleic Acids Res *48*, D307-D313.
Licatalosi, D.D., Mele, A., Fak, J.J., Ule, J., Kayikci, M., Chi, S.W., Clark, T.A., Schweitzer, A.C., Blume, J.E., Wang, X.*, et al.* (2008). HITS-CLIP yields genome-wide insights into brain alternative RNA processing. Nature *456*, 464-469.
Lledo, P.-M., Alonso, M., and Grubb, M.S. (2006). Adult neurogenesis and functional plasticity in neuronal circuits. Nature Reviews Neuroscience *7*, 179-193.
Lopez-Bertoni, H., Kozielski, K.L., Rui, Y., Lal, B., Vaughan, H., Wilson, D.R., Mihelson, N., Eberhart, C.G., Laterra, J., and Green, J.J. (2018). Bioreducible Polymeric Nanoparticles Containing Multiplexed Cancer Stem Cell Regulating miRNAs Inhibit Glioblastoma Growth and Prolong Survival. Nano Letters *18*, 4086-4094.
Lopez-Bertoni, H., Lal, B., Li, A., Caplan, M., Guerrero-Cazares, H., Eberhart, C.G., Quinones-Hinojosa, A., Glas, M., Scheffler, B., Laterra, J.*, et al.* (2015). DNMT-dependent suppression of microRNA regulates the induction of GBM tumor-propagating phenotype by Oct4 and Sox2. Oncogene *34*, 3994-4004.
Lugert, S., Basak, O., Knuckles, P., Haussler, U., Fabel, K., Gotz, M., Haas, C.A., Kempermann, G., Taylor, V., and Giachino, C. (2010).

Quiescent and active hippocampal neural stem cells with distinct morphologies respond selectively to physiological and pathological stimuli and aging. Cell Stem Cell *6*, 445-456.
Lugert, S., Vogt, M., Tchorz, J.S., Muller, M., Giachino, C., and Taylor, V. (2012). Homeostatic neurogenesis in the adult hippocampus does not involve amplification of Ascl1(high) intermediate progenitors. Nat Commun *3*, 670.
Lukong, K.E., Chang, K.W., Khandjian, E.W., and Richard, S. (2008). RNA-binding proteins in human genetic disease. Trends Genet *24*, 416-425.
Lunde, B.M., Moore, C., and Varani, G. (2007). RNA-binding proteins: modular design for efficient function. Nat Rev Mol Cell Biol *8*, 479-490.
Luo, Y., Shan, G., Guo, W., Smrt, R.D., Johnson, E.B., Li, X., Pfeiffer, R.L., Szulwach, K.E., Duan, R., Barkho, B.Z.*, et al.* (2010). Fragile x mental retardation protein regulates proliferation and differentiation of adult neural stem/progenitor cells. PLoS Genet *6*, e1000898.
Macias, S., Cordiner, Ross A., Gautier, P., Plass, M., and Cáceres, Javier F. (2015). DGCR8 Acts as an Adaptor for the Exosome Complex to Degrade Double-Stranded Structured RNAs. Molecular Cell *60*, 873-885.
Mackenzie, I.R.A., Rademakers, R., and Neumann, M. (2010). TDP-43 and FUS in amyotrophic lateral sclerosis and frontotemporal dementia. The Lancet Neurology *9*, 995-1007.
Marinaro, F., Marzi, M.J., Hoffmann, N., Amin, H., Pelizzoli, R., Niola, F., Nicassio, F., and De Pietri Tonelli, D. (2017). MicroRNA-independent functions of DGCR8 are essential for neocortical development and TBR1 expression. EMBO Rep *18*, 603-618.
McGeary, S.E., Lin, K.S., Shi, C.Y., Pham, T.M., Bisaria, N., Kelley, G.M., and Bartel, D.P. (2019). The biochemical basis of microRNA targeting efficacy. Science *366*.
Melamed, Z.e., Levy, A., Ashwal-Fluss, R., Lev-Maor, G., Mekahel, K., Atias, N., Gilad, S., Sharan, R., Levy, C., Kadener, S.*, et al.* (2013). Alternative Splicing Regulates Biogenesis of miRNAs Located across Exon-Intron Junctions. Molecular Cell *50*, 869-881.
Mira, H., Andreu, Z., Suh, H., Lie, D.C., Jessberger, S., Consiglio, A., San Emeterio, J., Hortigüela, R., Marqués-Torrejón, M.Á., Nakashima, K.*, et al.* (2010). Signaling through BMPR-IA Regulates Quiescence and Long-Term Activity of Neural Stem Cells in the Adult Hippocampus. Cell Stem Cell *7*, 78-89.
Nguyen, T.A., Jo, M.H., Choi, Y.G., Park, J., Kwon, S.C., Hohng, S., Kim, V.N., and Woo, J.S. (2015). Functional Anatomy of the Human Microprocessor. Cell *161*, 1374-1387.
Nishino, J., Kim, I., Chada, K., and Morrison, S.J. (2008). Hmga2 promotes neural stem cell self-renewal in young but not old mice by reducing p16Ink4a and p19Arf Expression. Cell *135*, 227-239.
Pan, W.L., Chopp, M., Fan, B., Zhang, R., Wang, X., Hu, J., Zhang, X.M., Zhang, Z.G., and Liu, X.S. (2019). Ablation of the microRNA-17-92 cluster in neural stem cells diminishes adult hippocampal neurogenesis and cognitive function. FASEB J *33*, 5257-5267.

Patzlaff, N.E., Shen, M., and Zhao, X. (2018). Regulation of Adult Neurogenesis by the Fragile X Family of RNA Binding Proteins. Brain Plast *3*, 205-223.
Pilz, G.A., Bottes, S., Betizeau, M., Jorg, D.J., Carta, S., Simons, B.D., Helmchen, F., and Jessberger, S. (2018). Live imaging of neurogenesis in the adult mouse hippocampus. Science *359*, 658-662.
Rolando, C., Erni, A., Grison, A., Beattie, R., Engler, A., Gokhale, P.J., Milo, M., Wegleiter, T., Jessberger, S., and Taylor, V. (2016). Multipotency of Adult Hippocampal NSCs In Vivo Is Restricted by Drosha/NFIB. Cell Stem Cell *19*, 653-662.
Rolando, C., and Taylor, V. (2017). Non-canonical post-transcriptional RNA regulation of neural stem cell potential. Brain Plast *3*, 111-116.
Romer-Seibert, J.S., Hartman, N.W., and Moss, E.G. (2019). The RNA-binding protein LIN28 controls progenitor and neuronal cell fate during postnatal neurogenesis. The FASEB Journal *33*, 3291-3303.
Rosenberg, M., Blum, R., Kesner, B., Maier, V.K., Szanto, A., and Lee, J.T. (2017). Denaturing CLIP, dCLIP, Pipeline Identifies Discrete RNA Footprints on Chromatin-Associated Proteins and Reveals that CBX7 Targets 3' UTRs to Regulate mRNA Expression. Cell Syst *5*, 368-385 e315.
Rouillard, A.D., Gundersen, G.W., Fernandez, N.F., Wang, Z., Monteiro, C.D., McDermott, M.G., and Ma'ayan, A. (2016). The harmonizome: a collection of processed datasets gathered to serve and mine knowledge about genes and proteins. Database (Oxford) *2016*.
Seri, B., Garcia-Verdugo, J.M., Collado-Morente, L., McEwen, B.S., and Alvarez-Buylla, A. (2004). Cell types, lineage, and architecture of the germinal zone in the adult dentate gyrus. J Comp Neurol *478*, 359-378.
Shcherbata, H.R. (2019). miRNA functions in stem cells and their niches: lessons from the Drosophila ovary. Curr Opin Insect Sci *31*, 29-36.
Sorrells, S.F., Paredes, M.F., Cebrian-Silla, A., Sandoval, K., Qi, D., Kelley, K.W., James, D., Mayer, S., Chang, J., Auguste, K.I.*, et al.* (2018). Human hippocampal neurogenesis drops sharply in children to undetectable levels in adults. Nature *555*, 377-381.
Stappert, L., Klaus, F., and Brüstle, O. (2018). MicroRNAs Engage in Complex Circuits Regulating Adult Neurogenesis. Frontiers in Neuroscience *12*.
Tobin, M.K., Musaraca, K., Disouky, A., Shetti, A., Bheri, A., Honer, W.G., Kim, N., Dawe, R.J., Bennett, D.A., Arfanakis, K.*, et al.* (2019). Human Hippocampal Neurogenesis Persists in Aged Adults and Alzheimer's Disease Patients. Cell Stem Cell *24*, 974-982 e973.
Trendel, J., Schwarzl, T., Horos, R., Prakash, A., Bateman, A., Hentze, M.W., and Krijgsveld, J. (2019). The Human RNA-Binding Proteome and Its Dynamics during Translational Arrest. Cell *176*, 391-403 e319.
Triboulet, R., Chang, H.M., Lapierre, R.J., and Gregory, R.I. (2009). Post-transcriptional control of DGCR8 expression by the Microprocessor. RNA *15*, 1005-1011.

Ule, J., Hwang, H.W., and Darnell, R.B. (2018). The Future of Cross-Linking and Immunoprecipitation (CLIP). Cold Spring Harb Perspect Biol *10*.
Ule, J., Jensen, K.B., Ruggiu, M., Mele, A., Ule, A., and Darnell, R.B. (2003). CLIP identifies Nova-regulated RNA networks in the brain. Science *302*, 1212-1215.
Van Nostrand, E.L., Pratt, G.A., Shishkin, A.A., Gelboin-Burkhart, C., Fang, M.Y., Sundararaman, B., Blue, S.M., Nguyen, T.B., Surka, C., Elkins, K.*, et al.* (2016). Robust transcriptome-wide discovery of RNA-binding protein binding sites with enhanced CLIP (eCLIP). Nat Methods *13*, 508-514.
Viswanathan, S.R., Daley, G.Q., and Gregory, R.I. (2008). Selective blockade of microRNA processing by Lin28. Science *320*, 97-100.
Wang, Y., Guo, Y., Tang, C., Han, X., Xu, M., Sun, J., Zhao, Y., Zhang, Y., Wang, M., Cao, X.*, et al.* (2019). Developmental Cytoplasmic-to-Nuclear Translocation of RNA-Binding Protein HuR Is Required for Adult Neurogenesis. Cell Reports *29*, 3101-3117.e3107.
Wu, H., Ye, C., Ramirez, D., and Manjunath, N. (2009). Alternative processing of primary microRNA transcripts by Drosha generates 5' end variation of mature microRNA. PLoS One *4*, e7566.
Zarnegar, B.J., Flynn, R.A., Shen, Y., Do, B.T., Chang, H.Y., and Khavari, P.A. (2016). irCLIP platform for efficient characterization of protein-RNA interactions. Nat Methods *13*, 489-492.
Zhang, R., Boareto, M., Engler, A., Louvi, A., Giachino, C., Iber, D., and Taylor, V. (2019). Id4 Downstream of Notch2 Maintains Neural Stem Cell Quiescence in the Adult Hippocampus. Cell Rep *28*, 1485-1498 e1486.
Zhao, C., Deng, W., and Gage, F.H. (2008). Mechanisms and functional implications of adult neurogenesis. Cell *132*, 645-660.
Zhao, Y., Zhang, Y., Teng, Y., Liu, K., Liu, Y., Li, W., and Wu, L. (2019). SpyCLIP: an easy-to-use and high-throughput compatible CLIP platform for the characterization of protein-RNA interactions with high accuracy. Nucleic Acids Res *47*, e33.

Questions and Aims

It has been known that Drosha targets and cleaves an evolutionary conserved hairpin in the 3' UTR of the mRNA of the transcription factor NFIB (Rolando et al., 2016). However, as Drosha is expressed in the entire brain at all times, it appears to be impossible that under the presence of Drosha any NFIB will be ever expressed. Yet, there are cells that express this important driver of oligodendrogenesis and become oligodendrocytes. Hence, there must be a regulatory mechanism that allows expression of NFIB in the cell, even if Drosha is expressed in parallel. In this study, we aim to solve this mystery and investigate, how cells can escape Drosha-mediated cleavage of NFIB. Another important aspect is to find out, how the hairpin targeting between the different mRNA targets can be specific and off-target cleavage is avoided. We postulate the hypothesis, that there must be RBPs, that specifically regulate Drosha cleavage of non-canonical mRNA targets.

Results

Paper title, authors & status

Analysis of Drosha interactome unravels Safb1 as novel regulator of neural stem cell fate;
Niklas Iffländer, Chiara Rolando, Elli-Anna Balta, Tanzila Mukhtar, Thomas Bock, Verdon Taylor;
submitted

Contribution

I planned, performed and analyzed all major experiments, prepared the manuscript and the figures. The FACS experiments were performed in collaboration with CR and the SVZ experiments with EAB.

Short summary

In this study we investigated the non-canonical function of Drosha to target and cleave the mRNA of the transcription factor NFIB. We asked how the widely active RNAse can specifically target this RNA transcript and how NFIB can be expressed despite the ubiquitously expressed Drosha. We identified Safb, a key regulator of Drosha-mediated cleavage of NFIB, and could show that Safb level changes via Drosha influence NFIB mRNA expression which affects NSC oligodendrogenesis.

Manuscript

Analysis of Drosha interactome unravels Safb1 as novel regulator of neural stem cell fate

Niklas Iffländer,[1,4] Chiara Rolando,[1,2,4] Elli-Anna Balta,[1] Tanzila Mukhtar,[1] Thomas Bock,[3] and Verdon Taylor[1,5,*]

[1]Department of Biomedicine, University of Basel, CH-4058 Basel, Switzerland

[2]Present address: Department of Biosciences, University of Milan, I-20133 Milan, Italy

[3]Proteomics Core Facility, Biozentrum, University of Basel, CH-4056 Basel, Switzerland

[4]These authors contributed equally

[5]Lead contact

*Correspondence to: verdon.taylor@unibas.ch

SUMMARY

The ribonuclease Drosha is an integral component of the microRNA biogenesis machinery but also regulates gene expression by targeted cleavage of specific mRNAs. Drosha regulates hippocampal neural stem cell (NSC) fate by cleaving mRNAs of the transcription factor NFIB, thereby enabling differentiation into neurons at the expense of oligodendrocytes. We addressed how mRNA destabilization is regulated by ubiquitously expressed Drosha, and identified 165 NSC proteins that interact with Drosha and 102 that bind the Drosha interacting regions on the NFIB mRNA. We show that one of these proteins, Scaffold Attachment Factor B1 (Safb1), modulates Drosha endonucleic activity and potentiates NFIB mRNA degradation. Safb1 reduces oligodendrocyte production and its expression is reduced in oligodendrogenic NSCs. Our results reveal specific regulations of Drosha activity on a target mRNA by a novel partner and RNA binding protein Safb1 which has important implications for cell-specific, post-transcriptional regulation of gene expression.

KEYWORDS: Drosha, Safb1, NFIB, adult neurogenesis, oligodendrogenesis, neural stem cells, fate regulation, mRNA hairpin, post-transcriptional gene regulation

INTRODUCTION

Neurogenesis is a fundamental biological process for brain development where neural stem cells (NSCs) generate new neurons. While heavily active at embryonic stages, in the postnatal vertebrate brain neurogenesis continues in restricted brain regions. The two niches that maintain adult NSCs are the subventricular zone (SVZ) of the lateral ventricles and the subgranular zone of the hippocampal dentate gyrus (DG) (Goncalves et al., 2016; Obernier and Alvarez-Buylla, 2019). DG NSCs predominantly generate glutamatergic granule neurons and to less extent astrocytes (Bonaguidi et al., 2011; Bonzano et al., 2018; Pilz et al., 2018; Seri et al., 2004). Adult hippocampal neurogenesis plays a central role in memory formation, plasticity and learning in rodents, but also in other species including humans (Berg et al., 2019; Boldrini et al., 2018; Eriksson et al., 1998; Gage, 2019; Moreno-Jimenez et al., 2019; Spalding et al., 2013). Although still controversially discussed (Beckervordersandforth and Rolando, 2019; Kempermann et al., 2018; Sorrells et al., 2018), recent studies suggest that hippocampal neurogenesis persists until late decades of life in humans (Boldrini et al., 2018; Tobin et al., 2019) and that it might be linked to neurodegenerative diseases, such as Alzheimer's Disease (Moreno-Jimenez et al., 2019; Tobin et al., 2019). In rodents, adult NSC regulation is fairly well understood on the molecular and physiological levels, however, the influence and importance of post-transcriptional regulation in adult neurogenesis is becoming clearer (Baser et al., 2019; Pilaz and Silver, 2015).

The RNase III Drosha is involved in different post-transcriptional regulatory mechanisms beyond its primary function in microRNA biogenesis (Chong et al., 2010; Lee and Shin, 2017; Rolando and Taylor, 2017). Drosha is a core component of the microRNA (miRNA) pathway and forms a trimeric complex with two DGCR8 proteins to generate the miRNA Microprocessor (Han et al., 2004; Nguyen et al., 2015). The main function of the Microprocessor is the processing of pri-miRNA hairpins (HPs), where Drosha, assisted by DGCR8, cleaves the pri-miRNA HP stem in a specific

pattern (Kim et al., 2017). Although microRNAs are fundamental for terminal neuronal differentiation (Yoo et al., 2011), Drosha maintains the NSC pool independently of miRNA activity (Knuckles et al., 2012; Rolando et al., 2016). The expression of proneural genes is tightly controlled by a non-canonical Drosha pathway, in which Drosha negatively regulates expression of its target mRNAs by cleaving their evolutionary conserved HPs (Knuckles et al., 2012). Different Drosha mRNA targets have been identified in NSCs, including Neurogenin2, NeuroD1, NeuroD6 and Nuclear Factor I/B (NFIB) (Knuckles et al., 2012; Rolando et al., 2016). The transcription factor NFIB is required and sufficient to promote glial-fate specification (Deneen et al., 2006). In the adult hippocampus, Drosha silences NFIB mRNA and prevents the acquisition of an oligodendrocytic fate by DG NSCs (Rolando et al., 2016). There are two Drosha interacting HPs located in the 5' UTR and 3' UTR of the NFIB mRNA. Despite that both are bound by Drosha, only the NFIB 3' UTR is cleaved. However, how the cleavage specificity towards the HPs is achieved has still to be investigated (Rolando et al., 2016).

Drosha is ubiquitously expressed and its interactions are not restricted to DGCR8. Different Drosha-binding partners have been identified underlining the diversity of Drosha function on RNA including splicing and transcriptional regulation (Rouillard et al., 2016; Spadotto et al., 2018). However, the composition of the Drosha complexes that allow for NSC maintenance in the adult brain are broadly unknown. Thus, it is unclear how Drosha-mediated cleavage of mRNAs is regulated to ensure NSC pool maintenance.

Here, we unraveled the Drosha interacting partners in DG hippocampal NSCs and identified novel RNA binding proteins (RBPs) involved in neurogenesis. We also identified RBPs that differentially contribute to the regulation of NFIB HPs and found fundamental differences between the HPs in post-transcriptional processes including mRNA translation. We investigated Drosha-interacting RBPs for their functions and identified the Scaffold Attachment Factor B1 (Safb1) as new regulator of NFIB mRNA

stability. We showed that Safb1 together with Drosha represses NFIB mRNA and that this regulation is crucial for preventing oligodendrocytic differentiation of NSCs. Therefore, we unraveled the Drosha/Safb1 complex as a novel regulator of RNA stability and translation during neurogenesis.

RESULTS

Identification of Drosha-binding partners in DG NSCs

In order to identify Drosha interacting proteins that may regulate its DG NSC fate controlling activity, we performed Drosha co-immunoprecipitation (Co-IP) followed by tandem mass spectrometry (MS^2) from adult mouse DG NSCs to establish a Drosha interactome (Figure 1A and Figure S1A,B). 165 proteins co-precipitated with Drosha from DG NSCs ($p < 0.05$, log2 fold change ≥ 3, FDR ≤ 0.001, peptide count ≥ 4; Figure 1B and Table S1), the majority of which are RBPs (138; 84%) (Gerstberger et al., 2014; Huang et al., 2018). We compared this dataset with a previous Drosha IP performed from human embryonic kidney cells (HEK293T) and found an overlap of 24 proteins (Macias et al., 2015). Comparison of our DG NSC Drosha interactome with the 20 protein components of the large Drosha complex described previously (CORUM protein complexes dataset) revealed an overlap of 11 proteins (Figure 1B,C) (Rouillard et al., 2016). Therefore, approximately 50% of the canonical large Drosha complex proteins identified in other cellular systems were identified as Drosha partner proteins in the DG NSC interactome (Figure 1B,C). As a proof of concept, the canonical Drosha interacting protein and partner in the miRNA Microprocessor complex DGCR8, was highly enriched in our DG NSC Drosha interactome (Figure 1B).

Process network analysis (MetaCore) indicated that 56 of the 165 Drosha interacting proteins (34%, $p = 10^{-61}$) are involved in the regulation of transcription and mRNA processing (Figure 1D). Conversely, only 2 - 7% (3 - 11) of the Drosha interacting proteins have been linked to other process networks including translation, cell cycle, cell adhesion and the cytoskeleton ($p = 10^{-1}$ - 10^{-3}) (Figure 1D). In order to gain insights into the biological functions of the Drosha interactors, we performed Gene Ontology (GO) enrichment analysis of biological processes. The top GO term of the Drosha interactors in NSCs was RNA splicing (GO:0008380) with >30-fold enrichment, followed by RNA processing (Figure 1E).

We performed a STRING functional protein association network analysis with the DG NSC Drosha interactome (considering only experimentally determined data and curated databases) (Szklarczyk et al., 2019). The resulting network culminated in only one known major complex, indicating the close connectivity between interactors (Figure 1F and S1C,D). Strikingly, many of the known Drosha interactors, including Drosha itself, were not positioned in the core of the complex indicating additional mediators between Drosha and distant co-interactors. In summary, we identified Drosha binding partners in adult DG NSCs and found that they are mainly involved in transcriptional regulation and RNA splicing.

Identification of interactors with NFIB 5' UTR and 3' UTR HP RNA sequences

NFIB is required and sufficient to induce glial-fate specification of NSCs and its expression is repressed in DG NSCs by Drosha-mediated post-transcriptional cleavage of its mRNA (Deneen et al., 2006; Rolando et al., 2016). The 5' UTR and 3' UTR of the NFIB mRNA contain evolutionary conserved HPs that are bound by Drosha (Rolando et al., 2016). To determine the Drosha complexes that potentially control NFIB mRNA stability, we performed RNA pull-down experiments using the critical regulatory regions of the NFIB mRNA as bait (Rolando et al., 2016).
We biotinylated the NFIB HPs including flanking sequences and pulled-down proteins from DG NSC lysates which were subsequently analyzed by MS^2 (Figure 2A). As a proof of concept, we confirmed that Drosha was precipitated with both the NFIB 5' UTR and 3' UTR HPs (Figure S2A). We identified 128 and 83 proteins by MS^2 that bound the NFIB 5' UTR and 3' UTR HPs, respectively ($p < 0.05$, log2 fold change ≥ 1, FDR ≤ 0.1, peptide count ≥ 4) and that were significantly enriched compared to pull-downs with the proximal 3' UTR of the androgen receptor (AR) mRNA that was used as a control bait (Figure 2B,C and Table S2).
The majority of the DG NSCs proteins that interact with the NIFB HPs (117 of 128 the 5' UTR HP bound proteins and 78 of 83 the 3' UTR HP bound

proteins) are known RBPs (Gerstberger et al., 2014; Huang et al., 2018). We performed MetaCore and GO term analysis of both the NFIB 5' UTR and 3' UTR HP bound protein datasets. Process networks analysis revealed that 22% and 27% of the NFIB 5' UTR HP and 3' UTR HP binding proteins, respectively, are involved in transcription (Figure 2D,E). Strikingly, translation initiation (21% of total, P-value 10^{-23}) and elongation (22% of total, P-value 10^{-21}) were strongly enriched in the 5' UTR HP bound proteins, but were far less relevant for the 3' UTR HP interacting proteins (9% of total, P-value 10^{-5} and 10^{-4}). Similarly, STRING network analysis of 3' UTR and 5' UTR HP bound proteins resulted in comparable findings (Figure 2F,G and S2B,C). While both interaction datasets displayed a complex including many heterogeneous nuclear ribonucleoproteins (hnRNPs), only the 5' UTR HP protein network showed an additional complex that included many ribosomal proteins (Figure 2G).

NFIB interacting RBPs bind the HP flanking regions

The binding of Drosha and its regulatory complexes to non-canonical cleavage sites in its target mRNAs is still not understood (Rolando et al., 2016). We assessed whether the potential regulators of Drosha activity bind to the HPs or the flanking sequences in the region of the NFIB 5' UTR and 3' UTR HPs. We compared the DG NSC proteins that bound to the NFIB 5' UTR HP and 3' UTR HP probes with those that bound to hybrid RNA controls (AR RNA / 5' UTR flanking and AR RNA / 3' UTR flanking) where the HP forming region had been replaced with the AR RNA sequence but which retained the NFIB 5' UTR and 3' UTR HP flanking regions, respectively (Figure S2D,F). Hnrnpa2b1, Purb, Vcp, Pura and Rbm25 were enriched as interactors of the NFIB 5' UTR HP whereas Rbmx was the only protein that selectively interacted with the NFIB 3' UTR HP (Figure S2D,F). These results indicated that the majority of the RBPs bind to the HP flanking regions in the 5' and 3' UTRs of the NFIB mRNA. Indeed, 808 proteins bound to the 5' UTR flanking region of NFIB mRNA and 892 proteins bound the 3' UTR HP flanking region (Table S2). Process networks analysis indicated that ~20 % of the proteins associated

with the 5’ UTR and 10% of the proteins associated with the 3’ UTR HP regions are involved in translation (Figure 2C). Similarly, GO biological process analysis revealed that translation (GO:0006412) was 10-fold enriched in the 5’ UTR HP flanking dataset compared to the random control prediction, whereas regulation of gene expression and RNA processing were most enriched in the 3’ UTR HP flanking region binding protein dataset (Figure S2E,G).

Previously, we had found that the 3’ UTR HP of NFIB mRNA is cleaved by Drosha and this contributes to the destabilization of the RNA and blockade of NFIB expression (Rolando et al., 2016). Therefore, we focused on the proteins that preferentially interact with the NFIB UTR HPs (Figure 2B,D; colored dots). We identified 18 proteins ($p < 0.05$, log2 fold change ≥ 1, FDR ≤ 0.1, peptide count ≥ 4) that preferentially bound to the NFIB 3’ UTR and not to the NFIB 5’ UTR HP (Figure S2H, Table S2), with the highest enrichment for Hnrnpl, Safb1, Sfpq and Nono. GO analysis of the NFIB 3’ UTR HP specific interacting proteins showed significant enrichment in negative regulation of mRNA metabolic processes (GO:1903312), consistent with 3' UTR-mediated mRNA stabilization (Figure S2I).

Identification of modulators of non-canonical Drosha activity

We hypothesized that the proteins interacting with Drosha and NFIB HPs could facilitate the Drosha-mediated cleavage of target mRNAs. We compared the lists of Drosha, NFIB 3’ and 5’ UTR interacting proteins (Figure 3A and Table S3) and identified 18 candidates, all of which have previously been reported to be RBPs (Gerstberger et al., 2014; Huang et al., 2018). As a proof of principle, this subset of 18 RBPs included the Hnrnp family members Hnrnpa1, Hnrnpa2b1 and Hnrnpu, which are known interactors of Drosha (Macias et al., 2015; Rouillard et al., 2016). In addition, we identified 5 RBPs that interacted only with Drosha and the 3’ UTR HP region of NFIB and 14 RBPs that bound only to Drosha and the 5’ UTR HP but not the 3’ UTR HP regions of NFIB. The majority of Drosha-binding partners, including the main partner of Drosha in miRNA

biogenesis, DGCR8, did not interact with the NFIB 3' UTR or 5' UTR HP regions (127 out of 165 identified proteins in the Drosha IP).

To elucidate potential regulatory functions of the NFIB mRNA-interacting RBPs in Drosha-mediated control of NFIB RNA stability, we developed a Drosha-cleavage activity reporter system in the DG NSC system. We generated stable DG NSC lines carrying a destabilized EGFP (EGFPd2), doxycycline-regulated expression cassette and floxed Drosha alleles (*Drosha*$^{fl/fl}$) (Li et al., 1998). One *Drosha*$^{fl/fl}$ DG NSC line stably expressed the control EGFPd2 reporter (Tet-on ctrl) (Figure 3B). Another *Drosha*$^{fl/fl}$ DG NSC line carried the same doxycycline-regulated EGFPd2 expression cassette but the NFIB 3' UTR HP sequence had been inserted downstream of the EGFPd2 coding region (Tet-on 3' UTR) thus mimicking the endogenous Drosha-mediated NFIB mRNA processing site (Figure 3B and S3A,B). Both Tet-on ctrl and Tet-on 3' UTR NSC lines retained stem cell properties including the capacity to generate neurons *in vitro* (Figure S3A).

EGFPd2 (referred to hereafter as GFP) expression was induced to submaximal levels by tittered administration of doxycycline (Figure S3C,D and G). To test whether these inducible DG NSC systems reproduce Drosha-mediate mRNA cleavage of the NFIB mRNA, we analyzed GFP expression following conditional *Drosha* ablation (cKO) induced by transient expression of Cre-recombinase (Cre-IRES-Tom) (Figure 3B and S3E) (Rolando et al., 2016). 48 hours after *Drosha* cKO, we administered doxycycline to induce GFP expression from the Tet-on ctrl and Tet-on 3' UTR HP reporter constructs (Figure 3C), and compared the expression of GFP from these reporters in wild-type (Tom^{-}) and *Drosha* cKO (Tom^{+}) NSCs by FACS analysis. *Drosha* cKO increased GFP expression from the Tet-on 3' UTR HP reporter compared to cells with Drosha. Conversely, *Drosha* cKO did not affect GFP levels produced from the Tet-on ctrl reporter (Figure 3D and S3F). Therefore, insertion of the NFIB 3' UTR HP into the Tet-on 3' UTR reporter construct conveyed Drosha sensitivity and the system enables quantification of Drosha cleavage of target mRNAs.

Drosha and NFIB RNA interacting proteins are novel regulators of NFIB HP processing

From the combined proteomic experiments, we hypothesized that the Drosha and NFIB RNA interacting proteins modulate the activity of Drosha towards its targets, including NFIB mRNA. To assess these effects, we selected RBPs from the Drosha interacting protein dataset and performed gain-of-function analysis in the Tet-on DG NSCs lines (Figure 3E). We expressed Bub3, Ddx5, Ddx17, DGCR8, Dhx9, Fus, Hnrnpa1, Hnrnpu, Khsrp, Pabpn1, Prpf6, Qki, Safb1, Sam68, Sart1, Sf1, Tdp4 and Trim9 in DG NSCs under the control of a CAG promoter (*CAG::RBP-IRES-CFP*) or expressed CFP as a control (*CAG::CFP*), and assessed the regulation of the Tet-on ctrl and Tet-on 3' UTR HP reporters. 24 hours after expression of the RBP or CFP alone (*CAG::CFP*), we induced the Tet-on ctrl and Tet-on 3' UTR reporters, respectively, by doxycycline induction, and quantified GFP expression in the single cells by FACS and populations after sorting by RT-qPCR (Figure 3E and Figure S3G).

We quantified the changes in GFP intensity (GFP protein) following RBP expression (CFP^+) in the Tet-on 3' UTR HP DG NSC line and standardized these changes to changes caused by the same RBP expressed in the Tet-on ctrl DG NSCs. This approach aimed to identify RBPs that acted directly on the NFIB 3' UTR HP sequences and not through indirect effects on the Tet-on EGFPd2 expression cassettes via transcriptional and translational regulation, independent of the NFIB 3' UTR HP sequences. Among the eighteen RBPs tested, Dhx9, Sf1, Hnrnpu and TDP-43 caused the most dramatic increases in GFP expression in a NFIB 3' UTR HP-dependent fashion. Conversely, Safb1, Qki, Sam68 and Sart1 induced the most pronounced reduction in GFP protein expression (Figure 3F, S3H). Of these 8 RBPs that showed the greatest effects on GFP levels from the Tet-on 3' UTR HP reporter, Fus and Safb1 were those that also showed a similar corresponding change in the GFP mRNA levels (Fus 824%, Safb1

48%) suggesting their actions were based on regulation of mRNA turnover (Figure 3F).

As Drosha destabilizes NFIB mRNA, reduces NFIB protein expression and reduces GFP expression from the Tet-on 3' UTR HP reporter, we hypothesized that Drosha partners that reduce GFP mRNA and protein expression from the Tet-on 3' UTR HP construct are potential positive regulators of Drosha activity. Safb1 was the only RBP that strongly reduced GFP mRNA and protein expression suggesting its direct involvement in NFIB 3' UTR HP regulation (Figure 3F).

Safb1 regulates NFIB 3' UTR HP stability via Drosha

Safb1 showed a strong binding preference towards the NFIB 3' UTR HP compared to the NFIB 5' UTR HP (Figure S2H). We addressed whether this specificity underlies differences in a functional regulation of the NFIB 5' UTR and 3' UTR HPs by Drosha. Therefore, we generated an independent stable DG NSC line expressing Tet-on 5' UTR GFP, where the NFIB 3' UTR HP sequence in the Tet-on 3' UTR HP construct had been exchanged with the NFIB 5' UTR HP sequence (Figure 4A and S4A,B).

We expressed Safb1 (*CAG::Safb1-IRES-CFP)* in Tet-on GFP, Tet-on 5' UTR and Tet-on 3' UTR reporter DG NSC lines and compared the levels of GFP protein and mRNA 48 hours after Doxycycline induction relative to the effects of expressing GFP alone (*CAG::CFP*) (Figure 4E). Safb1 overexpression significantly reduced GFP mRNA expression in Tet-on 3' UTR reporter cells (Figure 4B). Interestingly and in stark contrast, Safb1 overexpression increased GFP mRNA in Tet-on 5' UTR HP reporter NSCs indicating key differential roles of Safb1 on the two HPs (Figure 4B). Similarly, GFP protein intensity was also reduced in the Tet-on 3' UTR DG NSCs following Safb1 expression (Figure 4C). These data show that Safb1 could regulate NFIB mRNA stability through the 3' UTR HP.

To address whether Safb1 and Drosha cooperate to regulate NFIB mRNA, we first investigated whether Drosha and Safb1 physically interact in DG NSCs via a co-immunoprecipitation assay (co-IP). We immunoprecipitated

endogenous Drosha from DG NSCs with an anti-Drosha antibody and detected endogenous Safb1 in the IP but not PKC-α, which we used as a negative control as it has not been reported to interact with Drosha and was not identified in the MS of the Drosha IP (Figure 4D and S4C-E).
To address whether Safb1 and Drosha cooperate at the NFIB 3' UTR HP, we analyzed the effects of Safb1 overexpression on the Tet-on 3' UTR reporter in the presence and absence of Drosha (Figure 4E). In the former, Safb1 overexpression reduced GFP expression from the doxycycline-induced Tet-on 3' UTR reporter at the RNA (RT-qPCR) and protein level (FACS), respectively, compared to the Tet-on GFP reporter (Figure 4E-G). We then addressed the effects of Safb1 overexpression in the absence of Drosha. While *Drosha* cKO increased GFP expression from the Tet-on 3' UTR HP reporter at the RNA and proteins levels relative to the Tet-on GFP reporter, simultaneous *Drosha* cKO and overexpression of Safb1 reversed the effects of both mRNA and protein indicating that Drosha and Safb1 work together to regulate Tet-on 3' UTR HP expression (Figure 4E-G).

Safb1 represses NFIB expression in DG NSCs

Safb1 reduced expression of the NFIB 3' UTR HP reporter in a Drosha-dependent manner. We mapped Safb1 RNA binding motifs and found 12 potential binding sites in the NFIB 3' UTR HP sequence (Figure 5A) (Rivers et al., 2015). We evaluated Safb1 binding to the endogenous NFIB mRNA by crosslinking and immunoprecipitation (CLIP) with anti-Safb1 antibodies from DG NSCs followed by RT-qPCR analysis (Figure S5A). Both NFIB mRNA and the known Safb1 target, Hnrnpu mRNA, were bound and precipitated with Safb1 (Figure 5B). Therefore, we evaluated the effects of Safb1 overexpression on the endogenous NFIB mRNA levels in DG NSCs by RT-qPCR. Safb1 overexpression reduced NFIB mRNA levels similar to its effects on the Tet-on 3' UTR HP reporter and opposite to the effects of *Drosha* cKO (Figure 5C) (Knuckles et al., 2012; Rolando et al., 2016). Thus, Safb1 directly binds NFIB mRNA and represses its levels in DG NSCs.

Safb1 regulates oligodendrocyte differentiation from NSCs

The multipotent NSCs of the DG generate predominately granule neurons as well as astrocytes but not oligodendrocytes and their fate is controlled in part by Drosha and its post-transcriptional repression of NFIB expression (Rolando et al., 2016). To assess the expression of Safb1 in the hippocampus *in vivo*, we genetically labelled neurogenic DG NSCs in *Hes5::CreER^{T2}*, *Rosa26-CAG::EGFP* mice (Lugert et al., 2012). The Notch signal target *Hes5* is expressed only by NSCs in the DG and *Hes5::CreER^{T2}* can be used to lineage trace neurogenic and gliogenic cells in the adult mouse following Tamoxifen induction (Lugert et al., 2010; Lugert et al., 2012). Safb1 protein was expressed by most cells in the adult DG including GFAP^{+} and Hes5^{+} radial NSCs (Figures S5B). In line with this, DG NSC cultures also showed high levels of Safb1 expression indicating that Safb1 is expressed by DG NSCs both *in vivo* and *in vitro* (Figure S5C).

As Safb1 promotes Drosha cleavage of NFIB transcript and Drosha activity controls DG NSC fate *in vivo* and *in vitro* (Rolando et al., 2016), we evaluated the role of Safb1 in DG NSCs by esiRNA-mediated knockdown (KD) *in vitro*. Safb1 KD caused a rapid increase in activated Casp3 and loss of DG NSC within 48 hours, preventing further fate analysis (Figure S5D,E). Therefore, we undertook a different approach to address the role of Safb1 in NSC fate choice. While adult DG NSCs are fate restricted to generate neurons and astrocytes at the expense of oligodendrocytes, adult SVZ NSCs generate the three neural lineages including oligodendrocytes *in vivo* and *in vitro* (Kang et al., 2019; Lachapelle et al., 2002; Rolando et al., 2016; Sohn et al., 2012). We isolated SVZ NSCs from postnatal mice and expanded them *in vitro*. SVZ NSCs expressed Safb1 at lower levels than DG NSCs (Figure S5F). Sox10^{+} oligodendrocytic progenitors within the SVZ NSC cultures showed even lower Safb1 expression showing an inverse correlation between Safb1 expression and the oligodendrocytic differentiation marker Sox10 (Figure S5F).

As we were unable to address Safb1 KD DG NSCs due to their cell death, we evaluate the role of Safb1 during NSC differentiation by overexpressing Safb1 in SVZ NSCs (Figure S5G). We transfected SVZ NSCs with *CAG::Safb1-IRES-CFP* or *CAG::CFP* expression vectors and analyzed their fate 48 hours later (Figure 5D,E). Safb1 overexpression reduced $Sox10^{+}CFP^{+}$ oligodendrocyte differentiation (Safb1 overexpression: 19.9%±1.6%, $p < 0.01$; CFP ctrl: 33.2%±1.2%). Non-transfected cells in the cultures continued to produce oligodendrocytes. Therefore, Safb1 repressed oligodendrocytic differentiation of NSCs in a cell autonomous fashion.

DISCUSSION

Post-transcriptional regulation of gene expression contributes significantly to proteome regulation in NSCs (Pilaz and Silver, 2015; Ratti et al., 2006). miRNA-independent regulation of mRNA stability by Drosha recently emerged as crucial post-transcriptional regulator of NSC fate (Knuckles et al., 2012; Rolando et al., 2016). Several mRNAs are targets of Drosha and most contain evolutionarily conserved HP structures (Chong et al., 2010; Johanson et al., 2013; Knuckles et al., 2012; Rolando et al., 2016; Rolando and Taylor, 2017). More than 2000 human mRNAs are predicted to form secondary HPs that resemble pri-miRNAs, opening up a huge potential for non-canonical Drosha mRNA endonucleolytic function in different cells (Johanson et al., 2013; Pedersen et al., 2006). Non-canonical functions of Drosha influences NSC maintenance and differentiation in the embryonic and adult brain by regulating the expression of mRNAs encoding for cell fate determining transcription factors (Knuckles et al., 2012; Rolando et al., 2016). Nevertheless, how Drosha-mediated mRNA regulation is achieved to ensure physiological regulation of NSC activity and fate was unknown. Here, we uncovered novel Drosha-containing protein complexes in hippocampal NSCs and identify an RBP partner that modulates Drosha activity towards the mRNA of NFIB.

By MS^2, we identified 165 Drosha-interacting proteins in hippocampal NSCs and found that the majority of these are RBPs (Gerstberger et al., 2014; Huang et al., 2018). 15% of the NSC enriched Drosha-binding partners were also identified in HEK293T confirming that some Drosha partners and complexes are conserved across different cell types. Yet this findings further suggests that although ubiquitously expressed, there are also likely to be cell type-specific Drosha complexes (Macias et al., 2015; Rouillard et al., 2016). GO analysis showed the Drosha-interacting proteins have diverse functions but they frequently have established roles in RNA splicing and mRNA processing.

The role of DGCR8 together with Drosha in miRNA biogenesis has been well studied (Han et al., 2004). However, the contribution of DGCR8 to non-canonical Drosha functions in NSCs was unclear. We found that DGCR8 does not interact with NFIB UTR HPs and its overexpression does not affect NFIB HP cleavage. Therefore, these findings suggest that DGCR8 does not contribute to Drosha-mediated regulation of NFIB in adult NSCs and supports the requirement for other factors in cell-type specific regulation of RNA stability.

The top Drosha-interacting partner was Mex3c, an E3 ubiquitin ligase that post-transcriptionally regulates the 3' UTR of HLA-A2 mRNA by promoting mRNA decay. Its RNA binding domain is sufficient to prevent translation, but its ubiquitin ligase activity is required for mRNA degradation (Cano et al., 2012). It is not yet clear how Drosha interacts with Mex3c and why this interaction is highly enriched in NSCs, however, our dataset provides information of many novel interactions, that may serve as stepping stones for further investigation of proteome regulation.

NFIB transcript is a major target of Drosha in DG NSCs. NFIB mRNA has two HPs located in the UTR sequences that are both evolutionary conserved among species and convey Drosha sensitivity to the transcript (Rolando et al., 2016). Although Drosha binds both the 5’ and 3’ UTR HP regions of NFIB mRNAs, only the 3’ UTR HP is cleaved. To understand how Drosha activity on its mRNA targets is modulated, we identified NFIB-interacting proteins that bind the 3’ and 5’ UTR HP regions.

The NFIB 5’ UTR HP showed stronger interactions with ribosomal proteins including Rpl7, Rpl15, Rpl23a, Rpl27, Rpl31, Rps7, Rps15a and Rps25, compared to the NFIB 3’ UTR HP, suggesting additional regulatory mechanisms on NFIB protein expression.

In agreement, the top two 5’ UTR interacting partners were Rpl17, a ribosomal protein and translational regulator and the prolyl isomerase Fkbp3, a chromatin modifying enzyme responsible for cell cycle progression (Dilworth et al., 2018). These findings indicate that the Drosha targeted mRNA regions likely fulfill multiple roles in the regulation of NFIB

expression. In support of this hypothesis, *in silico* analysis of the NFIB HP interacting proteins revealed strong differences in the 5' and 3' UTR interacting complexes associated with translation.

The protein with the highest fold enrichment on the NFIB 3' UTR HP was SAFB-like transcription modulator (Sltm), which, together with Safb1 and Safb2, forms the Safb protein family. Sltm is expressed primarily in the nuclei and dendrites of cortical and hippocampal neurons, where it may affect mRNA processing and/or transport (Norman et al., 2016). Although Sltm does not selectively bind the 3' UTR HP region, it will be interesting to investigate the role of Sltm and Safb2 in DG NSC fate regulations to assess the full regulatory potential of this family of RBPs.

In silico analysis of the 78 (94%) 3' UTR HP binding proteins and the 117 (91%) 5' UTR HP binding proteins revealed to be RBPs (Gerstberger et al., 2014; Huang et al., 2018). However, the remaining putative non-RBPs might influence RNA processing via the formation of secondary complexes or have novel RNA binding domains that have not been described to date. Interestingly, both the NFIB 5' and 3' UTR HP regions are bound by many proteins that are involved in transcription and splicing. It remains to be determined whether these transcription and splicing functions require Drosha activity or not. As the RNA probes used in this assay did not require *in cyto* transcription or splicing, it suggests that preformed complexes in the cell recognize these RNA sequences independent of cellular localization and RNA biogenesis.

We investigated the functional contribution of Bub3, Ddx5, Ddx17, Dgcr8, Dhx9, Fus, Hnrnpa1, Hnrnpu, Khsrp, Pabpn1, Prpf6, Qki, Safb1, Sam68, Sart1, Sf1, Tdp4 and Trim9 in regulating NFIB HP containing transcripts. Qki displayed the second strongest reduction in reporter GFP expression. Qki is an RBP known to be involved in mRNA processing and splicing (Fagg et al., 2017; Wu et al., 2002). Although Qki is involved in oligodendrocyte differentiation (Larocque et al., 2005), our data suggests that it does not repress endogenous NFIB and, therefore, does not seem

to have a major role in Drosha-mediated NFIB-regulated oligodendrocyte fate shift by DG NSCs (Figure S5H).

Safb1 was the major regulator of Drosha-mediated NFIB mRNA cleavage identified in our screens. Safb1 binds AT-rich scaffold-matrix attachment regions (S/MARs) in DNA (Renz and Fackelmayer, 1996). However, Safb1 also binds RNA and is involved in RNA-dependent chromatin organization and mRNA processing (Huo et al., 2019; Rivers et al., 2015; Stoilov et al., 2004). Safb1 is implicated in multiple cellular processes, including cellular stress, DNA damage response, cell growth and has been linked to miRNA biogenesis (Altmeyer et al., 2013; Townson et al., 2000; Treiber et al., 2017). Although Safb1 is expressed in many tissues, its expression is particularly high in the brain (Rivers et al., 2015; Townson et al., 2003). Loss of Safb1 function results in embryonic or perinatal lethality and our attempts to induce a complete Safb1 knockdown also induced cells death (Ivanova et al., 2005). Hence, the function of Safb1 in the brain remains unclear. We show here that Safb1 prevents oligodendrogenesis by activating Drosha-mediated NFIB cleavage in NSCs. This is in line with the strong Safb1 expression in the adult DG NSCs (Rivers et al., 2015) where oligodendrogenesis does not occur under physiological conditions but Safb1 is expressed at lower levels in cells of the oligodendrocytic lineage and oligodendrogenic NSCs of the adult V-SVZ.

The Drosha requirements and binding sites for biogenesis of miRNA have been extensively studied (Kim et al., 2017). However, it remained to be shown how Drosha-mediated cleavage of target mRNAs is achieved, as this is clearly a separate mechanism (Kim et al., 2017; Rolando and Taylor, 2017). Previously, we showed that binding of Drosha to an mRNA region is not always conducive with cleavage (Rolando et al., 2016). This implies a multifaceted regulator control of targeting and cleavage and that these processes may not be necessarily linked. The differential targeting of Drosha to its cell-type specific targets has major functional implications in the dynamic control of Drosha activity. Our description of a strong binding preference of Safb1 towards the NFIB 3' UTR HP sequences

which promotes an inhibitory effect of the 3' UTR stability supports multifactorial control of Drosha specificity. Therefore, we propose that Drosha-mediated RNA cleavage requires interactions with specific RBPs that are able to direct its specificity to targets in the miRNA biogenesis pathway and for mRNA destabilization. Our data uncover novel Drosha interacting proteins and in the future it will be important to investigate these Drosha/RBP complexes and their functional involvement in NSC fate regulation as well as in other cellular systems and contexts.

STAR METHODS

Detailed methods are provided in the online version of this paper and include the following:

- KEY RESOURCES TABLE
- LEAD CONTACT AND MATERIALS AVAILABILITY
- EXPERIMENTAL MODEL AND SUBJECT DETAILS
- METHOD DETAILS
- QUANTIFICATION AND STATISTICAL ANALYSIS
- DATA AND CODE AVAILABILITY

SUPPLEMENTAL INFORMATION

Supplemental Information can be found online at LINK

ACKNOWLEDGMENTS

We thank the members of the V.T. laboratory for helpful discussions and Frank Sager for excellent technical assistance. We thank the Proteomics Facility of the Biozentrum Basel and the Animal Core Facility of the University of Basel. This work was supported by the Swiss National Science Foundation (31003A_162609 and 31003A_182388).

AUTHOR CONTRIBUTIONS

N.I., C.R., E.-A.B., T.M., and T.B. designed and performed experiments and evaluated and interpreted the data. V.T. conceived and designed the project and evaluated the data. N.I., C.R., and V.T. wrote the paper and prepared the figures. All authors edited and proofread the manuscript.

DECLARATION OF INTERESTS

The authors declare no competing interests

FIGURE LEGENDS

Figure 1: Drosha interacts with RNA regulatory proteins in neural stem cells

A. Scheme of the Drosha coimmunoprecipitation MS^2 procedure.

B. Volcano plot of MS^2 quantified proteins displaying log2 fold change (x-axis) versus -log10 P-value (y-axis). Significant enrichment for highlighted proteins (green dots) was assessed by considering P-value < 0.05, log2 fold change ≥ 3 and FDR ≤ 0.001. Known Drosha interactors are displayed by magenta framed dots.

C. Venn-Diagram showing overlaps of identified Drosha interactors in DG NSCs with Drosha-IP from Macias et al. and CORUM large Drosha complex dataset (Macias et al., 2015; Rouillard et al., 2016).

D. MetaCore enrichment analysis of process networks for identified Drosha-interacting proteins. Bar length corresponds to percentage of protein number out of total identified Drosha interacting proteins for each of the indicated category. P-values indicated by color.

E. GO terms (PANTHER) of biological processes for identified Drosha interacting proteins. Bar length corresponds to fold change enrichment per category. P-values indicated by color.

F. STRING network analysis of identified Drosha interacting proteins. Nodes are indicated by green dots, edges exclusively correspond to known interactions from experimental data and databases. Only nodes with one or more edges are displayed, protein isoforms are shown collectively.

Figure 2: Distinct interactions of NFIB 3' UTR and 5' UTR HPs with RNA binding proteins in NSCs.

A. Scheme of the NFIB HP pull-down and MS^2 procedure.

B. Volcano plot of MS quantified NFIB 5'UTR interacting proteins displaying log2 fold change (x-axis) versus -log10 P-value (y-axis). Significant enrichment for highlighted proteins (red dots) was achieved by

P-value < 0.05, log2 fold change ≥ 1 and FDR ≤ 0.1. Subset of interesting proteins is displayed (black framed dots).

C. MetaCore enrichment analysis of Process Networks and GO terms (PANTHER) of biological processes for identified NFIB 5' UTR interacting proteins. Bar length corresponds to percentage of protein out of total identified NFIB 5' UTR interacting proteins per category (Process Networks) or to fold change per category (GO biological processes). P-values indicated by color.

D. Volcano plot of MS^2 quantified NFIB 3' UTR interacting proteins displaying log2 fold change (x-axis) versus -log10 P-value (y-axis). Significant enrichment for highlighted proteins (blue dots) was achieved by P-value < 0.05, log2 fold change ≥ 1 and FDR ≤ 0.1. Subset of interesting proteins is displayed (black framed dots).

E. MetaCore enrichment analysis of Process Networks and GO terms (PANTHER) of biological processes for identified NFIB 3' UTR interacting proteins. Bar length corresponds to percentage of proteins out of total identified NFIB 3' UTR interacting proteins per category (Process Networks) or to fold change per category (GO biological processes). P-values are indicated by color.

F, G. STRING network analysis of identified NFIB 5' UTR HP and 3' UTR HP interacting proteins. Nodes are indicated by colored dots, edges exclusively correspond to known interactions from experimental data and databases. Only nodes with one or more edges are displayed, protein isoforms are shown collectively.

Figure 3: Overexpression of Drosha interactors affects Drosha mediated cleavage on NFIB 3' UTR.

A. Venn-diagram showing overlaps between identified Drosha interactors (green), NFIB 3' UTR (blue) and NFIB 5' UTR (red). Numbers indicate the total proteins, numbers in brackets indicate how many are known RBPs. Proteins selected for the functional assay are highlighted in bold.

B. Scheme of the experimental paradigm of Tet-on reporter lines.

C. Experimental setup for *Drosha* cKO experiments followed by FACS analysis.
D. FACS analysis of Tet-on 3' UTR and ctrl DG NSCs following *Drosha* cKO. Quantification of median fluorescence intensity of GFP from *Drosha* cKO over wt in Tet-on ctrl and 3' UTR lines, n = 5, two-tailed Mann-Whitney test: **p<0.01. Error bars SEM.
E. Scheme of the experimental setup for RBP overexpression experiments in Tet-on ctrl and 3'-UTR HP lines followed by FACS and RT-qPCR analysis.
F. Candidate RBP overexpression analysis in DG NSCs. Percentage of GFP change in Tet-on 3'UTR over ctrl line for protein fluorescence (FACS, x-axis) and mRNA (RT-qPCR, y-axis). Changes of +/- 50% were considered as significantly different (green area).

Figure 4: Safb1 overexpression leads to specific 3' UTR changes and is mediated by Drosha.
A. Scheme of the constructs used for generating Tet-on ctrl, Tet-on 3' UTR and Tet-on 5' UTR DG NSCs.
B. RT-qPCR analysis of GFP mRNA levels. Samples overexpressing CFP and Safb1 in Tet-on 3' UTR and Tet-on 5' UTR lines (x-axis). Percentage of mean GFP mRNA expression of Tet-on 3' and Tet-on 5' UTR DG NSCs compared to Tet-on ctrl DG NSCs (y-axis); n = 12, 5, 3; one-way ANOVA with Holm-Sidak's test: *p<0.05, **p<0.01, **p<0.001, Error bars SEM.
C. FACS analysis of EGFPd2 (GFP) protein fluorescence. Samples overexpressing CFP and Safb1 in Tet-on 3' UTR and 5' UTR DG NSCs as indicated (x-axis). Percentage of median GFP protein fluorescence of Tet-on 3' UTR and Tet-on 5' UTR DG NSCs over Tet-on ctrl DG NSCs (y-axis). n = 15, 6, 7; one-way ANOVA with Tukey's test: ***p<0.001. Error bars SEM.
D. Western blot validation of Drosha-Safb1 interaction. Drosha Co-IP shows enrichment for Drosha co-precipitation of Safb1. Negative control is PKC-α.

E. Experimental setup for Safb1 overexpression in Drosha cKO Tet-on ctrl and 3' UTR lines followed by FACS and RT-qPCR analysis.
F. RT-qPCR analysis of GFP mRNA levels. Samples OE Safb1 and/or *Drosha* cKO in Tet-on 3' UTR line (x-axis). Percentage of mean GFP mRNA expression of Tet-on 3' UTR over Tet-on ctrl reporter line (y-axis), 100% line indicates no change. n = 3, one-way ANOVA with Dunnett's test: *p<0.05. Error bars SEM
G. FACS analysis of GFP protein fluorescence. Samples OE Safb1 and/or cKO Drosha in Tet-on 3' UTR line (x-axis). Percentage of median GFP intensity of Tet-on 3' UTR over Tet-on ctrl reporter line (y-axis), 100% line indicates no change. n = 5, one-way ANOVA with Tukey's test: **p<0.01. Error bars SEM.

Figure 5: Safb1 overexpression leads to decreased levels of NFIB and affects oligodendrogenesis.
A. *In silico* motif analysis of Safb1 binding sites on NFIB 3' UTR.
B. RT-qPCR analysis of Safb1 CLIP. Relative expression (-ddct values) is calculated over input and -Ab control., Negative control: Ubc. positive control: Hnrnpu, Gene of interest: NFIB, n = 3, one-way ANOVA with Dunnett's test: *p<0.05, **p<0.01. Error bars SEM.
C. RT-qPCR analysis of NFIB mRNA in DG NSCs. Samples overexpressing CFP (mock) and Safb1 in DG NSCs, fold change of NFIB mRNA is calculated over wt. n = 4, two-tailed Mann-Whitney test: *p<0.05. Error bars SEM.
D. Safb1 overexpression assay in perinatal SVZ neurospheres. Cells were transfected with CFP (mock) or Safb1-CFP OE expressing vector. Staining for CFP, Safb1, Sox10. Scale bar: 20 μm.
E. Quantification of immunohistochemistry. Samples overexpressed for CFP (mock, n = 3) and Safb1 OE (n = 4) samples are shown as percentage of transfected (CFP^+) cells expressing Sox10. Two-tailed Welch's t-test: **p<0.01. Error bars SEM.

Figure S1: DG NSCs can differentiate and form a large Drosha complex. **Related to Figure 1.**

A. DG NSCs cells in the expansion and differentiation phases of culture. Immunohistochemistry for BLBP, MAP2 and Sox10. Scale Bar 50 μm.

B. Immunoblot (IB) validation of Drosha IP. IP with Drosha antibodies shows coprecipitation of Drosha. IP with Safb1 antibodies shows coprecipitation of Drosha. – negative control precipitation without antibody. Drosha protein and immunoglobulin (Ig) heavy chain from the precipitating antibody and detected in the Western blot are indicated.

C. STRING network analysis of identified Drosha interacting proteins (Related to Figure 1F). Node size corresponds to node degree, node color corresponds to betweenness centrality, edges exclusively correspond to known interactions of experimental data and databases. Only nodes with one or more edges are displayed, protein isoforms were analyzed collectively.

D. Common network parameters for Drosha IP network compared with a random network of similar node size. (Related to Figure 1F)

Figure S2: Both NFIB HPs interact with Drosha in DG NSCs and bind HP and flanking specific proteins. **Related to Figure 2.**

A. Immunoblot (IB) validation of Drosha precipitation with NFIB RNA 3' and 5' UTR pull-down probes. Negative control precipitation is bead-only control (Bead ctrl).

B, C. Common network parameters for pull-down networks compared with random networks of similar node size for the NFIB 5' UTR (**B**) and NFIB 3' UTR (**C**) probes.

D. Proteomics analysis of NFIB 5' UTR HP interactors. Volcano plot of MS^2 quantified proteins displaying log2 fold change (x-axis) versus -log10 P-value (y-axis).

E. NFIB 5' UTR HP flanking region protein association analysis. The dataset of flanking proteins includes proteins not enriched for 5' UTR HP or control in MS^2 analysis. Non-specific bead binding proteins were

subtracted from the analysis. MetaCore enrichment analysis of process networks and GO terms (PANTHER) of biological processes for identified NFIB 5' UTR HP flanking binding proteins.

F. Proteomics analysis of NFIB 3' UTR HP interactors. Volcano plot of MS^2 quantified proteins displaying log2 fold change (x-axis) versus. -log10 P-value (y-axis).

G. NFIB 3' UTR HP flanking region protein association analysis. The dataset of flanking proteins includes proteins not enriched for 3' UTR HP or control in MS^2 analysis. Non-specific bead binding proteins were subtracted from the analysis. MetaCore enrichment analysis of process networks and GO terms (PANTHER) of biological processes for identified NFIB 3' UTR HP flanking binding proteins.

H. Proteomics analysis of NFIB 3' versus 5' UTR HP interactors. Volcano plot of MS^2 quantified proteins displaying log2 fold change (x-axis) versus -log10 P-value (y-axis).

I. MetaCore enrichment analysis of process networks and GO terms (PANTHER) of biological processes for specific NFIB 3' UTR HP flanking proteins. Volcano plots: Significant enrichment for highlighted proteins (colored dots) was achieved by P-value < 0.05, log2 fold change ≥ 1 and FDR ≤ 0.1. Subset of protein names is displayed. Bar plots: Bar length corresponds to percentage of protein number out of total identified NFIB UTR HP interacting proteins per category or to fold change per category, respectively. P-values indicated by color.

Figure S3: Tet-on reporter lines have unchanged differentiation potential and respond to *Drosha* cKO. Related to Figure 3.

A. Characterization of the control (Tet-on ctrl) and NFIB 3' UTR HP (Tet-on 3' UTR) expressing DG NSCs cells in the expansion and differentiation phases of culture. Immunohistochemistry for the progenitor marker BLBP, neuronal protein Map2 and oligodendrocyte protein Sox10. Scale Bar 50 μm.

B. Genotyping control of the stable Tet-on 3' UTR DG NSC cell line. Agarose gel separation of amplicons and validation of stable insertion of Tet-on 3' UTR HP construct. Positive control (plasmid ctrl): plasmid construct - Tet-on 3' UTR HP construct, negative control (neg. ctrl): H_2O.
C. Expression of EGFPd2 from the doxycycline induced (48 hours) Tet-on control DG NSC line (Tet-on ctrl). Scale Bar 50 μm.
D. Doxycycline dose response curve on Tet-on control DG NSC line (Tet-on ctrl). Quantification of EGFPd2$^+$ (GFP) cells per visual field of a confluent culture.
E. RT-qPCR quantification of Drosha mRNA levels after *Drosha* cKO from Tet-on 3' UTR DG NSC line before (Ctrl) after infection with Adeno-Cre viruses (*Drosha* cKO). n = 4, two-tailed Mann-Whitney test: *p<0.05. Error bars SEM.
F. Flow cytometry analysis of EGFPd2 fluorescence in Tet-on 3' UTR and Tet-on ctrl DG NSC lines after doxycycline induction (48 hours). EGFPd2 intensity (x-axis) versus cell number normalized to mode (y-axis) of Tet-on ctrl and Tet-on 3' UTR DG NSC lines before Drosha knockout (ctrl: black) and after *Drosha* conditional knockout (cKO) (red).
G. Representative FACS plot from flow cytometric analyses of Tet-on ctrl DG NSC line after nucleofection with the control IRES CFP expression vector with or without doxycycline induction and no nucleofection (48 hours). Not nucleofected and not doxycycline induced Tet-on ctrl DG NSCs do not show EGFPd2 (GFP) or CFP expression compared to the induced and nucleofected cells.
H. Combined results of candidate RBP overexpression analysis in Tet-on 3' UTR DG NSCs. EGFPd2 (GFP) expression (x-axis) at the RNA assessed by RT-qPCR and protein levels (cytometry) following overexpression of RPBs from IRES CFP vectors relative to Tet-on 3' UTR DG NSCs transfected with control vector (CFP) plotted as percentage. RBP expressing cells were sorted by FACS by gating on the CFP expressing cells and RNA isolated for RT-qPCR. For quantitative flow cytometric analyses the nucleofected NSCs were gated in the CFP

channel and the GFP expression quantified. To eliminate effects of the RBPs on transcription, RNA stability or translation not linked to the NFIB 3' UTR HP, the changes were calculated as the differences in GFP expression as a result of RBP expression in the Tet-on 3' UTR DG NSCs and Tet-on ctrl DG NSCs (%GFP Tet-on 3' UTR HP/ Tet-on ctrl). Black dotted line indicates no change, red line indicates 50% increase or decrease in expression. Error bars SEM.

Figure S4: Safb1 is highly expressed in the murine DG Hippocampus and in DG NSCs. **Related to Figure 4.**

A. DG NSCs cells in the expansion (+bFGF/EGF) and differentiation (-bFGF/EGF) phases of culture. Immunohistochemistry for progenitor marker BLBP, neuronal marker Map2 and oligodendrocyte marker Sox10. Scale Bar 50 μm.

B. Genotyping of the stable Tet-on 3' UTR DG NSCs and Tet-on 5' UTR DG NSCs. Specific amplicons for the Tet-on 3' UTR HP construct and (514 bp) and 5' UTR HP construct (430 bp) are found only in the respective lines. left: primers for 3' UTR, right: primers for 5' UTR. neg. ctrl.: H_2O.

C. Immunoblot (IB) of Drosha-IP (related to Figure 4D), showing precipitation of Drosha. Immunoglobulin (Ig) heavy chain of the precipitating antibody detected in the immunoblots. Negative control precipitation without antibody (-).

D. Immunoblot (IB) of Drosha-IP (related to Figure 4D), showing coprecipitation of Safb1. Immunoglobulin (Ig) heavy chain of the precipitating antibody detected in the immunoblots. Negative control precipitation without antibody (-).

E. Immunoblot (IB) of Drosha-IP (related to Figure 4D), showing no precipitation of PKC-α. Immunoglobulin (Ig) heavy chain of the precipitating antibody detected in the immunoblots. Negative control precipitation without antibody (-).

Figure S5: Safb1 knock-down affects DG NSC cell survival and causes increased Casp3 activity. Related to Figure 5.

A. Scheme for the experimental setup for Safb1 CLIP from DG NSCs.

B. Safb1 expression in adult mouse DG. Immunofluorescent staining for Safb1, including by GFAP$^+$ *Hes5::GFP*$^+$ NSCs (GFP$^+$) (white arrow heads). Scale bars 50 μm for overview and 10 μm for high magnification images.

C. Safb1 expression in cultured DG NSCs. Immunofluorescent staining for Safb1 and GFAP. Scale bar 50 μm.

D Safb1 knockdown by esiRNA in DG NSCs after 48 hours compared to control Renilla Luciferase (rLuc esiRNA) treated cells. Fluorescent labeled RNA probes were used (red) as transfect control. DG NSCs were stained for Safb1 to validate knockdown.

E. Quantification of activated Caspase 3 expression in Safb1 esiRNA knockdown and control (rLuc esiRNA) transfected cells after 48h, 72h, and 96h. Safb1 knockdown results in a rapid induction of apoptosis. Two-tailed Students t-test: *$p<0.05$. Error bars SEM.

F. Safb1 and Sox10 expression by adult DG NSCs and adult V-SVZ NSCs *in vitro*. DG NSCs express higher levels of Safb1 than V-SVZ NSCs. Unlike DG NSCs, V-SVZ NSCs generate oligodendrocytes (Sox10$^+$).

G. Scheme for the experimental setup for Safb1 overexpression in postnatal V-SVZ NSCs (postnatal day 4: P4) expanded in EGF containing NSC medium as neurospheres followed by nucleofection with control (*CAG::CFP*) or Safb1 (*CAG::Safb1-IRES-CFP*) expression vectors and cell fate analysis after EGF withdrawal (-EGF) to induces differentiation.

H. RT-qPCR analysis of NFIB mRNA in DG NSCs overexpressing Qki (Qki OE) compared to control nucleofected DG NSCs expressing IRES CFP (CFP), NFIB mRNA fold change is calculated over CFP expressing DG NSCs. n = 4, two-tailed Mann-Whitney test. Error bars SEM.

STAR METHODS

KEY RESOURCES TABLE

LEAD CONTACT AND MATERIALS AVAILABILITY

Plasmids, cell lines and mouse lines generated by the Taylor lab can be obtained by requests. This study did not generate new unique reagents. Further information and requests for resources and reagents should be directed sent to and will be fulfilled by the Lead Contact, Verdon Taylor (verdon.taylor@unibas.ch).

EXPERIMENTAL MODEL AND SUBJECT DETAILS

Mouse strains and husbandry

The mouse models used in our experiments include: Rosa26R-CAG::GFP, Hes5::CreERT2 (Lugert et al., 2010; Rolando et al., 2016) and Drosha$^{fl/fl}$ (Chong et al., 2010). No gender differences were observed. Mice were randomly selected for the experiments based on birth date and genotype. According to Swiss Federal and Swiss Veterinary office regulations, all mice were bred and kept in a specific pathogen-free animal facility with 12 hours day-night cycle and free access to clean food and water. All mice were healthy and immunocompetent. All procedures were approved by the Basel Cantonal Veterinary Office under license number 2537 (Ethics commission Basel-Stadt, Basel Switzerland).

Hippocampal Adult NSC Cultures

DG NSCs were isolated from 8-week-old mice as described in the **Method Details** of *Hippocampal adult Neural Stem culture*. Papain-dissociated hippocampal cells from extracted mouse brain were resuspend in 350 *µ*l of DG NSCs media and plated in a 48-well plate, coated with 100 µg/ml Poly-L-Lysine (Sigma) and 1 µg/ml Laminin (Sigma) in DG stem cell medium containing DMEM:F12 (Gibco, Invitrogen), 2% B27 (Gibco, Invitrogen), FGF2 20 ng/ml (R&D Systems), EGF 20 ng/ml (R&D Systems). Cells were

passaged 6-20 times and characterized for marker expression and differentiation potential before use.

Neurospheres Culture

Perinatal neurospheres were isolated from postnatal day 4 (P4) C57BL/6 mouse pups as described in the **Method Details** of *Safb1 overexpression in postnatal neurosphere culture.* Papain-dissociated neurospheres were seeded in neurosphere medium (DMEM:F12 (Gibco, Invitrogen), 2% B27 (Gibco, Invitrogen), EGF 10 ng/ml (R&D Systems) and plated in a T25 flask. Every 2 days the cells were fed with 1ml of fresh neurosphere medium and passaged every 4 days.

METHOD DETAILS

Hippocampal adult neural stem cell cultures.

DG NSCs were isolated as described previously (Rolando et al., 2016; Zhang et al., 2019). 8-10 week old mice were sacrificed in a CO_2 chamber and decapitated. The brain was extracted, washed in ice cold sterile L15 medium (GIBCO) and live sectioned at 500 μm using a McIllwains tissue chopper. Brain slices were collected in cold HBSS, 10 mM HEPES and 100 I.U./mL penicillin and 100 (µg/mL) streptomycin in a 6 cm culture dish. After careful micro-dissection of the DG and removing the molecular layer and ventricular zone contaminants using a dissection binocular microscope, the dissected DGs were collected in cold HBSS, 10 mM HEPES and 100 I.U./mL penicillin and 100 (µg/mL) streptomycin in a 15 ml Falcon tube. After tissue sedimentation, the supernatant was removed and replaced by 100 μl pre-warmed Papain mix. The tissue pieces were incubated at 37°C in a water bath for 15 minutes with gentle agitation every 5 minutes, followed by addition of 50 μl of pre-warmed Trypsin inhibitor and incubation for 10 minutes at 37 °C. After adding 300 μl of DMEM/F12, the tissue was triturated with a 1 ml and 200 μl pipette tip. The sample was centrifuged at 80g to remove debris. The cell pellet was resuspended in DG NSC medium (DMEM:F12, Gibco, Invitrogen), 2% B27

(Gibco, Invitrogen), FGF2 20 ng/ml (R&D Systems), EGF 20 ng/ml (R&D Systems) and plated in a 48-well dish (Costar) coated with 100 µg/ml Poly-L-Lysine (Sigma) and 1 µg/ml Laminin (Sigma). Half of the cell medium was replaced every 2 days and cells were passaged every 6 days. Cell differentiation was induced by growth factor removal and continued culture for 6 days. Cell fixation for immunohistochemistry was performed for 10 minutes in 4% paraformaldehyde in 0.1M phosphate buffer.

Immunohistochemistry for brain tissues and NSC cultures

Mice were deeply anesthetized by injection of a ketamine/xylazine/acepromazine solution (150 mg, 7.5 and 0.6 mg per kg body weight, respectively). Animals were perfused with ice-cold 0.9% saline followed by 4% paraformaldehyde in 0.1M phosphate buffer. Brains were isolated and post-fixed overnight in 4% paraformaldehyde in 0.1M phosphate buffer, and then cryoprotected with 30% sucrose in phosphate buffer at 4°C overnight. Brains were embedded and frozen in OCT (TissueTEK) and sectioned as 30 µm floating sections by cryostat (Leica). Free-floating coronal sections were stored at -20°C in antifreeze solution until use.

DG NSCs fixation for immunohistochemistry was performed for 10 minutes in 4% paraformaldehyde in 0.1M phosphate buffer.

Sections were incubated overnight at room temperature, with the primary antibody diluted in blocking solution of 1.5% normal donkey serum (Jackson ImmunoResearch), 0.5% Triton X-100 in phosphate-buffered saline. DG NSC cultures were incubate overnight at 4°C, with the primary antibody diluted in blocking solution of 1.5% normal donkey serum, 1% BSA, 0.2% Triton X-100 in phosphate-buffered saline.

Antibodies used: activated cleavedCASP3 (Cell Signalling, rabbit, 1:500), BLBP (Chemicon, rabbit, 1:400), GFP (AbD Serotec, sheep, 1:250; Invitrogen, rabbit, 1:700; AvesLabs, chicken, 1:500), Map2 (Sigma, mouse, 1:200), SAFB1 (Abcam, rabbit, 1:200), Sox10 (Santa Cruz, goat, 1:500) and GFAP (Sigma, mouse, 1:200).

Sections were washed in phosphate-buffered saline and incubated at room temperature for 2 hours with the corresponding secondary antibodies in blocking solution. DG NSCs were washed in 1% BSA phosphate-buffered saline and incubated at room temperature for 35 minutes with the corresponding secondary antibodies in blocking solution.
Secondary antibodies and detection: Alexa488/Cy3/Alexa649 conjugated anti-chicken, mouse, goat, rabbit and sheep immunoglobulin (1:600, Jackson Immunoresearch). Sections were then washed and counter-stained with DAPI (1 µg/ml). Stained sections were mounted on Superfrost glass slides (Thermo Scientific), embedded in mounting medium containing diazabicyclo-octane (DABCO; Sigma) as an anti-fading agent. Brain sections and DG NSCs were visualized using a Zeiss LSM510 confocal microscope, Leica SP5 confocal microscope or Zeiss Apotome2 microscope.

Cell lysis

DG NSCs were washed with PBS and incubated with lysis buffer (20 mM Hepes-KOH pH 7.9; 100 mM KCl; 0.2 mM EDTA; 0.2 mM PMSF, 1x complete proteinase inhibitor (Roche); 5% glycerol; 0.5% Triton) for 10 minutes on ice. Cells were scraped off with cell scraper and lysate was transferred in Eppendorf tube, followed by sonication for 5 cycles (Bioruptor, 30s on/ 30s off, 320W) at 4°C. Lysate was centrifuged at 13'000 x g for 10 minutes at 4°C. The supernatant was transferred in a new tube and BCA assay (Thermo Fischer, #23250) was performed according to the protocol of the manufacturer to determine protein concentration.

Immunoprecipitation

1 mg of total protein lysate was incubated with antibody (Drosha, Cell Signaling, 1:50) on a rotating wheel overnight at 4°C. Magnetic beads (Dynabeads, Thermo Fisher) were washed with 1ml lysis buffer and DG

cell lysate/Ab mix was added to the beads, followed by incubation for 4h at 4°C on a rotating wheel. Beads were washed 5 times with activated lysis buffer and resuspended in milli-Q water.

Western blot

5x Laemmli Buffer was added to the samples to reach a final volume of 1x and heated 5 minutes at 95 °C at 700 rpm. Protein samples were separated on 10% SDS-polyacrylamide gels and transferred to nitrocellulose membrane (Protran). The membrane was blocked for 1h with 5% BSA in TBS-T followed by overnight incubation at 4°C with antibody (Drosha 1:1000; D28B1, Cell Signaling, in 5 %BSA; Safb1, 1:1000 ab187650, 2.5% BSA; PKC-alpha [H-7] (SC-8393) 1:500 1% BSA). Membrane was washed 3 times for 5 minutes with TBS-T followed by secondary antibody incubation (rabbit anti light chain HRP 211-032-171, 1:5000) for 1h at room temperature. Membrane was washed 3 times with TBS-T and once with TBS. Bands were detected by chemiluminescence (ECL, GE Healthcare).

Affinity purification and sample preparation for MS-based proteome analysis

IP and pull-down probes of DG NSCs were subjected to on-bead digestion (Hubner et al., 2010) by trypsin (5 μg/ml, Promega) in 1.6 M Urea / 0.1 M Ammonium bicarbonate buffer at 27 C for 30 minutes. Supernatant eluates containing active trypsin were further incubated with 1 mM TCEP at room temperature overnight. Carbamidomethylation of cysteins was performed next using 5 mM Chloroacetamide in the dark for 30 minutes. The tryptic digest was acidified (pH<3) using TFA and desalted using C18 reversed phase spin columns (Harvard Apparatus) according to the protocol of the manufacturer. Dried peptides were dissolved in 0.1% aqueous formic acid solution at a concentration of 0.2 mg/ml prior to injection into the mass spectrometer.

Mass Spectrometry Analysis

For each sample, aliquots of 0.4 µg of total peptides were subjected to LC-MS analysis using a dual pressure LTQ-Orbitrap Elite mass spectrometer connected to an electrospray ion source (both Thermo Fisher Scientific) and a custom-made column heater set to 60°C. Peptide separation was carried out using an EASY nLC-1000 system (Thermo Fisher Scientific) equipped with a RP-HPLC column (75µm × 30cm) packed in-house with C18 resin (ReproSil-Pur C18–AQ, 1.9 µm resin; Dr. Maisch GmbH, Germany) using a linear gradient from 95% solvent A (0.1% formic acid in water) and 5% solvent B (80% acetonitrile, 0.1% formic acid, in water) to 35% solvent B over 50 minutes to 50% solvent B over 10 minutes to 95% solvent B over 2 minutes and 95% solvent B over 18 minutes at a flow rate of 0.2 µl/min. The data acquisition mode was set to obtain one high resolution MS scan in the FT part of the mass spectrometer at a resolution of 240,000 full width at half maximum (at 400 m/z, MS1) followed by MS/MS (MS2) scans in the linear ion trap of the 20 most intense MS signals. The charged state screening modus was enabled to exclude unassigned and singly charged ions and the dynamic exclusion duration was set to 30 s. The collision energy was set to 35%, and one microscan was acquired for each spectrum.

Protein Identification and Label-free Quantification

The acquired raw-files were imported into the Progenesis QI software (v2.0, Nonlinear Dynamics Limited), which was used to extract peptide precursor ion intensities across all samples applying the default parameters. The generated mgf-files were searched using MASCOT against a decoy database containing normal and reverse sequences of the *Mus musculus* proteome (UniProt, April 2017) and commonly observed contaminants (in total 34490 sequences) generated using the SequenceReverser tool from the MaxQuant software (Version 1.0.13.13). The following search criteria were used: full tryptic specificity was required (cleavage after lysine or arginine residues, unless followed by proline); 3

missed cleavages were allowed; carbamidomethylation (C) was set as fixed modification; oxidation (M) and protein N-terminal acetylation were applied as variable modifications; mass tolerance of 10 ppm (precursor) and 0.6 Da (fragments). The database search results were filtered using the ion score to set the false discovery rate (FDR) to 1% on the peptide and protein level, respectively, based on the number of reverse protein sequence hits in the datasets.

Quantitative analysis results from label-free quantification were normalized and statically analyzed using the SafeQuant R package v.2.3.4 (https://github.com/eahrne/SafeQuant/) (Ahrne et al., 2016) to obtain protein relative abundances. This analysis included global data normalization by equalizing the total peak/reporter areas across all LC-MS runs, summation of peak areas per protein and LC-MS/MS run, followed by calculation of protein abundance ratios. Only isoform specific peptide ion signals were considered for quantification. The summarized protein expression values were used for statistical testing of between condition differentially abundant proteins. Here, empirical Bayes moderated t-Tests were applied, as implemented in the R/Bioconductor limma package (http://bioconductor.org/packages/release/bioc/html/limma.html). The resulting per protein and condition comparison P-values were adjusted for multiple testing using the Benjamini-Hochberg method.
All LC-MS analysis runs are acquired from independent biological samples. To meet additional assumptions (normality and homoscedasticity) underlying the use of linear regression models and Student t-Test MS-intensity signals are transformed from the linear to the log-scale.
Unless stated otherwise linear regression was performed using the ordinary least square (OLS) method as implemented in *base* package of R v.3.1.2 (http://www.R-project.org/).
The sample size of three biological replicates was chosen assuming a within-group MS-signal Coefficient of Variation of 10%. When applying a

two-sample, two-sided Student t-test this gives adequate power (80%) to detect protein abundance fold changes higher than 1.65, per statistical test. Note that the statistical package used to assess protein abundance changes, SafeQuant, employs a moderated t-Test, which has been shown to provide higher power than the Student t-test. We did not do any simulations to assess power, upon correction for multiple testing (Benjamini-Hochberg correction), as a function of different effect sizes and assumed proportions of differentially abundant proteins.

RNA biotinylation

NFIB 3' UTR and 5' UTR HP forming regions were *in vitro* transcribed using T7 transcriptase (NEB, E2040) and purified with Trizol extraction (described in RT-qPCR paragraph). RNA was biotinlylated using the Pierce™ RNA 3' End Desthiobiotinylation Kit (Thermo scientific). 50 pmol of RNA was incubated in T4 RNA ligase buffer at 16 °C overnight. RNA ligase was extracted with 100 µl chloroform:isoamyl alcohol (Sigma, C0549) and centrifuged 2 minutes at maximum speed. Aqueous phase was precipitated overnight in 5M NaCl. Sample was centrifuged at 13'000 x g for 20 minutes at 4 °C. Pellet was washed with 70% ethanol and resuspended in dH_2O. Labeling efficiency was determined by dot blotting using the chemiluminescent nucleic acid detection module kit (89880, Thermo Fisher scientific).

RNA pull-down

Experiment was performed as described in the manufacturers protocol (Pierce™ Magnetic RNA-Protein Pull-Down Kit, Thermo scientific, 20164). 50 µl of streptavidin magnetic beads were washed 3 times with 20 mM Tris, followed by 1x RNA capture buffer. 50 pmol of previously desthiobiotinylated RNA was added to the beads and incubated for 30 minutes on a heated shaker plate at 24 °C and 750 rpm. Beads were washed 3 times with 20 mM Tris and 100 µl 1x Protein-RNA Binding Buffer, followed by 100 µl of RNA Protein binding buffer including 60 µl of

Protein lysate (2mg/ml) (Cell lysis described in corresponding paragraph) for 60 minutes 4 °C with agitation.
The beads were washed 3 times with 100 μl of the kit 1x wash buffer and then further processed for WB or MS.

Enrichment Analysis and candidate selection

Datasets of significantly enriched proteins were analyzed for process networks by MetaCore (Cortellis) and molecular processes by GO terms (PANTHER, GENEONTOLOGY). An interaction network was drawn using STRING database (ELIXIR). Percental enrichment in MetaCore bar plot was calculated as listed in corresponding category out of total dataset. Significance is determined by P-value. For STRING network analysis, only experimentally determined data and curated databases were considered. Nodes with ≥ 1 Edge are displayed. Network was visualized and analyzed with Cytoscape software (Shannon et al., 2003). Prime candidates for functional analysis in reporter assay were selected using the following criteria: (i) enrichment in MS datasets; (ii) relevance in MetaCore, GO and STRING analysis; (iii) Drosha interactions reported in the literature

Stable cell line generation

NFIB 3' UTR, 5' UTR and EGFPd2 sequences were cloned in the multiple cloning site of pTet-One vector (Takara-Clontech, 634301). DG NSC Drosha$^{fl/fl}$ cells were brought in suspension by incubating with 0.25% trypsin (Gibco #15090) in Versene (Gibco #15040) for 5 min at 37°C followed by centrifugation at 80g for 5 minutes at RT. Cells were electroporated with the corresponding DNA vector using a 4D-Nucleofector (Lonza, program DS-112) according to protocol of manufacturer and re-plated in plastic dish (Costar) coated with 100 µg/ml Poly-L-Lysine (Sigma) and 1 µg/ml Laminin (Sigma).
Cells were induced with 1 µg/ml Doxycycline in DG medium. 48h post induction, cells were sorted for GFP$^+$ by flow cytometry (FACSaria III, BD Biosciences). All GFP$^+$ cells were collected, centrifuged at 80g for 5

minutes and resuspended in DG medium. Cells were re-plated, and passaged 3 times. Thereafter, cells were re-induced with 1 µg/ml Doxycycline and re-sorted two more times. Correct genotype of cell line was confirmed by genotyping using NFIB UTR and EGFPd2 specific primers.

RBP overexpression vector cloning

Coding sequences of selected prime candidates were cloned in a CAG-IRES-CFP expression vector, using the In-Fusion cloning kit (Takara) following manufactures protocols. Protein cDNAs from source vector were amplified by PCR and cloned upstream of IRES-CFP element of target vector. Sequences of all resulting vectors were verified by Sanger-Sequencing (Eurofins).

Tet-on DG NSC nucleofection and FACS

Tet-on no-HP ctrl., Tet-on 3' UTR and 5' UTR DG NSCs were brought in suspension by incubating with 0.25% trypsin (Gibco #15090) in Versene (Gibco #15040) for 4 minutes at 37°C followed by centrifugation at 80g for 5 minutes at RT. Cells were electroporated with either CFP-IRES or RBP-IRES-CFP vector (5μg) using a 4D-Nucleofector (Lonza, program DS-112) in 16-well stripes (500,000 cells/well) and re-plated in plastic dish (Costar) coated with 100 µg/ml Poly-L-Lysine (Sigma) and 1 µg/ml Laminin (Sigma).

For rescue experiments, Tet-on no-HP ctrl., Tet-on 3' UTR and 5' UTR Drosha$^{fl/fl}$ DG NSCs were electroporated with 1.6μg of Cre-IRES-Tomato and 3.4μg of CAG::IRES-CFP or CAG::Safb-IRES-CFP with 4D-Nucleofector (program DS-112).

After 24h or 48h cells were induced with 1 µg/ml Doxycycline in DG medium. 48h post induction, cells were brought in suspension with 0.25% trypsin in Versene collected in DMEM/F12 w/o red phenol, filtered through a 40 µm cell sieve (Miltenyi Biotec) and analyzed by flow cytometry (FACSaria III, BD Biosciences).

GFP and CFP double negative, GFP-single positive and CFP-single positive DG NSCs were used to create the compensation matrix and set the sorting gates. At least 100,000 events were recorded for each sample and MFI (Median Fluorescent Intensity) of the population of interest was subsequently analyzed with FlowJO (Becton Dickinson). GFP^+, CFP^+GFP^+, Tom^+ cells were sorted, centrifuged at 80g for 5 minutes and used for RNA isolation and gene expression analysis (see below).

Cross-linking immunoprecipitation (CLIP)

WT mouse DG NSCs in culture were washed with cold PBS and crosslinked at 254nm, 300mJ/cm2 in a BioLink UV-Crosslinker. Cells were lysed with RIPA buffer (0.1M sodium phosphate pH 7.2, 150 mM sodium chloride, 0.1% SDS, 1% sodium deoxycholate, 1% NP-40, 1mM activated Na_3VO_4, 1mM NaF, 1x complete protease inhibitor (Roche)). Lysate was collected and centrifuged for 5 minutes at 13'000 RPM at 4°C. Sample was treated with 10 μl DNase (Roche) and incubated for 5 minutes in a heated shaker at 37°C and 1000 RPM, followed by centrifugation at full speed at 4°C and Input probe separation. 50 μl magnetic beads (Dynabeads, Invitrogen) were washed with lysis buffer and incubated with target specific antibody (anti-Safb1, Abcam) for 1h at RT on a rotating wheel. Beads were washed twice with lysis buffer and incubated with cross-linked NSC lysate for 2h at 4°C on a rotating wheel. Beads were washed 5 times with lysis buffer, incubated with 4mg/ml ProteinaseK (Roche) in PK buffer (100 mM TrisHCL pH7.5, 50 mM NaCl, 10 mM EDTA) for 20 at 37°C at 1000 RPM, followed by downstream RNA analysis.

RNA isolation and RT-qPCR

Total RNA was isolated following the standard phenol-chloroform protocol from the manufacturer (Trizol, Life Technologies). 100% Trizol was added to the sample, followed by 20% of total volume chloroform. Sample was centrifuged at 12'000 x g for 15 minutes at 4°C. Aqueous phase was

extracted and RNA was precipitated with isopropanol and washed with ethanol. RNA pellet was resuspended in RNase-free Milli-Q water. Reverse transcription was performed using Superscript IV Vilo following manufacturers protocol (Thermo Fischer, 11766050). RNA was incubated for 5 minutes with ezDNAse enzyme at 37°C, followed by incubation with SuperScript™ IV VILO™ Master Mix at 25°C for 10 minutes, 50°C for 10 minutes and 85°C for 5 minutes. For expression analysis of genes of interest, we used the comparative Ct method using Rpl13a and Actin as normalizing genes. Experiments were performed using a qTOWER^3 real-time PCR machine (Analytik Jena). Three biological replicates for each genotype and three technical replicates for each gene were analyzed.

Safb1 RNA knock-down experiments

WT DG NSCs were brought in suspension with 0.25% trypsin in Versene followed by centrifugation at 80g for 5 minutes at RT. Cells were electroporated with either 70pmol esiRNA Luciferase or esiRNA Safb1 (Sigma) in combination with 30pmol RNA probe Alexa555 (Sigma) using a 4D-Nucleofector (Lonza, program DS-112) in 16-well stripes (500,000 cells/well) and re-plated on glass coverslips coated with 100 µg/ml Poly-L-Lysine (Sigma) and 1 µg/ml Laminin (Sigma). Cells were fixed 48, 72 and 96 hours after nucleofection in 4% paraformaldehyde in 0.1M phosphate buffer for 10 minutes.

Safb1 overexpression in postnatal neurosphere culture

Postnatal day 4 (P4) C57BL/6 mouse pups were sacrificed, decapitated and their brains collected in 6cm dishes containing sterile cold HBSS. With the aid of a stereoscope the meninges were carefully removed and the cortex was isolated by the removal of the midbrain, hindbrain and hippocampus. The cortex was dissociated in 500 μl pre-warmed Papain based solution at 37°C in a water bath for 30 minutes with gentle agitation every 5 minutes followed by addition of 500 μl of pre-warmed Trypsin inhibitor and incubation for 5 minutes at 37 °C. The tissue was then

mechanically dissociated with 1 ml and 200 μl pipette tip. After addition of 9 ml of DMEM/F12, the samples were centrifuged at 80g for 5 minutes to remove debris. The cell pellet from each animal was resuspended in neurosphere medium DMEM:F12 (Gibco, Invitrogen), 2% B27 (Gibco, Invitrogen), EGF 10 ng/ml (R&D Systems) and plated in a T25 flask. Every 2 days the cells were fed with 1ml of fresh neurosphere medium. The cells were passaged every 4 days.

Cells were electroporated with either CFP-IRES or Safb-IRES-CFP vector (5μg) using a 4D-Nucleofector (Lonza, program DS-112) in 16-well stripes (500,000 cells/well) and re-plated on cover glasses coated with 100 µg/ml Poly-L-Lysine (Sigma) and 1 µg/ml Laminin (Sigma) in neurosphere medium. Two days later, cell differentiation was induced by replacing the medium with neurosphere medium without EGF. The cells were let differentiating for 2 days and then fixed for immunocytochemical analysis by 10 minutes incubation in 4% paraformaldehyde in 0.1M phosphate buffer. The cells were then stained using antibodies against anti-GFP (Chicken, Aves labs, 1:500), anti-Safb1 (Rabbit, Abcam, 1:300) and anti-Sox10 (Goat, Santa Cruz, 1:200) antibodies (see Key Resources Table). The experiment was repeated three times with 3 biological replicates each.

QUANTIFICATION AND STATISTICAL ANALYSIS

Images of immunostainings were captured and processed on a Confocal Leica SP5 and Apotome2 (Zeiss). According to the Swiss governmental guidelines and requirements, the principles of the 3Rs for animal research were taking into consideration to reduce the number of mice used in the experiment. Data are presented as averages of indicated number of samples. Data representation and statistical analysis were performed using GraphPad Prism software. Statistical comparisons were conducted by two-tailed unpaired Student's t test, Mann-Whitney test or one-way ANOVA test, as indicated. The size of samples (n) is described in the figure legends. Statistical significance is determined by p values (*$p < 0.05$, **$p < 0.01$, ***$p < 0.001$) and error bars are presented as SEM.

For Safb1 motif analysis, the top 20 of pentamers (ranked for the highest Z-scores) identified in previous Safb1 iCLIP experiments (Rivers et al., 2015) were mapped on the NFIB 3'UTR sequence. These most enriched pentamers were also used to create the consensus binding motif with the web-based WebLogo software (http://weblogo.berkeley.edu/).

DATA AND CODE AVAILABILITY

The mass spectrometry proteomics data have been deposited to the ProteomeXchange Consortium via the PRIDE (Perez-Riverol et al., 2019) partner repository with the dataset identifier PXD017677 and 10.6019/PXD017677

SUPPLEMENTAL INFORMATION

Supplemental Information can be found online at LINK

Supplemental Item Titles

Table S1, related to Figure 1: MS Drosha IP

Table S2, related to Figure 2: MS RNA pull-down

Table S3, related to Figure 3: iVenn

REFERENCES

Ahrne, E., Glatter, T., Vigano, C., Schubert, C., Nigg, E.A., and Schmidt, A. (2016). Evaluation and Improvement of Quantification Accuracy in Isobaric Mass Tag-Based Protein Quantification Experiments. J Proteome Res *15*, 2537-2547.

Altmeyer, M., Toledo, L., Gudjonsson, T., Grofte, M., Rask, M.B., Lukas, C., Akimov, V., Blagoev, B., Bartek, J., and Lukas, J. (2013). The chromatin scaffold protein SAFB1 renders chromatin permissive for DNA damage signaling. Mol Cell *52*, 206-220.

Baser, A., Skabkin, M., Kleber, S., Dang, Y., Gulculer Balta, G.S., Kalamakis, G., Gopferich, M., Ibanez, D.C., Schefzik, R., Lopez, A.S.*, et al.* (2019). Onset of differentiation is post-transcriptionally controlled in adult neural stem cells. Nature *566*, 100-104.

Beckervordersandforth, R., and Rolando, C. (2019). Untangling human neurogenesis to understand and counteract brain disorders. Curr Opin Pharmacol *50*, 67-73.

Berg, D.A., Su, Y., Jimenez-Cyrus, D., Patel, A., Huang, N., Morizet, D., Lee, S., Shah, R., Ringeling, F.R., Jain, R.*, et al.* (2019). A Common Embryonic Origin of Stem Cells Drives Developmental and Adult Neurogenesis. Cell *177*, 654-668 e615.

Boldrini, M., Fulmore, C.A., Tartt, A.N., Simeon, L.R., Pavlova, I., Poposka, V., Rosoklija, G.B., Stankov, A., Arango, V., Dwork, A.J.*, et al.* (2018). Human Hippocampal Neurogenesis Persists throughout Aging. Cell Stem Cell *22*, 589-599 e585.

Bonaguidi, M.A., Wheeler, M.A., Shapiro, J.S., Stadel, R.P., Sun, G.J., Ming, G.L., and Song, H. (2011). In vivo clonal analysis reveals self-renewing and multipotent adult neural stem cell characteristics. Cell *145*, 1142-1155.

Bonzano, S., Crisci, I., Podlesny-Drabiniok, A., Rolando, C., Krezel, W., Studer, M., and De Marchis, S. (2018). Neuron-Astroglia Cell Fate Decision in the Adult Mouse Hippocampal Neurogenic Niche Is Cell-Intrinsically Controlled by COUP-TFI In Vivo. Cell Rep *24*, 329-341.

Cano, F., Bye, H., Duncan, L.M., Buchet-Poyau, K., Billaud, M., Wills, M.R., and Lehner, P.J. (2012). The RNA-binding E3 ubiquitin ligase MEX-3C links ubiquitination with MHC-I mRNA degradation. EMBO J *31*, 3596-3606.

Chong, M.M., Zhang, G., Cheloufi, S., Neubert, T.A., Hannon, G.J., and Littman, D.R. (2010). Canonical and alternate functions of the microRNA biogenesis machinery. Genes Dev *24*, 1951-1960.

Deneen, B., Ho, R., Lukaszewicz, A., Hochstim, C.J., Gronostajski, R.M., and Anderson, D.J. (2006). The transcription factor NFIA controls the onset of gliogenesis in the developing spinal cord. Neuron *52*, 953-968.

Dilworth, D., Gudavicius, G., Xu, X., Boyce, A.K.J., O'Sullivan, C., Serpa, J.J., Bilenky, M., Petrochenko, E.V., Borchers, C.H., Hirst, M.*, et al.* (2018). The prolyl isomerase FKBP25 regulates microtubule polymerization impacting cell cycle progression and genomic stability. Nucleic Acids Res *46*, 2459-2478.

Eriksson, P.S., Perfilieva, E., Bjork-Eriksson, T., Alborn, A.M., Nordborg, C., Peterson, D.A., and Gage, F.H. (1998). Neurogenesis in the adult human hippocampus. Nat Med *4*, 1313-1317.

Fagg, W.S., Liu, N., Fair, J.H., Shiue, L., Katzman, S., Donohue, J.P., and Ares, M., Jr. (2017). Autogenous cross-regulation of Quaking mRNA processing and translation balances Quaking functions in splicing and translation. Genes Dev *31*, 1894-1909.

Gage, F.H. (2019). Adult neurogenesis in mammals. Science *364*, 827-828.

Gerstberger, S., Hafner, M., and Tuschl, T. (2014). A census of human RNA-binding proteins. Nat Rev Genet *15*, 829-845.

Goncalves, J.T., Schafer, S.T., and Gage, F.H. (2016). Adult Neurogenesis in the Hippocampus: From Stem Cells to Behavior. Cell *167*, 897-914.

Han, J., Lee, Y., Yeom, K.H., Kim, Y.K., Jin, H., and Kim, V.N. (2004). The Drosha-DGCR8 complex in primary microRNA processing. Genes Dev *18*, 3016-3027.

Huang, R., Han, M., Meng, L., and Chen, X. (2018). Transcriptome-wide discovery of coding and noncoding RNA-binding proteins. Proc Natl Acad Sci U S A *115*, E3879-E3887.

Hubner, N.C., Bird, A.W., Cox, J., Splettstoesser, B., Bandilla, P., Poser, I., Hyman, A., and Mann, M. (2010). Quantitative proteomics combined with BAC TransgeneOmics reveals in vivo protein interactions. J Cell Biol *189*, 739-754.

Huo, X., Ji, L., Zhang, Y., Lv, P., Cao, X., Wang, Q., Yan, Z., Dong, S., Du, D., Zhang, F.*, et al.* (2019). The Nuclear Matrix Protein SAFB Cooperates with Major Satellite RNAs to Stabilize Heterochromatin Architecture Partially through Phase Separation. Molecular Cell.

Ivanova, M., Dobrzycka, K.M., Jiang, S., Michaelis, K., Meyer, R., Kang, K., Adkins, B., Barski, O.A., Zubairy, S., Divisova, J.*, et al.* (2005). Scaffold attachment factor B1 functions in development, growth, and reproduction. Mol Cell Biol *25*, 2995-3006.

Johanson, T.M., Lew, A.M., and Chong, M.M.W. (2013). MicroRNA-independent roles of the RNase III enzymes Drosha and Dicer. Open Biology *3*, 130144-130144.

Kang, W., Nguyen, K.C.Q., and Hebert, J.M. (2019). Transient Redirection of SVZ Stem Cells to Oligodendrogenesis by FGFR3 Activation Promotes Remyelination. Stem Cell Reports *12*, 1223-1231.

Kempermann, G., Gage, F.H., Aigner, L., Song, H., Curtis, M.A., Thuret, S., Kuhn, H.G., Jessberger, S., Frankland, P.W., Cameron, H.A.*, et al.* (2018). Human Adult Neurogenesis: Evidence and Remaining Questions. Cell Stem Cell *23*, 25-30.

Kim, B., Jeong, K., and Kim, V.N. (2017). Genome-wide Mapping of DROSHA Cleavage Sites on Primary MicroRNAs and Noncanonical Substrates. Mol Cell *66*, 258-269 e255.

Knuckles, P., Vogt, M.A., Lugert, S., Milo, M., Chong, M.M., Hautbergue, G.M., Wilson, S.A., Littman, D.R., and Taylor, V. (2012). Drosha regulates neurogenesis by controlling neurogenin 2 expression independent of microRNAs. Nat Neurosci *15*, 962-969.

Lachapelle, F., Avellana-Adalid, V., Nait-Oumesmar, B., and Baron-Van Evercooren, A. (2002). Fibroblast growth factor-2 (FGF-2) and platelet-derived growth factor AB (PDGF AB) promote adult SVZ-derived oligodendrogenesis in vivo. Mol Cell Neurosci *20*, 390-403.

Larocque, D., Galarneau, A., Liu, H.N., Scott, M., Almazan, G., and Richard, S. (2005). Protection of p27(Kip1) mRNA by quaking RNA binding proteins promotes oligodendrocyte differentiation. Nat Neurosci *8*, 27-33.

Lee, D., and Shin, C. (2017). Emerging roles of DROSHA beyond primary microRNA processing. RNA Biol, 1-8.

Li, X., Zhao, X., Fang, Y., Jiang, X., Duong, T., Fan, C., Huang, C.C., and Kain, S.R. (1998). Generation of destabilized green fluorescent protein as a transcription reporter. J Biol Chem *273*, 34970-34975.

Lugert, S., Basak, O., Knuckles, P., Haussler, U., Fabel, K., Gotz, M., Haas, C.A., Kempermann, G., Taylor, V., and Giachino, C. (2010). Quiescent and active hippocampal neural stem cells with distinct morphologies respond selectively to physiological and pathological stimuli and aging. Cell Stem Cell *6*, 445-456.

Lugert, S., Vogt, M., Tchorz, J.S., Muller, M., Giachino, C., and Taylor, V. (2012). Homeostatic neurogenesis in the adult hippocampus does not involve amplification of Ascl1(high) intermediate progenitors. Nat Commun *3*, 670.

Macias, S., Cordiner, Ross A., Gautier, P., Plass, M., and Cáceres, Javier F. (2015). DGCR8 Acts as an Adaptor for the Exosome Complex to Degrade Double-Stranded Structured RNAs. Molecular Cell *60*, 873-885.

Moreno-Jimenez, E.P., Flor-Garcia, M., Terreros-Roncal, J., Rabano, A., Cafini, F., Pallas-Bazarra, N., Avila, J., and Llorens-Martin, M. (2019). Adult hippocampal neurogenesis is abundant in neurologically healthy subjects and drops sharply in patients with Alzheimer's disease. Nat Med *25*, 554-560.

Nguyen, T.A., Jo, M.H., Choi, Y.G., Park, J., Kwon, S.C., Hohng, S., Kim, V.N., and Woo, J.S. (2015). Functional Anatomy of the Human Microprocessor. Cell *161*, 1374-1387.

Norman, M., Rivers, C., Lee, Y.B., Idris, J., and Uney, J. (2016). The increasing diversity of functions attributed to the SAFB family of RNA-/DNA-binding proteins. Biochem J *473*, 4271-4288.

Obernier, K., and Alvarez-Buylla, A. (2019). Neural stem cells: origin, heterogeneity and regulation in the adult mammalian brain. Development *146*, dev156059.

Pedersen, J.S., Bejerano, G., Siepel, A., Rosenbloom, K., Lindblad-Toh, K., Lander, E.S., Kent, J., Miller, W., and Haussler, D. (2006). Identification and classification of conserved RNA secondary structures in the human genome. PLoS Comput Biol *2*, e33.

Perez-Riverol, Y., Csordas, A., Bai, J., Bernal-Llinares, M., Hewapathirana, S., Kundu, D.J., Inuganti, A., Griss, J., Mayer, G., Eisenacher, M.*, et al.* (2019). The PRIDE database and related tools and resources in 2019: improving support for quantification data. Nucleic Acids Res *47*, D442-D450.

Pilaz, L.J., and Silver, D.L. (2015). Post-transcriptional regulation in corticogenesis: how RNA-binding proteins help build the brain. Wiley Interdiscip Rev RNA *6*, 501-515.

Pilz, G.A., Bottes, S., Betizeau, M., Jorg, D.J., Carta, S., Simons, B.D., Helmchen, F., and Jessberger, S. (2018). Live imaging of neurogenesis in the adult mouse hippocampus. Science *359*, 658-662.

Ratti, A., Fallini, C., Cova, L., Fantozzi, R., Calzarossa, C., Zennaro, E., Pascale, A., Quattrone, A., and Silani, V. (2006). A role for the ELAV RNA-binding proteins in neural stem cells: stabilization of Msi1 mRNA. J Cell Sci *119*, 1442-1452.

Renz, A., and Fackelmayer, F.O. (1996). Purification and molecular cloning of the scaffold attachment factor B (SAF-B), a novel human nuclear protein that specifically binds to S/MAR-DNA. Nucleic Acids Research *24*, 843-849.

Rivers, C., Idris, J., Scott, H., Rogers, M., Lee, Y.B., Gaunt, J., Phylactou, L., Curk, T., Campbell, C., Ule, J.*, et al.* (2015). iCLIP identifies novel roles for SAFB1 in regulating RNA processing and neuronal function. BMC Biol *13*, 111.

Rolando, C., Erni, A., Grison, A., Beattie, R., Engler, A., Gokhale, P.J., Milo, M., Wegleiter, T., Jessberger, S., and Taylor, V. (2016). Multipotency of Adult Hippocampal NSCs In Vivo Is Restricted by Drosha/NFIB. Cell Stem Cell *19*, 653-662.

Rolando, C., and Taylor, V. (2017). Non-canonical post-transcriptional RNA regulation of neural stem cell potential. Brain Plast *3*, 111-116.

Rouillard, A.D., Gundersen, G.W., Fernandez, N.F., Wang, Z., Monteiro, C.D., McDermott, M.G., and Ma'ayan, A. (2016). The harmonizome: a collection of processed datasets gathered to serve and mine knowledge about genes and proteins. Database (Oxford) *2016*.

Seri, B., Garcia-Verdugo, J.M., Collado-Morente, L., McEwen, B.S., and Alvarez-Buylla, A. (2004). Cell types, lineage, and architecture of the germinal zone in the adult dentate gyrus. J Comp Neurol *478*, 359-378.

Shannon, P., Markiel, A., Ozier, O., Baliga, N.S., Wang, J.T., Ramage, D., Amin, N., Schwikowski, B., and Ideker, T. (2003). Cytoscape: a software environment for integrated models of biomolecular interaction networks. Genome Res *13*, 2498-2504.

Sohn, J., Selvaraj, V., Wakayama, K., Orosco, L., Lee, E., Crawford, S.E., Guo, F., Lang, J., Horiuchi, M., Zarbalis, K.*, et al.* (2012). PEDF is a novel oligodendrogenic morphogen acting on the adult SVZ and corpus callosum. J Neurosci *32*, 12152-12164.

Sorrells, S.F., Paredes, M.F., Cebrian-Silla, A., Sandoval, K., Qi, D., Kelley, K.W., James, D., Mayer, S., Chang, J., Auguste, K.I.*, et al.* (2018). Human hippocampal neurogenesis drops sharply in children to undetectable levels in adults. Nature *555*, 377-381.

Spadotto, V., Giambruno, R., Massignani, E., Mihailovich, M., Patuzzo, F., Ghini, F., Nicassio, F., and Bonaldi, T. (2018).

Spalding, K.L., Bergmann, O., Alkass, K., Bernard, S., Salehpour, M., Huttner, H.B., Bostrom, E., Westerlund, I., Vial, C., Buchholz, B.A.*, et al.* (2013). Dynamics of hippocampal neurogenesis in adult humans. Cell *153*, 1219-1227.

Stoilov, P., Daoud, R., Nayler, O., and Stamm, S. (2004). Human tra2-beta1 autoregulates its protein concentration by influencing alternative splicing of its pre-mRNA. Hum Mol Genet *13*, 509-524.

Szklarczyk, D., Gable, A.L., Lyon, D., Junge, A., Wyder, S., Huerta-Cepas, J., Simonovic, M., Doncheva, N.T., Morris, J.H., Bork, P.*, et al.* (2019). STRING v11: protein-protein association networks with increased coverage, supporting functional discovery in genome-wide experimental datasets. Nucleic Acids Res *47*, D607-D613.

Tobin, M.K., Musaraca, K., Disouky, A., Shetti, A., Bheri, A., Honer, W.G., Kim, N., Dawe, R.J., Bennett, D.A., Arfanakis, K.*, et al.* (2019). Human Hippocampal Neurogenesis Persists in Aged Adults and Alzheimer's Disease Patients. Cell Stem Cell *24*, 974-982 e973.

Townson, S.M., Dobrzycka, K.M., Lee, A.V., Air, M., Deng, W., Kang, K., Jiang, S., Kioka, N., Michaelis, K., and Oesterreich, S. (2003). SAFB2, a New Scaffold Attachment Factor Homolog and Estrogen Receptor Corepressor. Journal of Biological Chemistry *278*, 20059-20068.

Townson, S.M., Sullivan, T., Zhang, Q.P., Clark, G.M., Osborne, C.K., Lee, A.V., and Oesterreich, S. (2000). HET/SAF-B overexpression causes growth arrest and multinuclearity and is associated with aneuploidy in human breast cancer. Clinical Cancer Research *6*, 3788-3796.

Treiber, T., Treiber, N., Plessmann, U., Harlander, S., Daiss, J.L., Eichner, N., Lehmann, G., Schall, K., Urlaub, H., and Meister, G. (2017). A Compendium of RNA-Binding Proteins that Regulate MicroRNA Biogenesis. Mol Cell *66*, 270-284 e213.

Wu, J.I., Reed, R.B., Grabowski, P.J., and Artzt, K. (2002). Function of quaking in myelination: regulation of alternative splicing. Proc Natl Acad Sci U S A *99*, 4233-4238.

Yoo, A.S., Sun, A.X., Li, L., Shcheglovitov, A., Portmann, T., Li, Y., Lee-Messer, C., Dolmetsch, R.E., Tsien, R.W., and Crabtree, G.R. (2011). MicroRNA-mediated conversion of human fibroblasts to neurons. Nature *476*, 228-231.

Zhang, R., Boareto, M., Engler, A., Louvi, A., Giachino, C., Iber, D., and Taylor, V. (2019). Id4 Downstream of Notch2 Maintains Neural Stem Cell Quiescence in the Adult Hippocampus. Cell Rep *28*, 1485-1498 e1486.

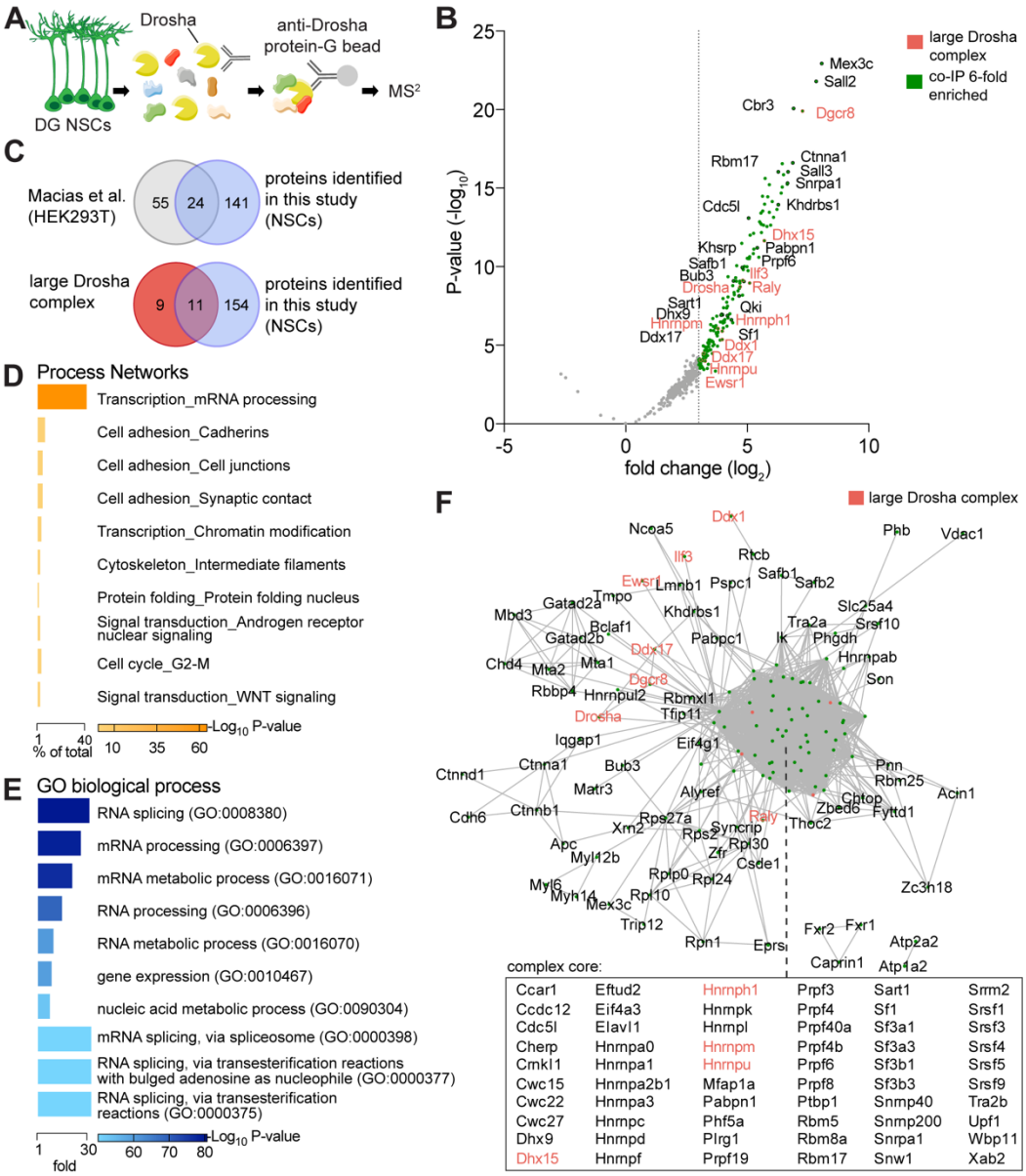

Iffländer et al., Figure 1

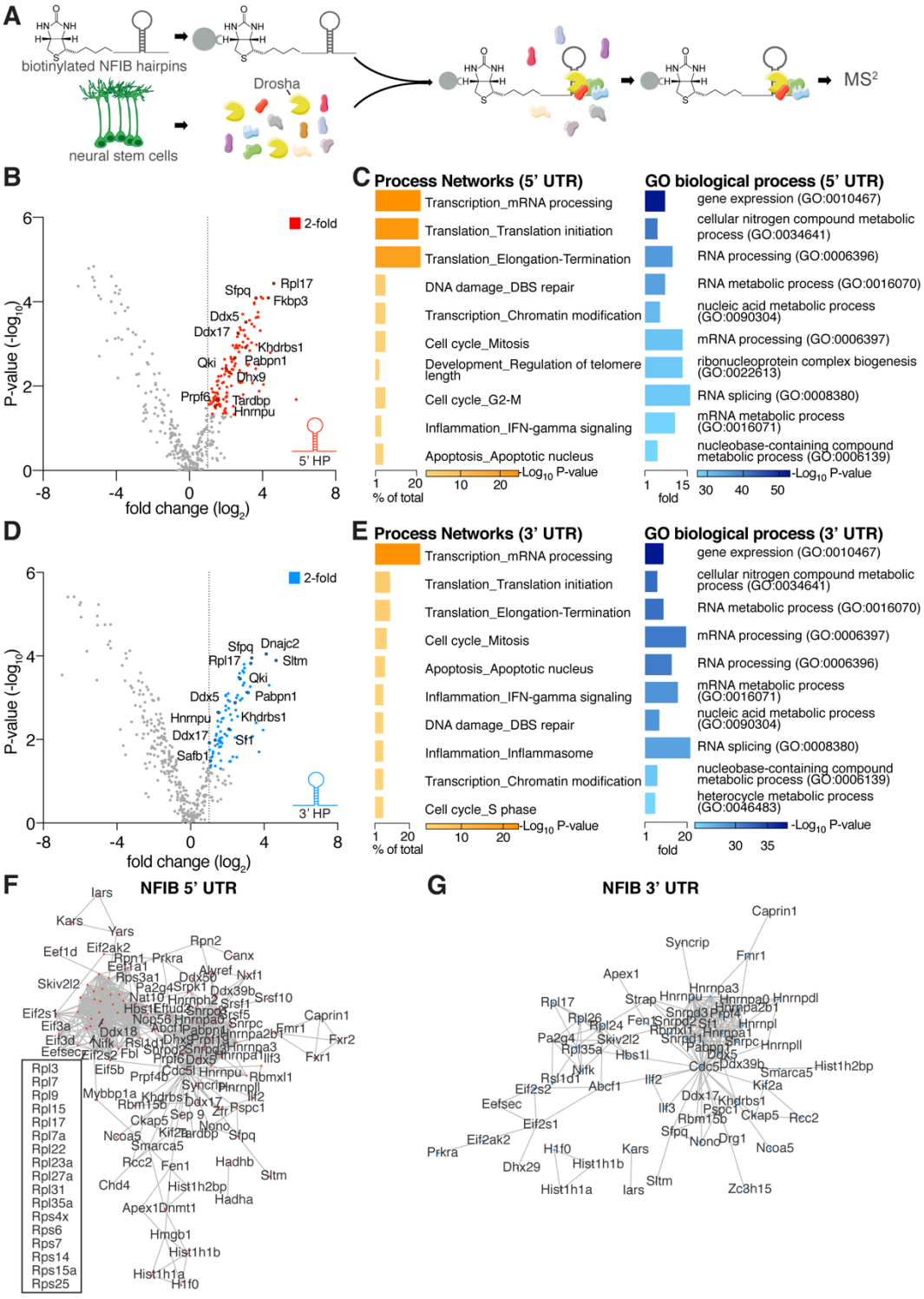

Iffländer et al., Figure 2

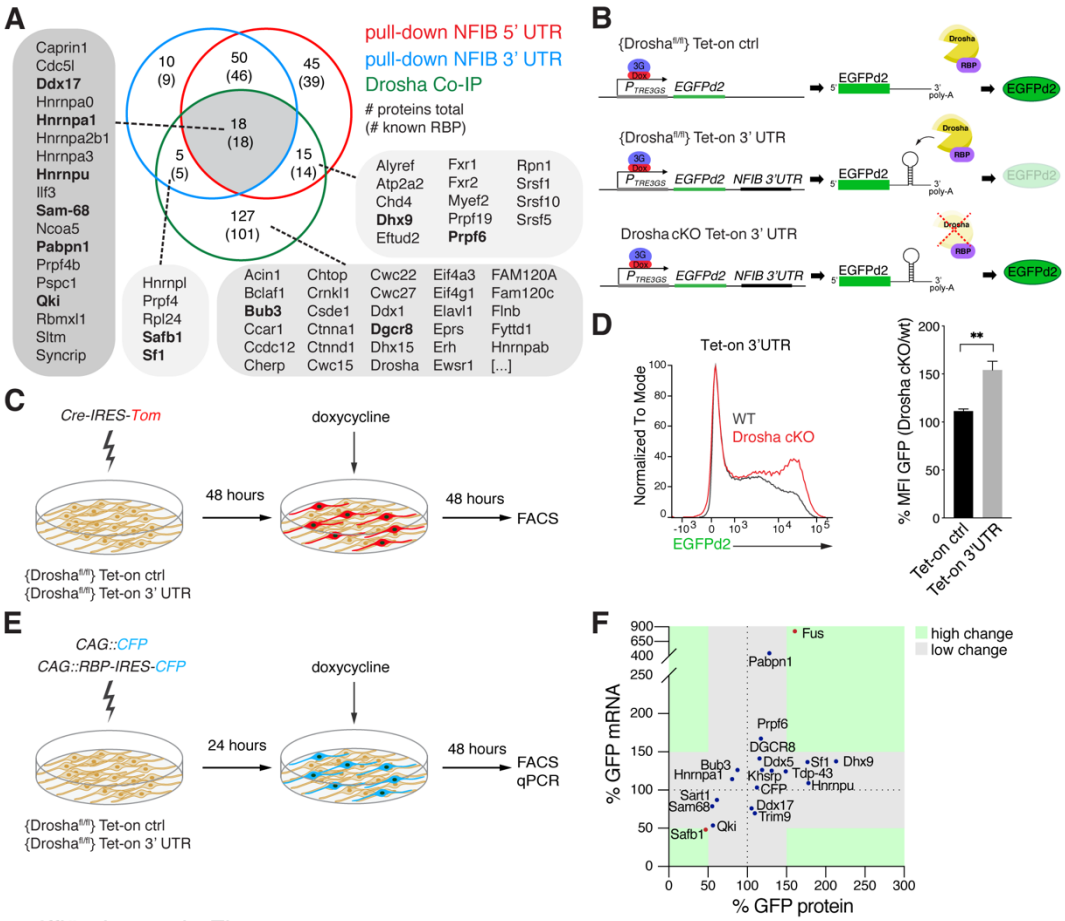

Iffländer et al., Figure 3

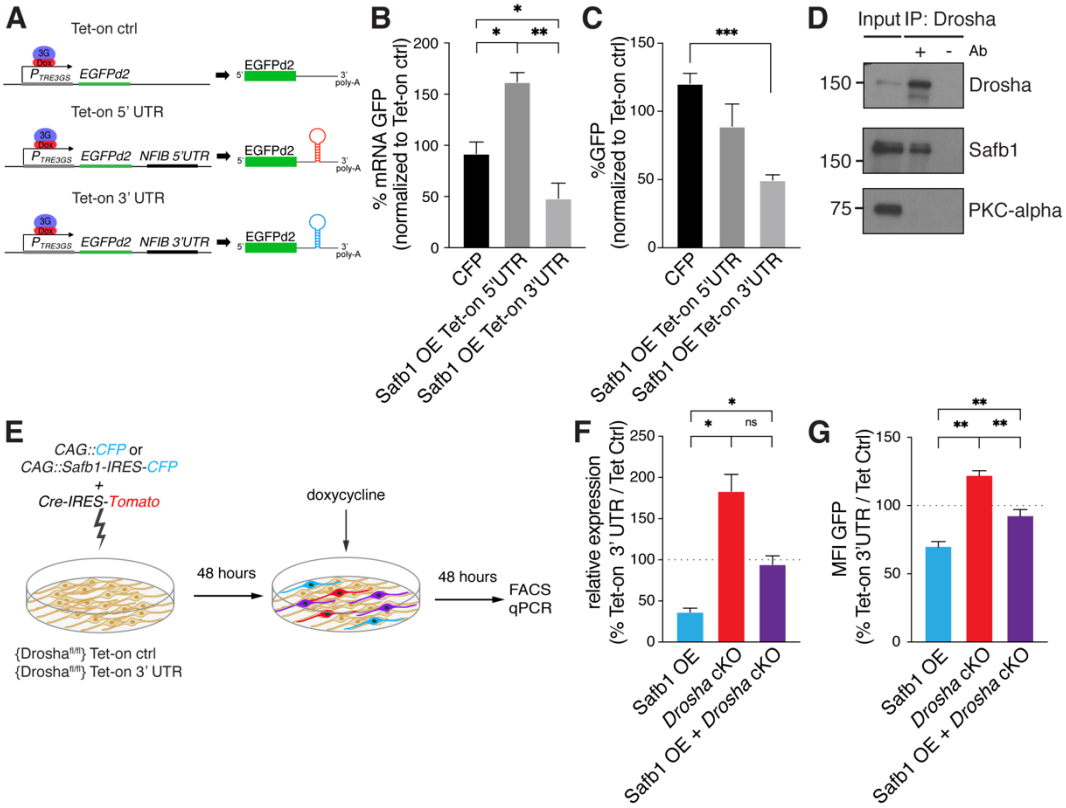

Iffländer et al., Figure 4

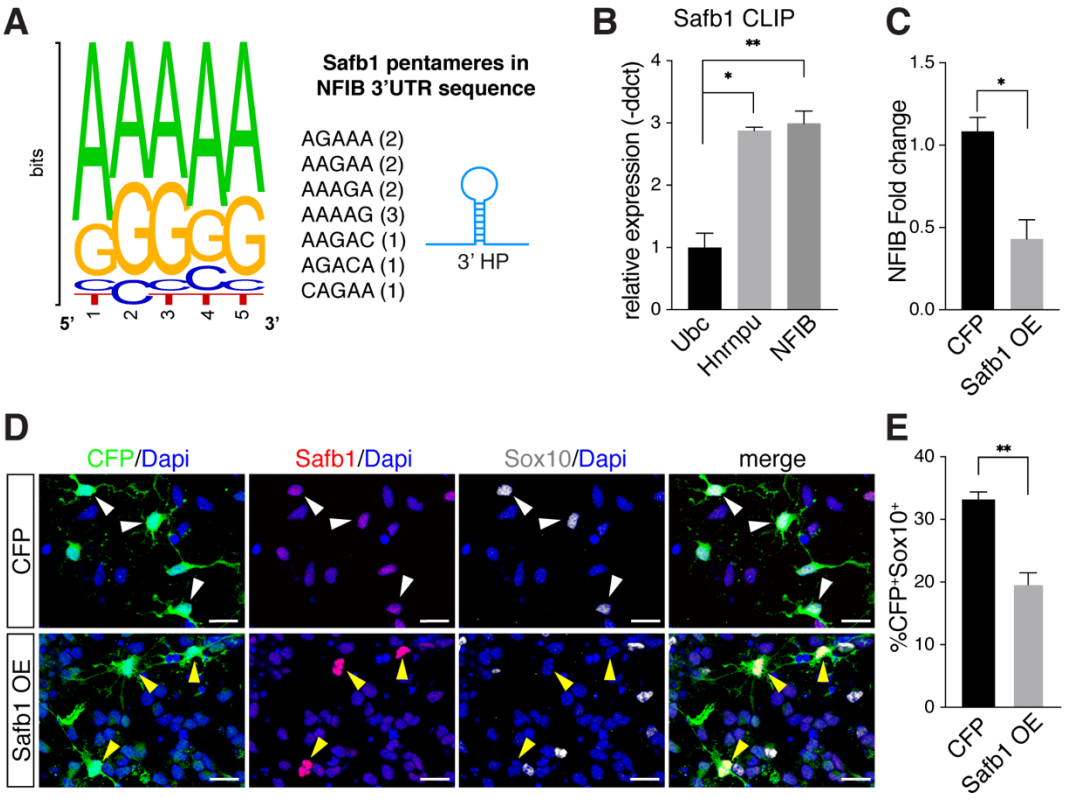

Iffländer et al., Figure 5

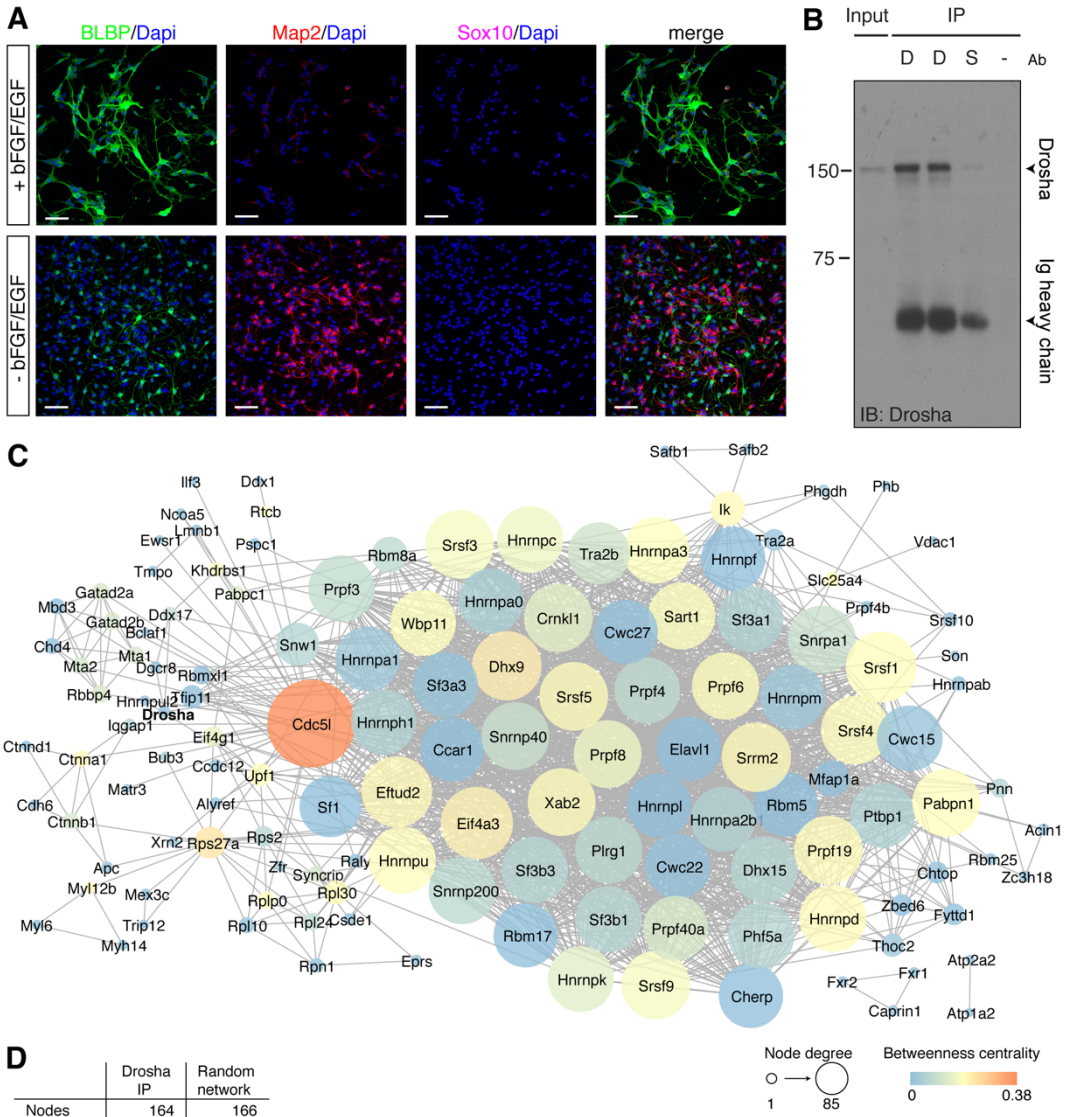

D

	Drosha IP	Random network
Nodes	164	166
Edges	1746	35
Clustering coefficient	0.66	0.17
Avg. node degree	21.3	0.422
P-value	1 x 10^{-16}	0.313

Iffländer et al., Figure S1

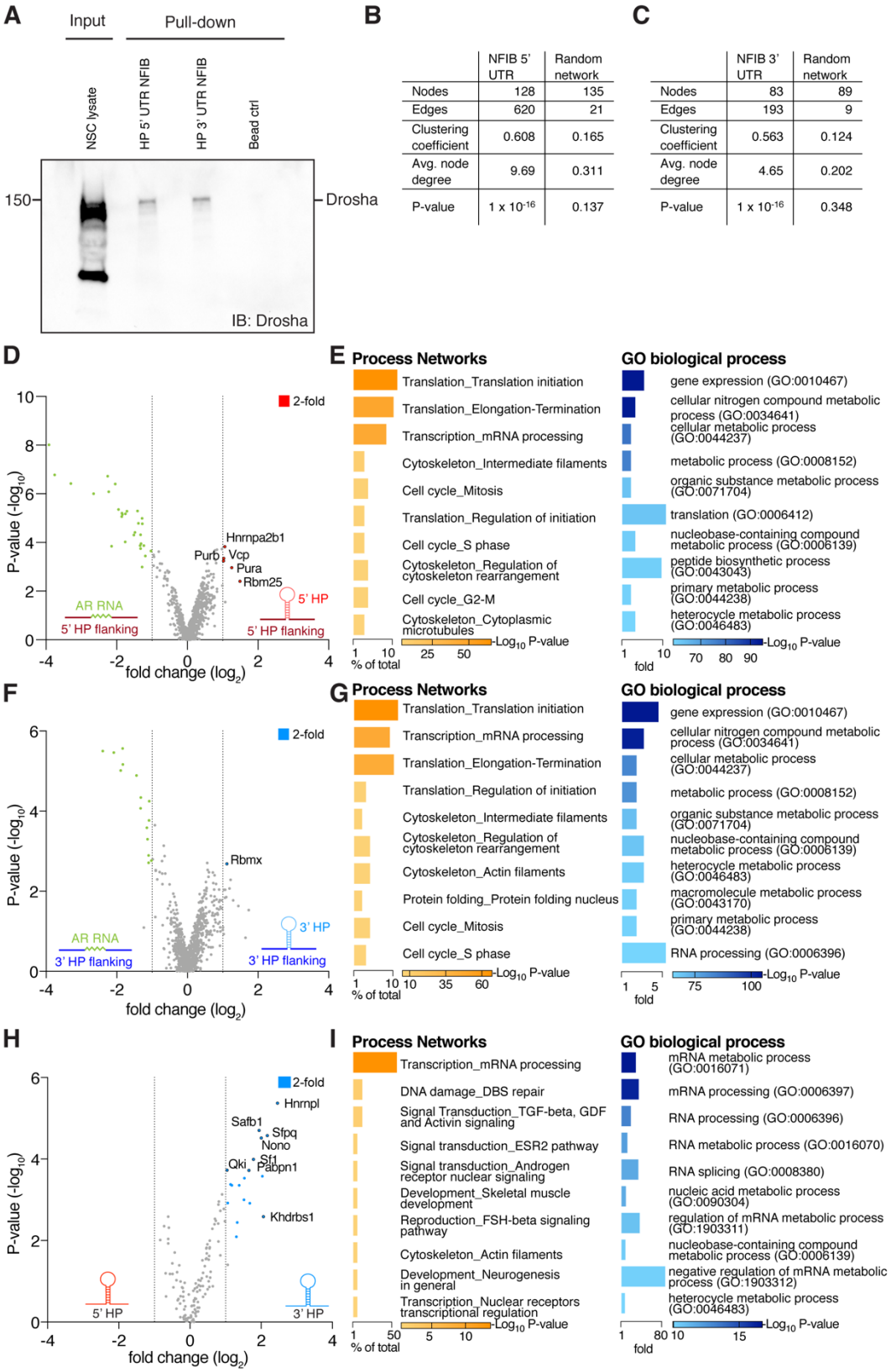

	NFIB 5' UTR	Random network
Nodes	128	135
Edges	620	21
Clustering coefficient	0.608	0.165
Avg. node degree	9.69	0.311
P-value	1 x 10^{-16}	0.137

	NFIB 3' UTR	Random network
Nodes	83	89
Edges	193	9
Clustering coefficient	0.563	0.124
Avg. node degree	4.65	0.202
P-value	1 x 10^{-16}	0.348

Iffländer et al., Figure S2

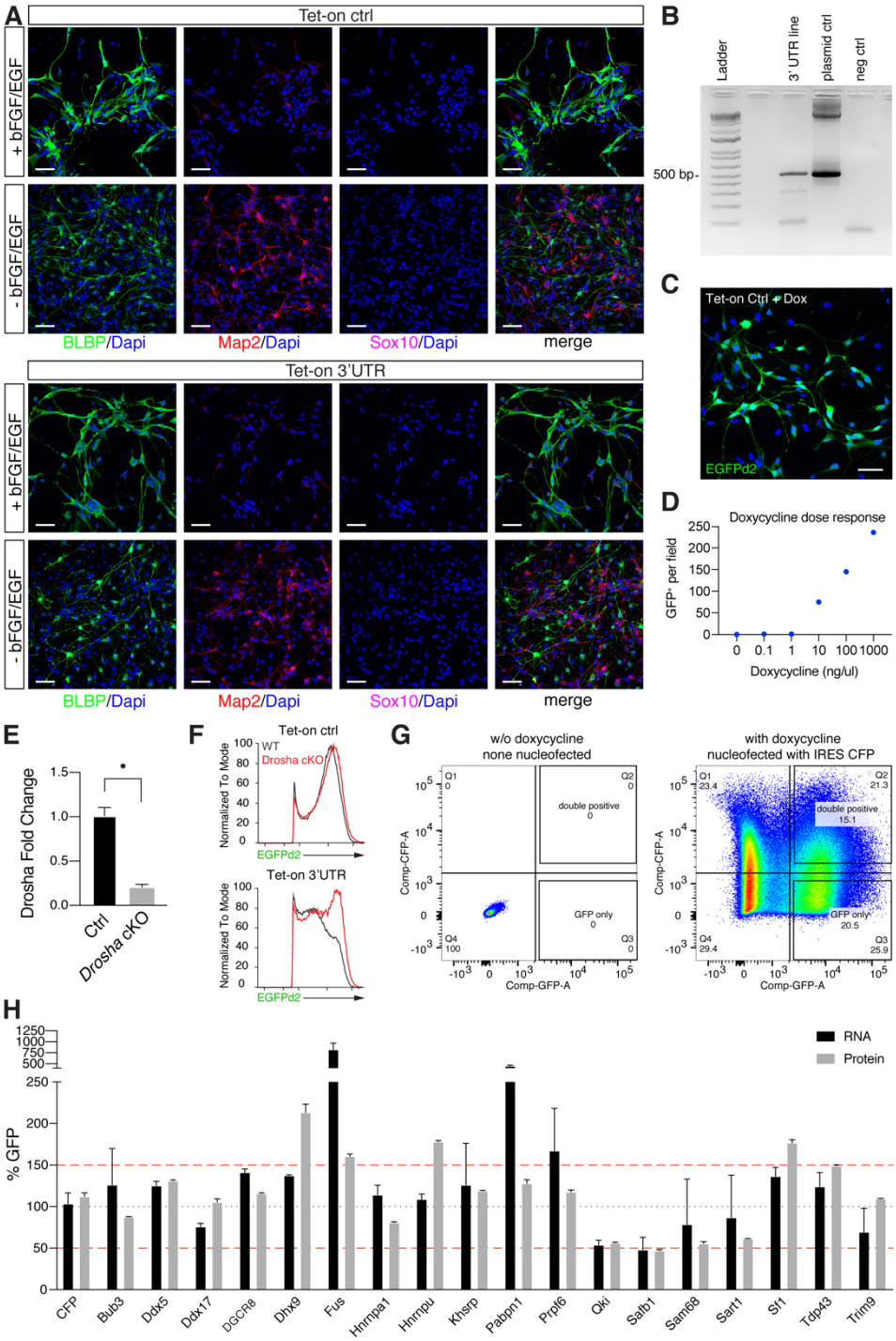

Iffländer et al., Figure S3

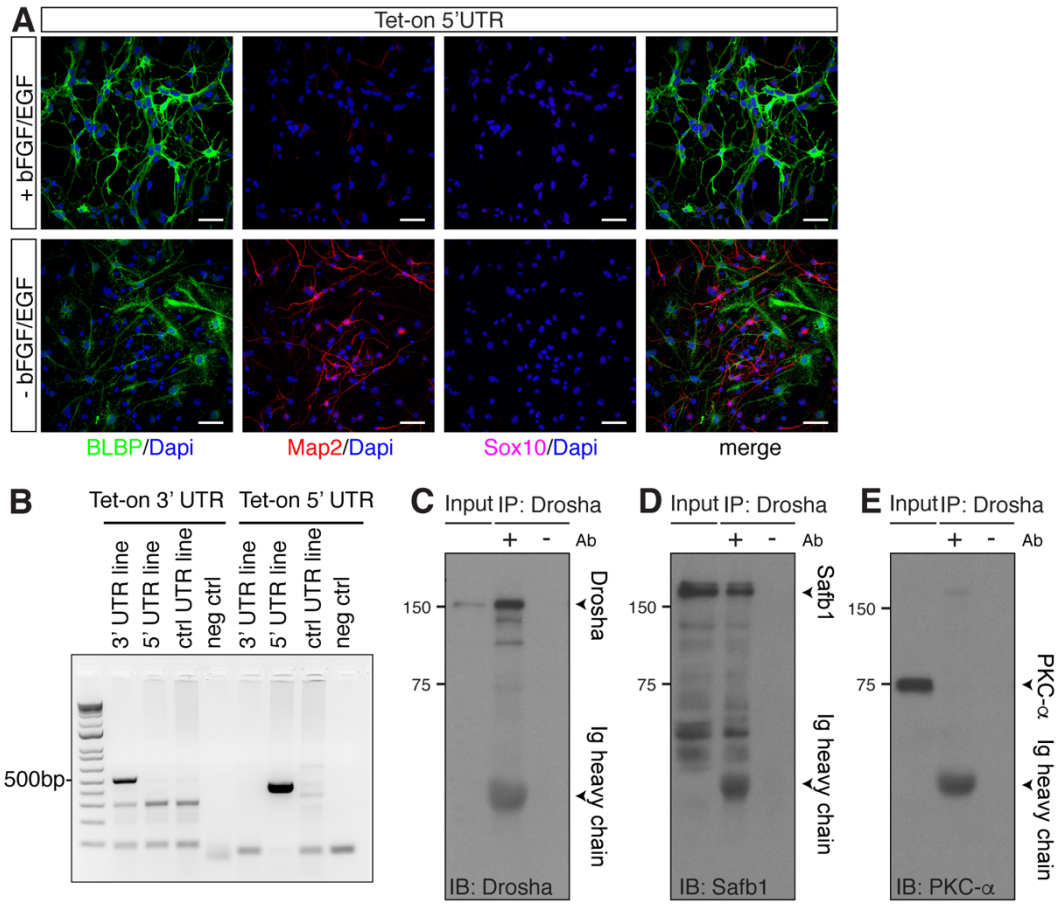

Iffländer et al., Figure S4

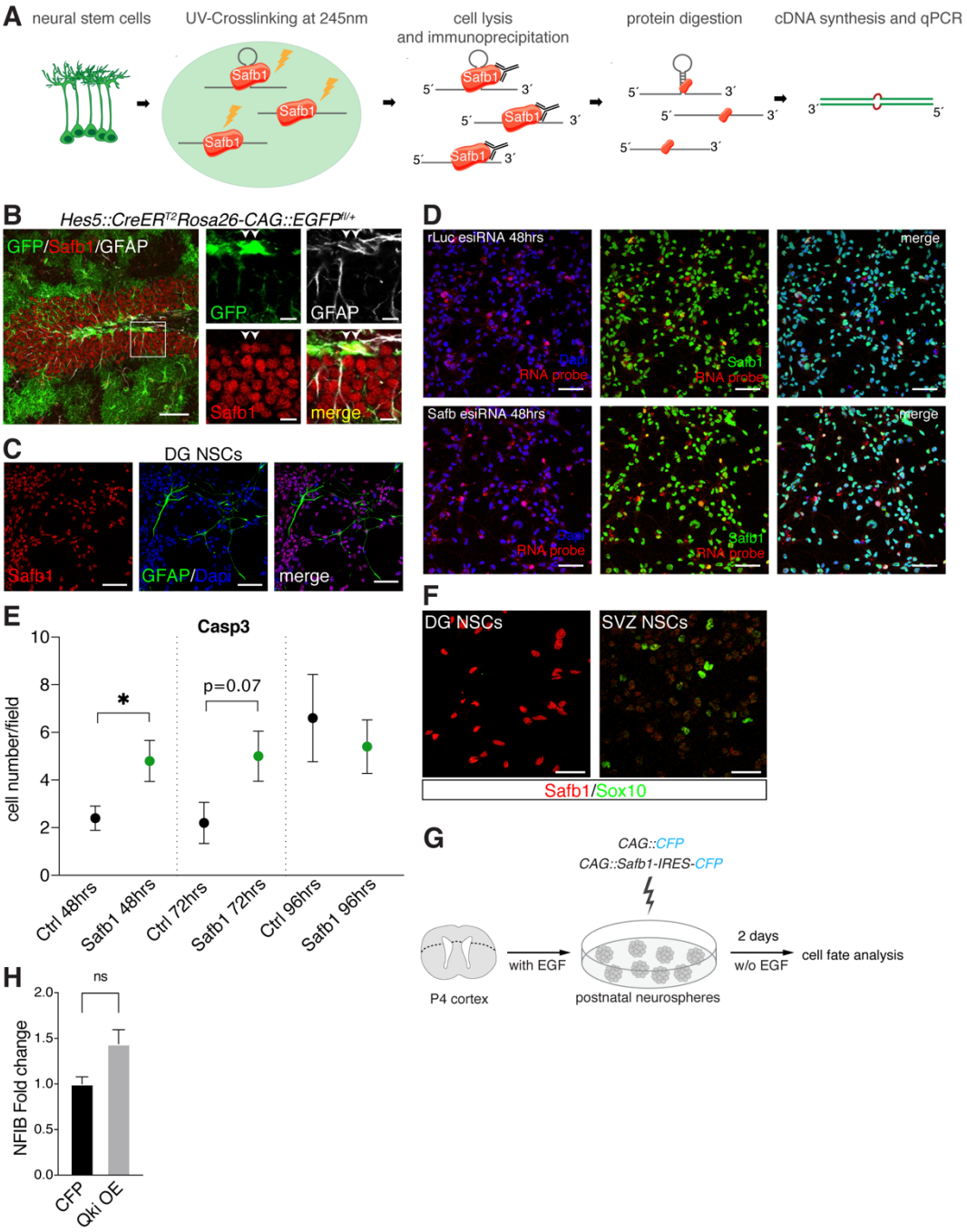

Iffländer et al., Figure S5

Discussion and future perspectives

Protein interaction studies

The first goal of this project was to find interacting proteins of Drosha and the 3' UTR and 5' UTR HP of NFIB. For these HP, we used an RNA-pull down approach using the biotinylated *in vitro* transcript as a bait. An alternative approach would have been a StreptoTag based approach (Bachler et al., 1999) or using streptomycin-binding RNA aptamers (Windbichler and Schroeder, 2006). The advantage of an aptamer based approach is to express the construct *in vitro* prior to cell lysis and to affinity purify the mRNA and their bound RBPS directly from the cell lysate. However, as we aim to continue the Drosha studies by not only investigate NFIB but also other non-canonical Drosha mRNA targets like neuogenin2, neuoD1 and neuroD6 (Knuckles et al., 2012) and also potential novel Drosha targets, it was beneficial to establish the RNA biotinylation approach, which will be easily applicable to any RNA sequence without designing a new aptamer. Yet, we had to overcome the methodological challenges in our approach like precise 5' end labeling, RNA bait competition with endogenous expressed transcript and premature Drosha cleavage prior to bait extraction etc. As I was able to successfully establish this protocol in our lab and to pull-down and identify RBP interaction partners of NFIB, this will now allow us to more easily investigate additional Drosha mRNA target interactors in future experiments. In collaboration with the proteomics facility of the Biozentrum of the University of Basel we were for the first time able to discover the Drosha interactome in DG NSCs. This dataset allowed us to better understand the large-complex formation of Drosha and identify potential novel interactors that could have additional Drosha regulatory functions in NSCs. It will be interesting for future experiments to closer investigate certain RBP interactors with gain and loss-of function and see potential effects of NSC development. In a next step, we would investigate the Drosha dependence in this process by *Drosha* cKO or OE in our established cell culture

systems and could potentially find novel non-canonical functions of Drosha.

Moreover, it would be interesting to follow up on the interactions observed for the two NFIB hairpins. The particular mechanistic role of the 5' UTR still remains uncertain. Thanks to our analysis, we know that the 5'UTR has a special role in translation. However, how this influences NFIB protein expression is still unclear. As NFIB is required and sufficient for oligodendrogenesis (Deneen et al., 2006), it would be interesting to learn more about this important cell fate determining transcription factor even if the mechanism extends beyond Drosha regulation.

Function assessment and identification of Safb1

The second main goal of our study was to test for the actual functional contribution towards Drosha-mediated cleavage of some selected interactors that we had identified in the MS analysis. In order to be able to directly monitor Drosha cleavage activity in NSCs, we established a reporter GFP assay mimicking the physiological process of NFIB degradation. Thanks to the doxycycline inducible promotor, we were able to express the reporter at the correct level for the endogenous Drosha to process. Using a destabilized eGFP variant (eGFPd2) helped us to always just monitor the immediate translated eGFP. The establishment of this method in the lab provides a great tool and will make future studies of Drosha cleavage behavior of NIFB mRNA more easy to proceed. Moreover, the hairpin sequence in the original reporter vector can be easily replaced with alternative hairpin sequences and thus brings a broader investigation of Drosha cleavage for multiple targets in to close range. For NFIB, we tested 18 RBPs in our cell assay and found that Safb1 significantly reduced reporter GFP expression on mRNA and protein level. Moreover, we could show that endogenous NFIB was also reduced after Safb1 OE. Additionally, we could observe that the regulation is 3' UTR specific as the effect could not be observed at the 5' UTR and found, that *Drosha* cKO could partially rescue the phenotype. Moreover we could

confirm interaction of Drosha and Safb1 by western blot analysis and the interaction of Safb1 and NFIB by CLIP. Altogether this results prove that Safb1 is a regulator of Drosha-mediated cleavage of NFIB. Nonetheless, the detailed mechanism needs further investigation. It is not yet clear, where exactly Safb1 binds the 3'UTR hairpin nor are the NFIB mRNA binding sites known for Drosha after all. Based on our MS results it seems likely that Safb1 binds the NFIB 3' UTR on the flanking region, where we could also identify several putative binding sites suiting the known Safb1 RNA binding motifs (Rivers et al., 2015). The best way to uncover the exact binding sites for Safb1 but also Drosha will be a precise mapping of the nucleotides that are retrieved by protein precipitation, similar to the mapping of the exact Drosha binding motif on miRNA by fCLIP-seq (Kim et al., 2017). As we found several valid Safb1 target sites and a strong MS signal on the 3' UTR transcript, it might be that several copies of the Safb1/Drosha complex could actually bind at different locations around the same hairpin. This hypothesis is still in accordance with the findings of this study but could explain, why investigation of the NFIB hairpin fragments by a rapid amplification of cDNA ends (RACE) approach did not lead to a clear cleavage site but rather an accumulation of transcript fragments of variant lengths (Rolando et al., 2016). This cleavage pattern could be explained by multiple copies of Safb1 recruiting Drosha to several locations on the RNA transcript inducing multiple Drosha cleavage sites. Our postulated mechanism does also not exclude the contribution of additional factors that join the Drosha/Safb1 complex in a co-regulatory, complex assembling or catalyzing fashion. Based on our Drosha interactome experiments, we found Drosha interacting with 165 proteins and STRING network interaction analysis indicated no direct protein interaction between Drosha and Safb1, which might imply the presence of a linking protein. Considering those facts, the theory of a more complex mechanism with several involved proteins seems possible and does not contradict our current findings, but in contrast, it will be inspiring to determine if Safb1 and Drosha indeed directly bind each other or are

assembled in a larger “non-canonical Drosha complex” with a potential exciting novel mega-regulatory function in the cell.
We have shown that Safb1 gets co-precipitated by Drosha IP in MS and direct western blot analysis. Also for the other way around, preliminary data of Safb1 IP indicate that Drosha gets precipitated by Safb1 as well. However, due to the high expression of Safb1, this binding is not saturated which pushed Drosha to the detection limit. Future analysis has to overcome this problem and confirm the inverse binding. Interestingly, preliminary data also suggests that the addition of RNAse enzyme to the Drosha IP cell lysate did not reduce the amount of bound Safb1, indicating that Safb1 and Drosha is direct and not via a mutual RNA transcript. Again, future experiments will show, if this assumption remains true. Another unsolved question is the order of binding. It is not yet known if Safb1 binds first to Drosha and the complex is then targeted towards the RNA hairpin as a whole or Safb1 binds first the mRNA and then recruits Drosha to this site. Despite similar outcome, mechanistically it makes an interesting difference, if Safb1 is present in a free floating Drosha complex with potential different functions for Safb1 or if Safb1 would work as a specific marker of NFIB degradation - similar to ubiquitin for proteins - but in a more specific fashion. It will be fundamental to determine all these details of Drosha/Safb1-mediated cleavage in order to fully understand the general process.

Safb1 regulation

As our experiments demonstrated, the problem of an ubiquitously expressed Drosha can be circumvented by expressing the Drosha regulator Safb1 at different levels in order to favor or hinder NFIB mRNA cleavage. The arguably most interesting follow-up question that raises from this study is the problem, how Safb1 expression levels get regulated themselves in NSCs. Safb1 fulfills many important functions in the cell ranging from chromatin-modifications to DNA repair, RNA splicing, stress response and apoptosis (Norman et al., 2016). We have seen increased

cell death after Safb1 knockdown and Safb1 OE was reported to have negative effects on cell growth in human breast cancer cells (Townson et al., 2000), an observation we also made during our own Safb1 OE experiments in NSCs. This indicates that disturbance of Safb1 expression levels induce drastic negative effects, which makes it interesting to address, how Safb1 level changes can be achieved under physiological conditions despite these adverse effects. One possible mechanism could be, that Safb1 regulation also occurs on the post-transcriptional level. It will be interesting to investigate, what RBPs bind to the mRNA transcript of Safb1 itself in NSCs and how they influence Safb1 expression in the brain.

As high levels of Safb1 increase Drosha cleavage, we hypothesize that low levels of Safb1 would have an opposite effect. Unfortunately, apoptosis after Safb1 knockdown was so severe that we could not perform any Safb1 loss-of-function experiments in our NSC reporter system. This effect seems particularly severe in NSCs, as in other cell types like SH-SY5Y neuroblastoma a Safb1 knockdown could be accomplished (Rivers et al., 2015). However, such a loss-of-function analysis of Safb1 in the DG would be the ideal experiment to investigate Safb1 induced fate shifts directly in DG NSCs. Although the creation of a *Safb1*$^{-/-}$ mutant mouse was successful, the evaluation revealed the mutation to induce strong perinatal lethality (Ivanova et al., 2005). The few mice that survived showed drastic malformations and developmental defects. Although the creation of a cKO mutant mouse line for NSCs might allow a more direct investigation of the brain, it remains uncertain, if *Safb1* cKO also causes NSC apoptosis or would allow the necessary cell survival.

Additional mechanisms and cell fate

As it has been shown that pri-miRNAs can function as mRNA (Cai et al., 2004) and vice versa miRNAs can derive from 3' flanking regions of genes (Morlando et al., 2008), the question arises, if the cleaved hairpin of the NFIB 3'UTR can serve as pre-miRNA and regulate other mRNA transcripts

or act as miRNA sponge. So far, we could not find any evidence for such a second life of the NFIB 3'UTR hairpin. However, a larger and designated investigation was not yet addressed and would be interesting as a future study. We can overexpress the cleaved NFIB HP in NSCs and address self-renewal and differentiation. An *in silico* analysis of sequences complementary to potential target transcripts would provide putative targets that we can test for their mRNA expression by RT-qPCR. Although such an secondary regulatory role of the NFIB 3'UTR HP would theoretically be possible, it would be restricted to cells in which Drosha-mediated cleavage via Safb1 takes place. Moreover, as there is no exactly known Drosha cleavage site and several different RNA fragments could be detected after the cleavage (Rolando et al., 2016), already the identification of the functional fragment might be challenging.

We started this project by looking for regulating RBPs in both an activating or inhibitory role. With the identification of Safb1 it became clear, that Drosha activation has a clear effect on its non-canonical cleavage behavior. However, an additional inhibitory role of other co-factors cannot be excluded. It has been shown that Lin28 can bind the pri-miRNA of Let-7 and prevent the hairpin from being cleaved by Drosha (Viswanathan et al., 2008). It would be interesting to follow up on such an inhibitory mechanism, especially as we could observe that OE of FUS significantly increased the level of reporter GFP for mRNA and protein. Hence, FUS does positively influence the expression of NFIB. To see if this effect is Drosha dependent, the experiment needs to be repeated in a *Drosha* cKO background.

We have seen that Safb1 OE leads to reduced NFIB levels and we know that lower NFIB levels lead to a reduction of oligodendrocytes (Rolando et al., 2016). We could show in NSCs of the SVZ, that we find reduced oligodendrogenesis after Safb1 OE. As a next logical step, we are preparing to experimentally determine the NFIB levels of these SVZ derived NSCs after Safb1 OE to confirm that the reduced number of

oligodendrocytes is indeed caused by the lower levels of NFIB. This data will solidify our proposed mechanism of Safb1 activated Drosha-mediated cleavage of NFIB mRNA to prevent NSCs to commit oligodendrogenesis.

Altogether, the findings of this study helped to understand the non-canonical function of Drosha to target and cleave the mRNA of the transcription factor NFIB and the consequent regulation of NSC fate. This knowledge will help us for future studies to better understand the exact mechanism and possibly even design potential treatments in order to regulate and maintain adult neurogenesis.

References

Ahrne, E., Glatter, T., Vigano, C., Schubert, C., Nigg, E.A., and Schmidt, A. (2016). Evaluation and Improvement of Quantification Accuracy in Isobaric Mass Tag-Based Protein Quantification Experiments. J Proteome Res *15*, 2537-2547.

Altmeyer, M., Toledo, L., Gudjonsson, T., Grofte, M., Rask, M.B., Lukas, C., Akimov, V., Blagoev, B., Bartek, J., and Lukas, J. (2013). The chromatin scaffold protein SAFB1 renders chromatin permissive for DNA damage signaling. Mol Cell *52*, 206-220.

Alvarez-Buylla, A., and Lim, D.A. (2004). For the long run: maintaining germinal niches in the adult brain. Neuron *41*, 683-686.

Arellano, J.I., Harding, B., and Thomas, J.L. (2018). Adult Human Hippocampus: No New Neurons in Sight. Cereb Cortex *28*, 2479-2481.

Bachler, M., Schroeder, R., and von Ahsen, U. (1999). StreptoTag: a novel method for the isolation of RNA-binding proteins. RNA *5*, 1509-1516.

Basak, O., Giachino, C., Fiorini, E., Macdonald, H.R., and Taylor, V. (2012). Neurogenic subventricular zone stem/progenitor cells are Notch1-dependent in their active but not quiescent state. J Neurosci *32*, 5654-5666.

Baser, A., Skabkin, M., Kleber, S., Dang, Y., Gulculer Balta, G.S., Kalamakis, G., Gopferich, M., Ibanez, D.C., Schefzik, R., Lopez, A.S.*, et al.* (2019). Onset of differentiation is post-transcriptionally controlled in adult neural stem cells. Nature *566*, 100-104.

Beckervordersandforth, R., and Rolando, C. (2019). Untangling human neurogenesis to understand and counteract brain disorders. Curr Opin Pharmacol *50*, 67-73.

Benhalevy, D., Anastasakis, D.G., and Hafner, M. (2018). Proximity-CLIP provides a snapshot of protein-occupied RNA elements in subcellular compartments. Nat Methods *15*, 1074-1082.

Benoit Bouvrette, L.P., Bovaird, S., Blanchette, M., and Lecuyer, E. (2020). oRNAment: a database of putative RNA binding protein target sites in the transcriptomes of model species. Nucleic Acids Res *48*, D166-D173.
Berg, D.A., Su, Y., Jimenez-Cyrus, D., Patel, A., Huang, N., Morizet, D., Lee, S., Shah, R., Ringeling, F.R., Jain, R.*, et al.* (2019). A Common Embryonic Origin of Stem Cells Drives Developmental and Adult Neurogenesis. Cell *177*, 654-668 e615.
Boldrini, M., Fulmore, C.A., Tartt, A.N., Simeon, L.R., Pavlova, I., Poposka, V., Rosoklija, G.B., Stankov, A., Arango, V., Dwork, A.J.*, et al.* (2018). Human Hippocampal Neurogenesis Persists throughout Aging. Cell Stem Cell *22*, 589-599 e585.
Bonaguidi, M.A., Wheeler, M.A., Shapiro, J.S., Stadel, R.P., Sun, G.J., Ming, G.L., and Song, H. (2011). In vivo clonal analysis reveals self-renewing and multipotent adult neural stem cell characteristics. Cell *145*, 1142-1155.
Bonzano, S., Crisci, I., Podlesny-Drabiniok, A., Rolando, C., Krezel, W., Studer, M., and De Marchis, S. (2018). Neuron-Astroglia Cell Fate Decision in the Adult Mouse Hippocampal Neurogenic Niche Is Cell-Intrinsically Controlled by COUP-TFI In Vivo. Cell Rep *24*, 329-341.
Brett, J.O., Renault, V.M., Rafalski, V.A., Webb, A.E., and Brunet, A. (2011). The microRNA cluster miR-106b~25 regulates adult neural stem/progenitor cell proliferation and neuronal differentiation. Aging (Albany NY) *3*, 108-124.
Burger, K., and Gullerova, M. (2015). Swiss army knives: non-canonical functions of nuclear Drosha and Dicer. Nature reviews. Molecular cell biology *16*, 417-430.
Cai, X., Hagedorn, C.H., and Cullen, B.R. (2004). Human microRNAs are processed from capped, polyadenylated transcripts that can also function as mRNAs. RNA *10*, 1957-1966.
Cano, F., Bye, H., Duncan, L.M., Buchet-Poyau, K., Billaud, M., Wills, M.R., and Lehner, P.J. (2012). The RNA-binding E3 ubiquitin ligase MEX-3C links ubiquitination with MHC-I mRNA degradation. EMBO J *31*, 3596-3606.
Chong, M.M., Zhang, G., Cheloufi, S., Neubert, T.A., Hannon, G.J., and Littman, D.R. (2010). Canonical and alternate functions of the microRNA biogenesis machinery. Genes Dev *24*, 1951-1960.
Deneen, B., Ho, R., Lukaszewicz, A., Hochstim, C.J., Gronostajski, R.M., and Anderson, D.J. (2006). The transcription factor NFIA controls the onset of gliogenesis in the developing spinal cord. Neuron *52*, 953-968.
Deng, L., Ren, R., Liu, Z., Song, M., Li, J., Wu, Z., Ren, X., Fu, L., Li, W., Zhang, W.*, et al.* (2019). Stabilizing heterochromatin by DGCR8 alleviates senescence and osteoarthritis. Nat Commun *10*, 3329.
Dilworth, D., Gudavicius, G., Xu, X., Boyce, A.K.J., O'Sullivan, C., Serpa, J.J., Bilenky, M., Petrochenko, E.V., Borchers, C.H., Hirst, M.*, et al.* (2018). The prolyl isomerase FKBP25 regulates microtubule polymerization impacting cell cycle progression and genomic stability. Nucleic Acids Res *46*, 2459-2478.

Doetsch, F., Caillé, I., Lim, D.A., García-Verdugo, J.M., and Alvarez-Buylla, A. (1999). Subventricular Zone Astrocytes Are Neural Stem Cells in the Adult Mammalian Brain. Cell *97*, 703-716.
Ehm, O., Goritz, C., Covic, M., Schaffner, I., Schwarz, T.J., Karaca, E., Kempkes, B., Kremmer, E., Pfrieger, F.W., Espinosa, L.*, et al.* (2010). RBPJkappa-dependent signaling is essential for long-term maintenance of neural stem cells in the adult hippocampus. J Neurosci *30*, 13794-13807.
Engler, A., Rolando, C., Giachino, C., Saotome, I., Erni, A., Brien, C., Zhang, R., Zimber-Strobl, U., Radtke, F., Artavanis-Tsakonas, S.*, et al.* (2018). Notch2 Signaling Maintains NSC Quiescence in the Murine Ventricular-Subventricular Zone. Cell Rep *22*, 992-1002.
Eriksson, P.S., Perfilieva, E., Bjork-Eriksson, T., Alborn, A.M., Nordborg, C., Peterson, D.A., and Gage, F.H. (1998). Neurogenesis in the adult human hippocampus. Nat Med *4*, 1313-1317.
Esteves, M., Serra-Almeida, C., Saraiva, C., and Bernardino, L. (2020). New insights into the regulatory roles of microRNAs in adult neurogenesis. Current Opinion in Pharmacology *50*, 38-45.
Eulalio, A., Huntzinger, E., and Izaurralde, E. (2008). Getting to the Root of miRNA-Mediated Gene Silencing. Cell *132*, 9-14.
Fagg, W.S., Liu, N., Fair, J.H., Shiue, L., Katzman, S., Donohue, J.P., and Ares, M., Jr. (2017). Autogenous cross-regulation of Quaking mRNA processing and translation balances Quaking functions in splicing and translation. Genes Dev *31*, 1894-1909.
Furutachi, S., Miya, H., Watanabe, T., Kawai, H., Yamasaki, N., Harada, Y., Imayoshi, I., Nelson, M., Nakayama, K.I., Hirabayashi, Y.*, et al.* (2015). Slowly dividing neural progenitors are an embryonic origin of adult neural stem cells. Nature Neuroscience *18*, 657-665.
Gage, F.H. (2019). Adult neurogenesis in mammals. Science *364*, 827-828.
Gebert, L.F.R., and MacRae, I.J. (2018). Regulation of microRNA function in animals. Nature Reviews Molecular Cell Biology *20*, 21-37.
Gerstberger, S., Hafner, M., and Tuschl, T. (2014). A census of human RNA-binding proteins. Nat Rev Genet *15*, 829-845.
Giachino, C., and Taylor, V. (2014). Notching up neural stem cell homogeneity in homeostasis and disease. Front Neurosci *8*, 32.
Goncalves, J.T., Schafer, S.T., and Gage, F.H. (2016). Adult Neurogenesis in the Hippocampus: From Stem Cells to Behavior. Cell *167*, 897-914.
Gregory, R.I., Chendrimada, T.P., Cooch, N., and Shiekhattar, R. (2005). Human RISC couples microRNA biogenesis and posttranscriptional gene silencing. Cell *123*, 631-640.
Griffiths-Jones, S. (2006). miRBase: microRNA sequences, targets and gene nomenclature. Nucleic Acids Research *34*, D140-D144.
Gromak, N., Dienstbier, M., Macias, S., Plass, M., Eyras, E., Caceres, J.F., and Proudfoot, N.J. (2013). Drosha regulates gene expression independently of RNA cleavage function. Cell Reports *5*, 1499-1510.
Hafner, M., Landthaler, M., Burger, L., Khorshid, M., Hausser, J., Berninger, P., Rothballer, A., Ascano, M., Jr., Jungkamp, A.C.,

Munschauer, M.*, et al.* (2010). Transcriptome-wide identification of RNA-binding protein and microRNA target sites by PAR-CLIP. Cell *141*, 129-141.
Hagerman, P.J., and Hagerman, R.J. (2015). Fragile X-associated tremor/ataxia syndrome. Annals of the New York Academy of Sciences *1338*, 58-70.
Han, J., Kim, H.J., Schafer, S.T., Paquola, A., Clemenson, G.D., Toda, T., Oh, J., Pankonin, A.R., Lee, B.S., Johnston, S.T.*, et al.* (2016). Functional Implications of miR-19 in the Migration of Newborn Neurons in the Adult Brain. Neuron *91*, 79-89.
Han, J., Lee, Y., Yeom, K.H., Kim, Y.K., Jin, H., and Kim, V.N. (2004). The Drosha-DGCR8 complex in primary microRNA processing. Genes Dev *18*, 3016-3027.
Han, J., Pedersen, J.S., Kwon, S.C., Belair, C.D., Kim, Y.K., Yeom, K.H., Yang, W.Y., Haussler, D., Blelloch, R., and Kim, V.N. (2009). Posttranscriptional crossregulation between Drosha and DGCR8. Cell *136*, 75-84.
Hatfield, S.D., Shcherbata, H.R., Fischer, K.A., Nakahara, K., Carthew, R.W., and Ruohola-Baker, H. (2005). Stem cell division is regulated by the microRNA pathway. Nature *435*, 974-978.
Hocq, R., Paternina, J., Alasseur, Q., Genovesio, A., and Le Hir, H. (2018). Monitored eCLIP: high accuracy mapping of RNA-protein interactions. Nucleic Acids Res *46*, 11553-11565.
Huang, R., Han, M., Meng, L., and Chen, X. (2018). Transcriptome-wide discovery of coding and noncoding RNA-binding proteins. Proc Natl Acad Sci U S A *115*, E3879-E3887.
Hubner, N.C., Bird, A.W., Cox, J., Splettstoesser, B., Bandilla, P., Poser, I., Hyman, A., and Mann, M. (2010). Quantitative proteomics combined with BAC TransgeneOmics reveals in vivo protein interactions. J Cell Biol *189*, 739-754.
Huo, X., Ji, L., Zhang, Y., Lv, P., Cao, X., Wang, Q., Yan, Z., Dong, S., Du, D., Zhang, F.*, et al.* (2019). The Nuclear Matrix Protein SAFB Cooperates with Major Satellite RNAs to Stabilize Heterochromatin Architecture Partially through Phase Separation. Molecular Cell.
Ihrie, R.A., and Alvarez-Buylla, A. (2011). Lake-front property: a unique germinal niche by the lateral ventricles of the adult brain. Neuron *70*, 674-686.
Imig, J., Brunschweiger, A., Brummer, A., Guennewig, B., Mittal, N., Kishore, S., Tsikrika, P., Gerber, A.P., Zavolan, M., and Hall, J. (2015). miR-CLIP capture of a miRNA targetome uncovers a lincRNA H19-miR-106a interaction. Nat Chem Biol *11*, 107-114.
Ivanova, M., Dobrzycka, K.M., Jiang, S., Michaelis, K., Meyer, R., Kang, K., Adkins, B., Barski, O.A., Zubairy, S., Divisova, J.*, et al.* (2005). Scaffold attachment factor B1 functions in development, growth, and reproduction. Mol Cell Biol *25*, 2995-3006.
Johanson, T.M., Keown, A.A., Cmero, M., Yeo, J.H.C., Kumar, A., Lew, A.M., Zhan, Y., and Chong, M.M.W. (2015). Drosha controls dendritic cell

development by cleaving messenger RNAs encoding inhibitors of myelopoiesis. Nature immunology *16*, 1134-1141.
Johanson, T.M., Lew, A.M., and Chong, M.M.W. (2013). MicroRNA-independent roles of the RNase III enzymes Drosha and Dicer. Open Biology *3*, 130144-130144.
Kaczkowski, B., Torarinsson, E., Reiche, K., Havgaard, J.H., Stadler, P.F., and Gorodkin, J. (2008). Structural profiles of human miRNA families from pairwise clustering. Bioinformatics *25*, 291-294.
Kaczynski, T., Hussain, A., and Farkas, M. (2019). Quick-irCLIP: Interrogating protein-RNA interactions using a rapid and simple cross-linking and immunoprecipitation technique. MethodsX *6*, 1292-1304.
Kadener, S., Rodriguez, J., Abruzzi, K.C., Khodor, Y.L., Sugino, K., Marr, M.T., 2nd, Nelson, S., and Rosbash, M. (2009). Genome-wide identification of targets of the drosha-pasha/DGCR8 complex. RNA *15*, 537-545.
Kang, W., Nguyen, K.C.Q., and Hebert, J.M. (2019). Transient Redirection of SVZ Stem Cells to Oligodendrogenesis by FGFR3 Activation Promotes Remyelination. Stem Cell Reports *12*, 1223-1231.
Kargapolova, Y., Levin, M., Lackner, K., and Danckwardt, S. (2017). sCLIP-an integrated platform to study RNA-protein interactomes in biomedical research: identification of CSTF2tau in alternative processing of small nuclear RNAs. Nucleic Acids Res *45*, 6074-6086.
Katz, S., Cussigh, D., Urbán, N., Blomfield, I., Guillemot, F., Bally-Cuif, L., and Coolen, M. (2016). A Nuclear Role for miR-9 and Argonaute Proteins in Balancing Quiescent and Activated Neural Stem Cell States. Cell Reports *17*, 1383-1398.
Kempermann, G., Gage, F.H., Aigner, L., Song, H., Curtis, M.A., Thuret, S., Kuhn, H.G., Jessberger, S., Frankland, P.W., Cameron, H.A.*, et al.* (2018). Human Adult Neurogenesis: Evidence and Remaining Questions. Cell Stem Cell *23*, 25-30.
Kilchert, C., Strasser, K., Kunetsky, V., and Anko, M.L. (2019). From parts lists to functional significance-RNA-protein interactions in gene regulation. Wiley Interdiscip Rev RNA, e1582.
Kim, B., Jeong, K., and Kim, V.N. (2017). Genome-wide Mapping of DROSHA Cleavage Sites on Primary MicroRNAs and Noncanonical Substrates. Mol Cell *66*, 258-269 e255.
Kim, H., Kim, J., Kim, K., Chang, H., You, K., and Kim, V.N. (2019). Bias-minimized quantification of microRNA reveals widespread alternative processing and 3' end modification. Nucleic Acids Res *47*, 2630-2640.
Knuckles, P., Vogt, M.A., Lugert, S., Milo, M., Chong, M.M., Hautbergue, G.M., Wilson, S.A., Littman, D.R., and Taylor, V. (2012). Drosha regulates neurogenesis by controlling neurogenin 2 expression independent of microRNAs. Nat Neurosci *15*, 962-969.
König, J., Zarnack, K., Rot, G., Curk, T., Kayikci, M., Zupan, B., Turner, D.J., Luscombe, N.M., and Ule, J. (2010). iCLIP reveals the function of hnRNP particles in splicing at individual nucleotide resolution. Nat Struct Mol Biol *17*, 909-915.

Kwon, S.C., Baek, S.C., Choi, Y.G., Yang, J., Lee, Y.S., Woo, J.S., and Kim, V.N. (2019). Molecular Basis for the Single-Nucleotide Precision of Primary microRNA Processing. Mol Cell *73*, 505-518 e505.
Lachapelle, F., Avellana-Adalid, V., Nait-Oumesmar, B., and Baron-Van Evercooren, A. (2002). Fibroblast growth factor-2 (FGF-2) and platelet-derived growth factor AB (PDGF AB) promote adult SVZ-derived oligodendrogenesis in vivo. Mol Cell Neurosci *20*, 390-403.
Larocque, D., Galarneau, A., Liu, H.N., Scott, M., Almazan, G., and Richard, S. (2005). Protection of p27(Kip1) mRNA by quaking RNA binding proteins promotes oligodendrocyte differentiation. Nat Neurosci *8*, 27-33.
Lazarov, O., Demars, M.P., Da Tommy Zhao, K., Ali, H.M., Grauzas, V., Kney, A., and Larson, J. (2012). Impaired survival of neural progenitor cells in dentate gyrus of adult mice lacking FMRP. Hippocampus *22*, 1220-1224.
Lee, D., Nam, J.W., and Shin, C. (2017). DROSHA targets its own transcript to modulate alternative splicing. RNA *23*, 1035-1047.
Lee, D., and Shin, C. (2017). Emerging roles of DROSHA beyond primary microRNA processing. RNA Biol, 1-8.
Lee, F.C.Y., and Ule, J. (2018). Advances in CLIP Technologies for Studies of Protein-RNA Interactions. Mol Cell *69*, 354-369.
Lee, Y., Kim, M., Han, J., Yeom, K.H., Lee, S., Baek, S.H., and Kim, V.N. (2004). MicroRNA genes are transcribed by RNA polymerase II. EMBO J *23*, 4051-4060.
Letunic, I., and Bork, P. (2018). 20 years of the SMART protein domain annotation resource. Nucleic Acids Res *46*, D493-D496.
Li, X., Zhao, X., Fang, Y., Jiang, X., Duong, T., Fan, C., Huang, C.C., and Kain, S.R. (1998). Generation of destabilized green fluorescent protein as a transcription reporter. J Biol Chem *273*, 34970-34975.
Liao, J.Y., Yang, B., Zhang, Y.C., Wang, X.J., Ye, Y., Peng, J.W., Yang, Z.Z., He, J.H., Zhang, Y., Hu, K.*, et al.* (2020). EuRBPDB: a comprehensive resource for annotation, functional and oncological investigation of eukaryotic RNA binding proteins (RBPs). Nucleic Acids Res *48*, D307-D313.
Licatalosi, D.D., Mele, A., Fak, J.J., Ule, J., Kayikci, M., Chi, S.W., Clark, T.A., Schweitzer, A.C., Blume, J.E., Wang, X.*, et al.* (2008). HITS-CLIP yields genome-wide insights into brain alternative RNA processing. Nature *456*, 464-469.
Lledo, P.-M., Alonso, M., and Grubb, M.S. (2006). Adult neurogenesis and functional plasticity in neuronal circuits. Nature Reviews Neuroscience *7*, 179-193.
Lopez-Bertoni, H., Kozielski, K.L., Rui, Y., Lal, B., Vaughan, H., Wilson, D.R., Mihelson, N., Eberhart, C.G., Laterra, J., and Green, J.J. (2018). Bioreducible Polymeric Nanoparticles Containing Multiplexed Cancer Stem Cell Regulating miRNAs Inhibit Glioblastoma Growth and Prolong Survival. Nano Letters *18*, 4086-4094.
Lopez-Bertoni, H., Lal, B., Li, A., Caplan, M., Guerrero-Cazares, H., Eberhart, C.G., Quinones-Hinojosa, A., Glas, M., Scheffler, B., Laterra, J.*,*

et al. (2015). DNMT-dependent suppression of microRNA regulates the induction of GBM tumor-propagating phenotype by Oct4 and Sox2. Oncogene *34*, 3994-4004.
Lugert, S., Basak, O., Knuckles, P., Haussler, U., Fabel, K., Gotz, M., Haas, C.A., Kempermann, G., Taylor, V., and Giachino, C. (2010). Quiescent and active hippocampal neural stem cells with distinct morphologies respond selectively to physiological and pathological stimuli and aging. Cell Stem Cell *6*, 445-456.
Lugert, S., Vogt, M., Tchorz, J.S., Muller, M., Giachino, C., and Taylor, V. (2012). Homeostatic neurogenesis in the adult hippocampus does not involve amplification of Ascl1(high) intermediate progenitors. Nat Commun *3*, 670.
Lukong, K.E., Chang, K.W., Khandjian, E.W., and Richard, S. (2008). RNA-binding proteins in human genetic disease. Trends Genet *24*, 416-425.
Lunde, B.M., Moore, C., and Varani, G. (2007). RNA-binding proteins: modular design for efficient function. Nat Rev Mol Cell Biol *8*, 479-490.
Luo, Y., Shan, G., Guo, W., Smrt, R.D., Johnson, E.B., Li, X., Pfeiffer, R.L., Szulwach, K.E., Duan, R., Barkho, B.Z.*, et al.* (2010). Fragile x mental retardation protein regulates proliferation and differentiation of adult neural stem/progenitor cells. PLoS Genet *6*, e1000898.
Macias, S., Cordiner, Ross A., Gautier, P., Plass, M., and Cáceres, Javier F. (2015). DGCR8 Acts as an Adaptor for the Exosome Complex to Degrade Double-Stranded Structured RNAs. Molecular Cell *60*, 873-885.
Mackenzie, I.R.A., Rademakers, R., and Neumann, M. (2010). TDP-43 and FUS in amyotrophic lateral sclerosis and frontotemporal dementia. The Lancet Neurology *9*, 995-1007.
Marinaro, F., Marzi, M.J., Hoffmann, N., Amin, H., Pelizzoli, R., Niola, F., Nicassio, F., and De Pietri Tonelli, D. (2017). MicroRNA-independent functions of DGCR8 are essential for neocortical development and TBR1 expression. EMBO Rep *18*, 603-618.
McGeary, S.E., Lin, K.S., Shi, C.Y., Pham, T.M., Bisaria, N., Kelley, G.M., and Bartel, D.P. (2019). The biochemical basis of microRNA targeting efficacy. Science *366*.
Melamed, Z.e., Levy, A., Ashwal-Fluss, R., Lev-Maor, G., Mekahel, K., Atias, N., Gilad, S., Sharan, R., Levy, C., Kadener, S.*, et al.* (2013). Alternative Splicing Regulates Biogenesis of miRNAs Located across Exon-Intron Junctions. Molecular Cell *50*, 869-881.
Mira, H., Andreu, Z., Suh, H., Lie, D.C., Jessberger, S., Consiglio, A., San Emeterio, J., Hortigüela, R., Marqués-Torrejón, M.Á., Nakashima, K.*, et al.* (2010). Signaling through BMPR-IA Regulates Quiescence and Long-Term Activity of Neural Stem Cells in the Adult Hippocampus. Cell Stem Cell *7*, 78-89.
Moreno-Jimenez, E.P., Flor-Garcia, M., Terreros-Roncal, J., Rabano, A., Cafini, F., Pallas-Bazarra, N., Avila, J., and Llorens-Martin, M. (2019). Adult hippocampal neurogenesis is abundant in neurologically healthy subjects and drops sharply in patients with Alzheimer's disease. Nat Med *25*, 554-560.

Morlando, M., Ballarino, M., Gromak, N., Pagano, F., Bozzoni, I., and Proudfoot, N.J. (2008). Primary microRNA transcripts are processed co-transcriptionally. Nat Struct Mol Biol *15*, 902-909.
Nguyen, T.A., Jo, M.H., Choi, Y.G., Park, J., Kwon, S.C., Hohng, S., Kim, V.N., and Woo, J.S. (2015). Functional Anatomy of the Human Microprocessor. Cell *161*, 1374-1387.
Nishino, J., Kim, I., Chada, K., and Morrison, S.J. (2008). Hmga2 promotes neural stem cell self-renewal in young but not old mice by reducing p16Ink4a and p19Arf Expression. Cell *135*, 227-239.
Norman, M., Rivers, C., Lee, Y.B., Idris, J., and Uney, J. (2016). The increasing diversity of functions attributed to the SAFB family of RNA-/DNA-binding proteins. Biochem J *473*, 4271-4288.
Obernier, K., and Alvarez-Buylla, A. (2019). Neural stem cells: origin, heterogeneity and regulation in the adult mammalian brain. Development *146*, dev156059.
Pan, W.L., Chopp, M., Fan, B., Zhang, R., Wang, X., Hu, J., Zhang, X.M., Zhang, Z.G., and Liu, X.S. (2019). Ablation of the microRNA-17-92 cluster in neural stem cells diminishes adult hippocampal neurogenesis and cognitive function. FASEB J *33*, 5257-5267.
Patzlaff, N.E., Shen, M., and Zhao, X. (2018). Regulation of Adult Neurogenesis by the Fragile X Family of RNA Binding Proteins. Brain Plast *3*, 205-223.
Pedersen, J.S., Bejerano, G., Siepel, A., Rosenbloom, K., Lindblad-Toh, K., Lander, E.S., Kent, J., Miller, W., and Haussler, D. (2006). Identification and classification of conserved RNA secondary structures in the human genome. PLoS Comput Biol *2*, e33.
Perez-Riverol, Y., Csordas, A., Bai, J., Bernal-Llinares, M., Hewapathirana, S., Kundu, D.J., Inuganti, A., Griss, J., Mayer, G., Eisenacher, M.*, et al.* (2019). The PRIDE database and related tools and resources in 2019: improving support for quantification data. Nucleic Acids Res *47*, D442-D450.
Pilaz, L.J., and Silver, D.L. (2015). Post-transcriptional regulation in corticogenesis: how RNA-binding proteins help build the brain. Wiley Interdiscip Rev RNA *6*, 501-515.
Pilz, G.A., Bottes, S., Betizeau, M., Jorg, D.J., Carta, S., Simons, B.D., Helmchen, F., and Jessberger, S. (2018). Live imaging of neurogenesis in the adult mouse hippocampus. Science *359*, 658-662.
Ratti, A., Fallini, C., Cova, L., Fantozzi, R., Calzarossa, C., Zennaro, E., Pascale, A., Quattrone, A., and Silani, V. (2006). A role for the ELAV RNA-binding proteins in neural stem cells: stabilization of Msi1 mRNA. J Cell Sci *119*, 1442-1452.
Renz, A., and Fackelmayer, F.O. (1996). Purification and molecular cloning of the scaffold attachment factor B (SAF-B), a novel human nuclear protein that specifically binds to S/MAR-DNA. Nucleic Acids Research *24*, 843-849.
Rivers, C., Idris, J., Scott, H., Rogers, M., Lee, Y.B., Gaunt, J., Phylactou, L., Curk, T., Campbell, C., Ule, J.*, et al.* (2015). iCLIP identifies novel roles

for SAFB1 in regulating RNA processing and neuronal function. BMC Biol *13*, 111.
Rolando, C., Erni, A., Grison, A., Beattie, R., Engler, A., Gokhale, P.J., Milo, M., Wegleiter, T., Jessberger, S., and Taylor, V. (2016). Multipotency of Adult Hippocampal NSCs In Vivo Is Restricted by Drosha/NFIB. Cell Stem Cell *19*, 653-662.
Rolando, C., and Taylor, V. (2017). Non-canonical post-transcriptional RNA regulation of neural stem cell potential. Brain Plast *3*, 111-116.
Romer-Seibert, J.S., Hartman, N.W., and Moss, E.G. (2019). The RNA-binding protein LIN28 controls progenitor and neuronal cell fate during postnatal neurogenesis. The FASEB Journal *33*, 3291-3303.
Rosenberg, M., Blum, R., Kesner, B., Maier, V.K., Szanto, A., and Lee, J.T. (2017). Denaturing CLIP, dCLIP, Pipeline Identifies Discrete RNA Footprints on Chromatin-Associated Proteins and Reveals that CBX7 Targets 3' UTRs to Regulate mRNA Expression. Cell Syst *5*, 368-385 e315.
Rouillard, A.D., Gundersen, G.W., Fernandez, N.F., Wang, Z., Monteiro, C.D., McDermott, M.G., and Ma'ayan, A. (2016). The harmonizome: a collection of processed datasets gathered to serve and mine knowledge about genes and proteins. Database (Oxford) *2016*.
Seri, B., Garcia-Verdugo, J.M., Collado-Morente, L., McEwen, B.S., and Alvarez-Buylla, A. (2004). Cell types, lineage, and architecture of the germinal zone in the adult dentate gyrus. J Comp Neurol *478*, 359-378.
Shannon, P., Markiel, A., Ozier, O., Baliga, N.S., Wang, J.T., Ramage, D., Amin, N., Schwikowski, B., and Ideker, T. (2003). Cytoscape: a software environment for integrated models of biomolecular interaction networks. Genome Res *13*, 2498-2504.
Shcherbata, H.R. (2019). miRNA functions in stem cells and their niches: lessons from the Drosophila ovary. Curr Opin Insect Sci *31*, 29-36.
Sohn, J., Selvaraj, V., Wakayama, K., Orosco, L., Lee, E., Crawford, S.E., Guo, F., Lang, J., Horiuchi, M., Zarbalis, K.*, et al.* (2012). PEDF is a novel oligodendrogenic morphogen acting on the adult SVZ and corpus callosum. J Neurosci *32*, 12152-12164.
Sorrells, S.F., Paredes, M.F., Cebrian-Silla, A., Sandoval, K., Qi, D., Kelley, K.W., James, D., Mayer, S., Chang, J., Auguste, K.I.*, et al.* (2018). Human hippocampal neurogenesis drops sharply in children to undetectable levels in adults. Nature *555*, 377-381.
Spadotto, V., Giambruno, R., Massignani, E., Mihailovich, M., Patuzzo, F., Ghini, F., Nicassio, F., and Bonaldi, T. (2018).
Spalding, K.L., Bergmann, O., Alkass, K., Bernard, S., Salehpour, M., Huttner, H.B., Bostrom, E., Westerlund, I., Vial, C., Buchholz, B.A.*, et al.* (2013). Dynamics of hippocampal neurogenesis in adult humans. Cell *153*, 1219-1227.
Stappert, L., Klaus, F., and Brüstle, O. (2018). MicroRNAs Engage in Complex Circuits Regulating Adult Neurogenesis. Frontiers in Neuroscience *12*.

Stoilov, P., Daoud, R., Nayler, O., and Stamm, S. (2004). Human tra2-beta1 autoregulates its protein concentration by influencing alternative splicing of its pre-mRNA. Hum Mol Genet *13*, 509-524.
Szklarczyk, D., Gable, A.L., Lyon, D., Junge, A., Wyder, S., Huerta-Cepas, J., Simonovic, M., Doncheva, N.T., Morris, J.H., Bork, P.*, et al.* (2019). STRING v11: protein-protein association networks with increased coverage, supporting functional discovery in genome-wide experimental datasets. Nucleic Acids Res *47*, D607-D613.
Tobin, M.K., Musaraca, K., Disouky, A., Shetti, A., Bheri, A., Honer, W.G., Kim, N., Dawe, R.J., Bennett, D.A., Arfanakis, K.*, et al.* (2019). Human Hippocampal Neurogenesis Persists in Aged Adults and Alzheimer's Disease Patients. Cell Stem Cell *24*, 974-982 e973.
Townson, S.M., Dobrzycka, K.M., Lee, A.V., Air, M., Deng, W., Kang, K., Jiang, S., Kioka, N., Michaelis, K., and Oesterreich, S. (2003). SAFB2, a New Scaffold Attachment Factor Homolog and Estrogen Receptor Corepressor. Journal of Biological Chemistry *278*, 20059-20068.
Townson, S.M., Sullivan, T., Zhang, Q.P., Clark, G.M., Osborne, C.K., Lee, A.V., and Oesterreich, S. (2000). HET/SAF-B overexpression causes growth arrest and multinuclearity and is associated with aneuploidy in human breast cancer. Clinical Cancer Research *6*, 3788-3796.
Treiber, T., Treiber, N., Plessmann, U., Harlander, S., Daiss, J.L., Eichner, N., Lehmann, G., Schall, K., Urlaub, H., and Meister, G. (2017). A Compendium of RNA-Binding Proteins that Regulate MicroRNA Biogenesis. Mol Cell *66*, 270-284 e213.
Trendel, J., Schwarzl, T., Horos, R., Prakash, A., Bateman, A., Hentze, M.W., and Krijgsveld, J. (2019). The Human RNA-Binding Proteome and Its Dynamics during Translational Arrest. Cell *176*, 391-403 e319.
Triboulet, R., Chang, H.M., Lapierre, R.J., and Gregory, R.I. (2009). Post-transcriptional control of DGCR8 expression by the Microprocessor. RNA *15*, 1005-1011.
Ule, J., Hwang, H.W., and Darnell, R.B. (2018). The Future of Cross-Linking and Immunoprecipitation (CLIP). Cold Spring Harb Perspect Biol *10*.
Ule, J., Jensen, K.B., Ruggiu, M., Mele, A., Ule, A., and Darnell, R.B. (2003). CLIP identifies Nova-regulated RNA networks in the brain. Science *302*, 1212-1215.
Van Nostrand, E.L., Pratt, G.A., Shishkin, A.A., Gelboin-Burkhart, C., Fang, M.Y., Sundararaman, B., Blue, S.M., Nguyen, T.B., Surka, C., Elkins, K.*, et al.* (2016). Robust transcriptome-wide discovery of RNA-binding protein binding sites with enhanced CLIP (eCLIP). Nat Methods *13*, 508-514.
Viswanathan, S.R., Daley, G.Q., and Gregory, R.I. (2008). Selective blockade of microRNA processing by Lin28. Science *320*, 97-100.
Wang, Y., Guo, Y., Tang, C., Han, X., Xu, M., Sun, J., Zhao, Y., Zhang, Y., Wang, M., Cao, X.*, et al.* (2019). Developmental Cytoplasmic-to-Nuclear Translocation of RNA-Binding Protein HuR Is Required for Adult Neurogenesis. Cell Reports *29*, 3101-3117.e3107.

Windbichler, N., and Schroeder, R. (2006). Isolation of specific RNA-binding proteins using the streptomycin-binding RNA aptamer. Nat Protoc *1*, 637-640.
Wu, H., Ye, C., Ramirez, D., and Manjunath, N. (2009). Alternative processing of primary microRNA transcripts by Drosha generates 5' end variation of mature microRNA. PLoS One *4*, e7566.
Wu, J.I., Reed, R.B., Grabowski, P.J., and Artzt, K. (2002). Function of quaking in myelination: regulation of alternative splicing. Proc Natl Acad Sci U S A *99*, 4233-4238.
Yoo, A.S., Sun, A.X., Li, L., Shcheglovitov, A., Portmann, T., Li, Y., Lee-Messer, C., Dolmetsch, R.E., Tsien, R.W., and Crabtree, G.R. (2011). MicroRNA-mediated conversion of human fibroblasts to neurons. Nature *476*, 228-231.
Zarnegar, B.J., Flynn, R.A., Shen, Y., Do, B.T., Chang, H.Y., and Khavari, P.A. (2016). irCLIP platform for efficient characterization of protein-RNA interactions. Nat Methods *13*, 489-492.
Zhang, R., Boareto, M., Engler, A., Louvi, A., Giachino, C., Iber, D., and Taylor, V. (2019). Id4 Downstream of Notch2 Maintains Neural Stem Cell Quiescence in the Adult Hippocampus. Cell Rep *28*, 1485-1498 e1486.
Zhao, C., Deng, W., and Gage, F.H. (2008). Mechanisms and functional implications of adult neurogenesis. Cell *132*, 645-660.
Zhao, Y., Zhang, Y., Teng, Y., Liu, K., Liu, Y., Li, W., and Wu, L. (2019). SpyCLIP: an easy-to-use and high-throughput compatible CLIP platform for the characterization of protein-RNA interactions with high accuracy. Nucleic Acids Res *47*, e33.